



Dissertations

Graduate College

8-2006

The Effects of Paper Physical Properties on Print Gloss and Ink Mileage

Renmei Xu
Western Michigan University

Follow this and additional works at: <https://scholarworks.wmich.edu/dissertations>



Part of the Engineering Commons

Recommended Citation

Xu, Renmei, "The Effects of Paper Physical Properties on Print Gloss and Ink Mileage" (2006).

Dissertations. 1005.

<https://scholarworks.wmich.edu/dissertations/1005>

This Dissertation-Open Access is brought to you for free and open access by the Graduate College at ScholarWorks at WMU. It has been accepted for inclusion in Dissertations by an authorized administrator of ScholarWorks at WMU. For more information, please contact wmu-scholarworks@wmich.edu.



**THE EFFECTS OF PAPER PHYSICAL PROPERTIES ON PRINT GLOSS AND
INK MILEAGE**

by

Renmei Xu

**A Dissertation
Submitted to the
Faculty of The Graduate College
in partial fulfillment of the
requirements for the
Degree of Doctor of Philosophy
Department of Paper Engineering, Chemical Engineering, and Imaging
Advisor: Paul D. Fleming III, Ph.D.**

**Western Michigan University
Kalamazoo, Michigan
August 2006**

THE EFFECTS OF PAPER PHYSICAL PROPERTIES ON PRINT GLOSS AND INK MILEAGE

Renmei Xu, Ph.D.

Western Michigan University, 2006

This research involved two kinds of printing process, inkjet printing and gravure printing.

Five commercial Epson and Kodak inkjet papers were printed on three Epson ink jet printers. Paper surface roughness was tested by a Parker Print-Surf (PPS) tester, a stylus profilometer and an atomic force microscopy (AFM). AFM and profilometer roughness showed higher correlations with paper gloss and print gloss. For microporous Epson papers, higher print gloss was found with the Pro 5500 and Photo 2200 printers using pigment-based inks than the Pro 5000 printer using dye-based inks. The ink types had less effect on print gloss for resinous Kodak papers. Study of the black ink film surface using AFM proved that dyed ink films resulted in smoother ink film surfaces than pigmented ones.

Two gravure printing trials were performed on a rotogravure web press. Five commercial LWC papers were used in the first trial, and five trial coated papers were used in the second trial. AFM roughness showed the best correlations with both 60° and 75° paper and print gloss, while PPS roughness was the worst.

Ink film coat weight was measured using an internal tracer method. Commercial toluene based gravure inks were marked with the tracer, which can be detected analytically and used to calculate ink film coat weight. The ink film coat weight versus relative print density data was plotted and curve fitting was performed

using six previous proposed models. The models that were used to fit laboratory results were also found useful for pilot plant press results. Oittinen model and Calabro-Savagnone model fitted the experimental data better than the other four models, measured by the sum of the square of residuals and their distribution around zero point. These two models were used to study ink mileage characteristics. Permeability and pore size were found to have more effects on regression coefficients derived from curve fitting than roughness. Ink requirement of black ink is much less than those of cyan and magenta inks. Magenta ink had higher ink mileage than cyan ink except at very low coat weight.

UMI Number: 3234892

INFORMATION TO USERS

The quality of this reproduction is dependent upon the quality of the copy submitted. Broken or indistinct print, colored or poor quality illustrations and photographs, print bleed-through, substandard margins, and improper alignment can adversely affect reproduction.

In the unlikely event that the author did not send a complete manuscript and there are missing pages, these will be noted. Also, if unauthorized copyright material had to be removed, a note will indicate the deletion.

UMI[®]

UMI Microform 3234892

Copyright 2006 by ProQuest Information and Learning Company.

All rights reserved. This microform edition is protected against unauthorized copying under Title 17, United States Code.

ProQuest Information and Learning Company
300 North Zeeb Road
P.O. Box 1346
Ann Arbor, MI 48106-1346

Copyright by
Renmei Xu
2006

ACKNOWLEDGMENTS

First, I would like to thank Dr. Paul D. Fleming III, my advisor and mentor, who has opened my mind since I entered this totally new paper and imaging world in 2003. His enthusiasm inspired me to pursue the subject. The work contained in this dissertation could not be done without him.

I also want to thank the members of my dissertation committee, Dr. Alexandra Pekarovicova, Dr. Margaret K. Joyce, and Dr. Valery N. Bliznyuk, for taking the time to review my work. I would particularly like to thank Dr. Pekarovicova for helping me with the printing trials and for all the countless discussions that solved the problems along the way.

The last and most important person is my husband, Weijiang. There is no word that can describe how grateful I am, so all I can do is to give him the same support he has given to me all these years.

Renmei Xu

TABLE OF CONTENTS

ACKNOWLEDGMENTS	ii
LIST OF TABLES	vi
LIST OF FIGURES	viii
CHAPTER	
I. INTRODUCTION	1
II. LITERATURE REVIEW	2
Printing Technologies.....	2
Future of Printing Technologies	2
Digital Printing	3
Gravure Printing.....	8
Gloss.....	10
Basic Optical Theories	10
Gloss and Microgloss Uniformity.....	12
Relationship between Gloss and Surface Topography.....	17
Factors Affecting Print Gloss.....	23
Ink Mileage.....	31
Definition	31
Ink Film Optics	32
Ink Mileage Curve	34
Ink Film Coat Weight Measurement.....	42

Table of Contents—continued

CHAPTER	
III. EXPERIMENTAL.....	44
Substrates.....	44
Inkjet Printing	44
Gravure Printing Trial One	44
Gravure Printing Trial Two	44
Paper Physical Properties	45
Roughness	45
Air Permeability.....	46
Pore Size Distribution	46
Printing Processes.....	47
Inkjet Printing	47
Gravure Printing Trial One	47
Gravure Printing Trial Two	48
Paper and Print Gloss	49
Gravure Ink Mileage.....	49
Gravure Printing Trial One	49
Gravure Printing Trial Two	50
IV. RESULTS AND DISCUSSION.....	51
Inkjet Printing.....	51
AFM Images of Paper Topography	51
Relationships between Roughness and Paper Gloss	52

Table of Contents—continued

CHAPTER		
	Relationships between Roughness and Print Gloss	54
	AFM Images of Ink Film Topography.....	58
	Ink Film Thickness	59
	Gravure Printing Trial One.....	60
	Paper Physical Properties.....	60
	Paper and Print Gloss.....	65
	Reflection Density	68
	Ink Film Coat Weight	68
	Relationships between Paper Physical Properties and Ink Film Coat Weight.....	70
	Gravure Printing Trial Two.....	71
	Paper Physical Properties.....	71
	Paper and Print Gloss.....	72
	Ink Mileage Curves.....	73
	Effects of Paper Physical Properties on Ink Mileage Characteristics.....	78
	Comparison of Cyan and Magenta Ink Mileage Curves	84
	V. CONCLUSIONS.....	85
APPENDIX		
	Ink Mileage Curve Fitting Results.....	87
BIBLIOGRAPHY		118

LIST OF TABLES

1. Cylinder engraving information.....	48
2. Correlation coefficients between surface roughness and paper gloss.....	53
3. Correlation coefficients between paper roughness and print gloss for Photo 2200 Inkjet Printer	54
4. Correlation coefficients between paper roughness and print gloss for Pro 5000 Inkjet Printer	55
5. Correlation coefficients between paper roughness and print gloss for Pro 5500 Inkjet Printer	56
6. Surface roughness measured by different methods.....	61
7. Comparison of PPS porosity.....	62
8. Comparison of pore sizes.....	64
9. Paper and print gloss at 60°.....	65
10. Paper and print gloss at 75°.....	66
11. Correlation matrix of paper and print gloss at 60°.....	66
12. Correlation matrix of paper and print gloss at 75°.....	67
13. Ink film coat weight results.....	69
14. Correlation matrix of ink film coat weight	71
15. Paper physical properties	71
16. Paper and print gloss at 60° and 75°.....	72
17. Correlation matrix of paper and print gloss at 60°.....	73
18. Correlation matrix of paper and print gloss at 75°.....	73
19. Ink film coat weights and relative reflection densities at different tones.....	74

List of Tables—continued

20. Regression coefficients of Oittinen model.....	81
21. Regression coefficients of Calabro-Savagnone model	81
22. Correlation matrix of regression coefficients of Oittinen model	82
23. Correlation matrix of regression coefficients of Calabro-Savagnone model.....	82

LIST OF FIGURES

1. Proportion of the use of various printing technologies, based on the value of printed products sold.....	2
2. Paths of light on a perfectly smooth surface	10
3. A goniophotometric curve for a paper sample	13
4. STFI gloss-variation measurement instrument	15
5. The setup for microgloss uniformity.....	16
6. Schematic of AFM.....	19
7. Principle of the CLSM	22
8. Thin film leveling on a rough surface	25
9. Model results showing predicted profile of a 2 μm ink film on a rough substrate at time = 0 (dashed line) and after 0.2, 0.5, 1, 2, 5, 10, 20 s (the thick curve at the bottom is the substrate surface).....	26
10. Model results showing predicted profile of a 1 μm ink film on a rough substrate at time = 0 (dashed line) and after 1, 5, 10, 50, 100 s.....	26
11. Model results showing predicted profile of a 2 μm ink film on a rough substrate at time = 0 (dashed line) and after 0.01, 0.02, 0.05, 0.1 s.....	27
12. Schematic of experimental setup to record changes in printed gloss right after printing nip	28
13. Pictorial representation of gloss, roughness and refractive index.....	30
14. Major paths of light in ink and paper.....	32
15. First-surface reflection of glossy surface	34
16. First-surface reflection of matte surface	34
17. Multiple internal reflections in the ink layer.....	34

List of Figures—continued

18. Ink mileage curve.....	35
19. AFM images of topography of the inkjet papers (A: Epson Glossy, B: Epson Luster, C: Kodak Gloss, D: Kodak Satin).....	51
20. Comparisons of print gloss at 60° (left) and 75° (right) between three printers for all five papers, with dotted line indicating paper gloss value (print gloss lower than the paper gloss results in negative delta gloss)	57
21. AFM images of black ink film topography on Epson Glossy paper printed by all three printers (A: Pro 5500 Printer, B: Photo 2200 Printer, C: Pro 5000 Printer).....	59
22. Ink film thickness measurement using AFM	60
23. AFM images of sample No. 5 (left) and No. 10 (right)	61
24. Pore size distributions from mercury porosimetry curves	63
25. AFM image of LWC#4	64
26. AFM image of a black half-tone dot.....	67
27. Comparison of relative reflection density	68
28. Comparison of ink film coat weight	70
29. Curve fitting results of cyan ink film on sample 1 using Oittinen model	75
30. Sum of the square of reflection density residuals and their distributions for various models.....	78
31. Ink mileage curves of cyan ink film using Oittinen model	79
32. Ink mileage curves of magenta ink film using Oittinen model	79
33. Ink mileage curves of cyan ink film using Calabro-Savagnone model.....	80
34. Ink mileage curves of magenta ink film using Calabro-Savagnone model.....	80
35. Particle size distributions of magenta and cyan ink pigments	83
36. Cyan and magenta ink mileage curves of sample 1	84

CHAPTER I

INTRODUCTION

Print gloss is one of the most important quality properties of printed products and papermakers strive to improve the paper surface to gain higher and more even print gloss. Studies on the relation between print gloss and paper properties are consequently of high relevance for the paper industry. The primary subject of this dissertation was to study the effect of paper roughness on print gloss using atomic force microscopy, which can measure several microns and has been used recently in paper industry. Such small scale roughness is especially important in inkjet printing, due to small sizes of ink droplets and the use of non-impact technologies. Inkjet printing is growing very fast, and its market share is increasing.

After my research on inkjet papers, two great companies, OMNOVA Solutions and International Paper, provided another great opportunity to study ink mileage of gravure printing. Gravure printing is an old printing technology, but has a constant market share due to its high printing quality. However, it is always a goal for printers to achieve the same print quality with less consumption of printing inks. Compared to offset printing, there has been much less ink mileage research done in gravure printing because of the difficulty of measuring the ink film coat weight. Fortunately, a new internal tracer method was introduced recently, which might shed light on the study of gravure ink mileage characteristics.

CHAPTER II

LITERATURE REVIEW

Printing Technologies

Future of Printing Technologies

Most of the research on printing is focused on offset lithography, because it is the dominant method of printing in commercial use today. However, the main printing technologies have corresponding shares in the market, and it is of interest to estimate how their use for the production of printed products will develop in the future. Figure 1 shows an estimate of the extent to which the different printing technologies are used for the production of print media vs. the value of the printed products sold to the end user (Kipphan, 2001).

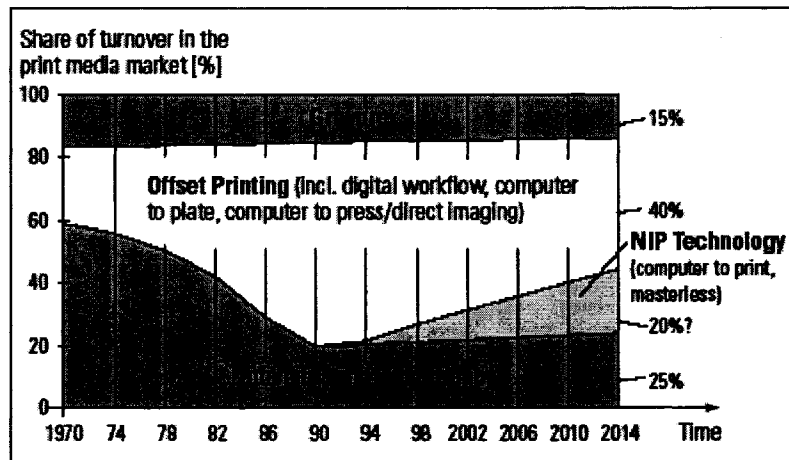


Figure 1. Proportion of the use of various printing technologies, based on the value of printed products sold (Kipphan, 2001).

It can be seen that gravure printing has a constant market share due to its high printing quality. However, this share is comparatively low, since this method is more economical with longer print runs, due to the high costs for producing the gravure cylinders.

For a long time, offset printing experienced an increasing share in the market at the expense of letterpress printing. This was a result of cost-effective platemaking, increased use of automation technology, a considerable reduction of makeready times, and printing at maximum quality level. Due to developments made in flexo printing, which led to a distinct increase in printing quality, and with the growing use of flexo printing in package printing, relief (letterpress and flexography) printing saw a slight increase.

Offset printing, in particular in the field of sheet-fed printing, is losing market shares to digital printing systems based on non-impact printing (NIP) technologies, such as laser printing, inkjet printing, etc. The spread of the NIP technologies results from their advantages when printing short or very short print run lengths and the possibility of new production strategies, such as print on demand, book on demand, and personalization, as well as improvements in printing quality and productivity (Kipphan, 2001).

Digital Printing

Digital Printing Revolution

The digital printing revolution started when rock musician Graham Nash wanted to have an exhibition of his photography collection and found out that he had no way to make the exhibition prints from the digital images he was working with on his Macintosh computer (Johnson, 2005). So he put together a team of experts in

various fields, including an art publicist, a sales representative, a computer wizard, and a silkscreen printer. They focused their efforts on something called an IRIS printer, which was used in the printing and graphic arts industries. The world's first series of all-digitally printed, photographic fine art were brought in front of the public at the New York gallery show on April 24, 1990.

The first photorealistic desktop digital printer didn't come onto the scene until Epson introduced their Stylus Color inkjet printer in 1994. The quality wasn't perfect, but it was the first of a long line of printers that could be purchased by anyone and that could produce photo prints in the comfort of the home. After a decade, there are many different models of digital printers manufactured by Epson, HP, Kodak, Xerox, etc., from high quality photo printers to copy machines, from wide format to 4 by 6 photo size, from high speed commercial printers to desktop ones for homes and offices.

Today, there are hundreds of thousands of individual "image-makers," photographers, and artists, from amateurs to pros, plus many more regular consumers, moms and dads, and scrapbookers who are able to print high-quality images in their own studios, homes, and offices. No longer constrained by the inconvenience and high costs of traditional printing methods, the production of photographic prints has been put in the hands of the people themselves.

Digital Printing and Traditional Printing

What is digital printing? Digital means using numbers to represent something, and that's exactly what a computer does. A normal image is converted into numerical data (a long string of ones and zeros) that describe or quantify each sample point or "pixel" (short for picture element, the basic unit of image information) in terms of

certain attributes such as color and intensity. This data can be stored, manipulated, and ultimately transformed with digital printing technologies back into a normally viewed image (Johnson, 2005).

Traditional (analog) printing, such as lithographic printing, flexographic printing, and gravure printing, is a mechanical process that uses a physical master or “matrix” for making repeatable prints. Commercial and even traditional fine-art printing presses use pressure or impact to transfer the image from a carrier, plate and blanket (in litho), flexible plate (in flexo), or cylinder (in gravure) – the matrix – to the receiving paper. Similarly, with old-style photography, the negative or a transparency is the matrix through which light travels to expose the print.

However, digital printing is different. There is no pressure or impact, which is why digital printing is also called non-impact printing (NIP). There is also no physical matrix. The matrix now sits in the computer in the form of digital data that can be converted repeatedly, with or without any variation, into a print by any image-maker who either does his own printing using a desktop printer or uses an outside printing service, lab, or retailer.

Advantages of Digital Printing

Digital printing is less costly for short runs when compared with traditional printing. It's fully digital from creation to printing, which means that it uses no film, no imagesetters, no plates, and no photo-chemicals. Once the initial setup and proofing stage is complete, digital prints can be made on an as-needed basis, so digital printing is true “print on demand”. By contrast, conventional non-photographic, print production methods require the entire print run to be produced all at once.

Digital printing is consistent. Because digital source files are stored on

computer hard disks, or onto other digital storage media, they can be reused over time to produce identical results, assuming the media, inks, and hardware/software have not changed. Related to the above, digital images take little physical room when stored on disk. Digital files can be long-lasting if the digital data remain intact and there is a way to read them.

Size is not much of an issue with digital, especially with wide-format inkjet printers, which come in four-, five-, and even six-foot-wide models. Printing on roll paper, the length of an inkjet image is only limited by the printer's software. For even larger prints, images can be "tiled" and assembled in pieces. And, of course, the same digital source file can be cropped, blown up, or shrunk, and printed in many sizes.

Digital printing provides freedom and flexibility. With desktop printing equipment, almost anyone has the freedom to print what he wants, when he wants. Using the same image file, image-makers can experiment with different sizes, cropping, or unconventional media. New images, variations, or new editions can be sampled and tested at minimal cost and with little risk, one at a time.

One final advantage of inkjet printing is that the NIP technology makes it possible to print with inkjet on almost any surface, regardless of surface texture, shape, or pressure resistance. Inkjet printing can place an image on a plastic container or bubble package as easily and as quickly as it can on paper, a textured surface such as sandpaper, or a curved surface such as a pill or capsule (Adams et al., 1996).

Inkjet Printing

The most common non-impact technology used for digital printing system is inkjet. The inkjet process is a computer to print technology in which ink is sprayed from nozzles, which means that no image carrier is needed. Imaging is done directly

onto the substrate. The data of the digital print job is transferred directly to control the imaging unit, which transfers the ink to the paper via nozzles (Kipphan, 2001).

There are two types of these processes, continuous inkjet and drop on demand inkjet. In the continuous inkjet process, only part of the continuously generated flow of small ink drops is directed onto the paper during printing in accordance with the image. In drop on demand inkjet processes drops of ink are only generated if the information to be printed requires them. Drop on demand inkjet processes can be classified into thermal inkjet, piezo inkjet, and electrostatic inkjet, according to the way that the individual ink drop is generated.

The multicolor inkjet technology is especially growing for the home and office markets (Williams, 2001). A large and growing consumer market for inkjet has become noticed in packaging, publication, and specialty areas. There are different inkjet systems for various, wide-spread applications. High-speed printing systems print predominantly with one color or with an additional spot color, while systems for proof purposes require high quality printing. Small-format multicolor inkjet printers are most widely used in office applications, desk-top publishing, and for private use. Inkjet systems for large-format printing, such as posters and billboards, are becoming more widely used. Inkjet systems are also used in connection with digital photography for printing high quality, small-format color images (Kipphan, 2001).

The quality of inkjet printing is influenced by the printers in use, as well as by the physical-chemical properties of printing ink and print substrate. To mention a few, these interactions are influenced by interfacial charges, wettability, and adsorption phenomena (Lee et al., 2004 and 2005a, b). An inkjet recording sheet comprises a support such as paper, at least one ink-receiving layer on the support, and a gloss-providing layer formed on the ink-receiving layer. The ink-receiving layer consists

essentially of a pigment and a binder. The gloss-providing layer consists of a pigment and a synthetic polymer formed from a latex or water soluble polymer as a binder.

Gravure Printing

Overview of Gravure Printing

Gravure printing is a very old printing process that dates back to early fifteenth century. Today, gravure printing accounts for a market share of 10-15% in industrialized nations. This percentage share has remained almost constant for two decades, with a slight downward tendency.

The distinctive feature of gravure printing technology is the fact that the image elements are engraved into the surface of the cylinder. The non-image areas are at a constant, original level. Prior to printing, the entire printing plate is inked and flooded with ink. Ink is removed from the non-image areas by a wiper or blade before printing, so that ink remains only in the cells. The ink is transferred from the cells to the printing substrate by a high printing pressure and the adhesive forces between printing substrate and ink (Kipphan, 2001).

Gravure printing is a very good illustration printing technology, achieving very high image quality. When variable-depth and electronically engraved gravure printing cylinders are used, the cells take up different amounts of ink. The different ink layer thickness produced on the substrate resulting from this corresponds to the tonal gradations of the original. The image effect is improved even more by the fact that, after the ink has been transferred, the liquid ink flows out somewhat in the areas of deeper shades on the substrate, as a result of which no sharply defined screen dots are produced and the cell walls of the printing cylinder are not visible.

The simplicity of the printing principle is, however, offset against the problem

of a labor-intensive and costly manufacture of the gravure cylinder. Hence, gravure printing is principally used for very long print runs. Typical gravure printed products are high-circulation, high-quality printed products such as periodicals, magazines, mail-order catalogs, plastic films, metal foils, transparent films, security papers, stamps, bank notes, etc.

Properties Required for Gravure Substrates

Smoothness or Roughness. Surface smoothness is the single most important property for fine gravure reproduction (Rutherford, 1991). A smooth paper is one whose surface is free of irregularities, so to measure smoothness we actually measure the extent of those irregularities, or roughness. Roughness is the deviation of a surface from an ideal plane. Paper roughness has two aspects: the roughness of the “free surface” versus the roughness of the surface under pressure. Since some pressure is applied to the paper substrate during gravure printing, a measurement of the roughness of the surface under pressure is of greater importance, which provides a means to evaluate compressibility.

Receptivity. Receptivity of the substrate is a measure of the surface’s ability to accept the gravure ink dot, and the quality of absorbency. If a coated paper surface is too dense because of surface sizing, coating and calendering, the ink will not transfer from the gravure cell quickly and fully, no matter how smooth the paper is.

Ink Holdout and Porosity. Although the paper must be receptive to ink, it must also possess the characteristics of holdout, retaining the ink pigment on the surface of the paper for a sharp image with the highest possible reflection density. Ink holdout is dependent upon the substrate’s porosity, and, to a lesser extent, upon roughness and

formation. Porosity must be sufficiently high for ink vehicles to be readily absorbed, but not so high that the ink dots spread or “feather” – or, worse yet, penetrate to the other side of the sheet. Ink holdout describes the extent to which a printed paper’s surface resists penetration by the vehicle and/or pigment of a given ink formulation (Rutherford, 1991).

Gloss

Gloss is an important optical property for either unprinted or printed paper since it determines the perceived quality of the finished products. It has been the subject of many studies for decades. The visual appearance of any surface, including glossiness, depends on how it reflects light. Therefore, it is important to understand some basic optical theories.

Basic Optical Theories

Perfectly Smooth Surfaces

The optical effects taking place on perfectly smooth surfaces are represented in Figure 2.

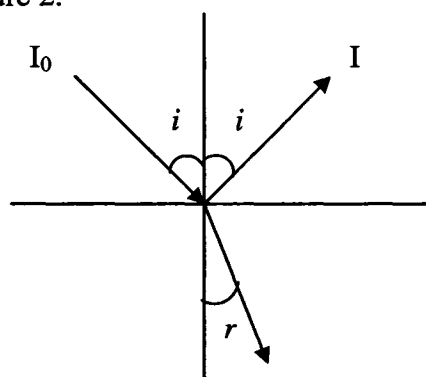


Figure 2. Paths of light on a perfectly smooth surface.

When light passes from one medium to another of different refractive index, some of it is reflected, according to the Fresnel's law (Harrison, 1945)

$$I/I_0 = \frac{1}{2} [\sin(i-r)/\sin(i+r)]^2 + \frac{1}{2} [\tan(i-r)/\tan(i+r)]^2 \quad (1)$$

where I and I_0 are the intensities of the reflected and the incident light, and i and r are the angles of incidence and refraction. These angles are related according to the formula

$$\sin i / \sin r = \mu \quad (2)$$

where μ is the ratio of the refractive index of the medium on which light is incident to that of the medium from which it comes. The refractive index of air is close to 1, therefore, in the case that the incident light comes from air, equation (2) can be expressed as

$$\sin i / \sin r = n \quad (3)$$

where n is the refractive index of the medium on which light is incident. With an angle of incidence of 45° , equation (2) can be written as

$$I/I_0 = [(n-1)/(n+1)]^2 \quad (4)$$

If n is 1.5, about 4% of the incident light is reflected at the surface.

Rough Surfaces

Rough surfaces reflect the incident light diffusely (that is, in all directions). Chinmayanandam (1919) hypothesized that the reflecting elements of an optically rough surface are distributed according to the probability law and derived the expression

$$I = \exp[(-8\pi^2 \cos^2 R)/\alpha\lambda^2] \quad (5)$$

where R is the angle of viewing and α is a constant having dimensions of length^{-2} . For moderate angles of incidence (up to 54°), it shows good agreement with practice. For

higher angles, Chinmayanandam fell back on an empirical formula, which has been found to give good agreement with observed value

$$I = \exp[-(a \tan^2 R + b \cos^2 R / \lambda^2)] + [1 - \exp(-a \tan^2 R)] \exp[-(c \cos R + d \cos^2 R) / \lambda] \quad (6)$$

Gloss and Microgloss Uniformity

Definition of Gloss

According to the terminology of appearance, gloss is the

“...angular selectivity of reflectance, involving surface-reflected light, responsible for the degree to which reflected highlights or images of objects may be seen as superimposed on a surface...” (ASTM, 1998)

This definition excludes that gloss is a psychophysical phenomenon that depends on the perception of a variety of reflection effects. Hunter (1952) studied different gloss measurement instrument, and attempted to characterize gloss, which led to the conclusion that at least six different visual criteria exist for ranking gloss. Six types of gloss have been measured: specular gloss, sheen gloss, contrast gloss, absence-of-bloom gloss, distinctness-of-reflected image gloss, and absence-of-surface texture gloss. This demonstrates the complexity of gloss measurement.

In goniophotometric measurements, the directions of the incident and reflected light can vary independently (Niskanen, 1998). It differs from a conventional gloss meter in that it enables measurement of the intensity of reflected light as a function of angular position, either side of the specular angle. The resulting curve in Figure 3, which is measured at incident angle of 45°, gives comprehensive information about gloss.

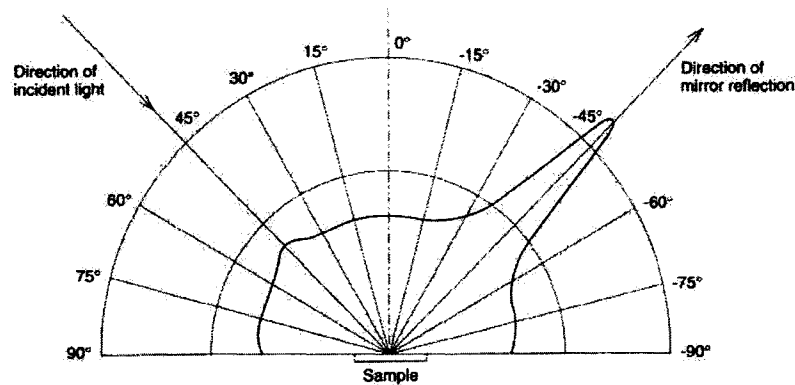


Figure 3. A goniophotometric curve for a paper sample (Judd and Wyszecki, 1975).

In the paper industry, the facet of gloss most frequently measured is specular reflectance. It is the intensity ratio of specularly reflected light to the incident light. The specular reflection occurs in the surface layer of paper because light that enters the paper undergoes many reflections and loses directionality.

Specular Gloss

Specular gloss is more exactly defined as the ratio of luminous flux reflected by the test surface into a specified angle to luminous flux from the standard reflecting surface. The specular reflection equation for rough surfaces like paper is as follows (Chinmayanandam, 1919)

$$I/I_0 = f(n, i) \exp[-(4\pi\sigma\cos i/\lambda)^2] \quad (7)$$

where $f(n, i)$ is the Fresnel coefficient of specular reflection as a function of refractive index n and angle of incident light i , σ is standard deviation of the surface roughness, and λ is the wavelength of incident light.

From Equation (7), the specular gloss is determined by the incident angle of light, the wavelength of light, refractive index and surface roughness. Instruments for

gloss measurement have a fixed angle for the incident and the reflected light direction. TAPPI (1992) standard defines the gloss as the specular reflectance of 75° incident light at $\lambda=0.55 \mu\text{m}$. Therefore, TAPPI 75° gloss is dependent on refractive index and surface roughness.

Small-Scale Gloss (Microgloss) Variation

Gloss is a psychophysical phenomenon. It has a complex nature. How the human visual system perceives gloss is still not well understood. It is true that there are aspects of the human perception that can not be quantified, but researchers are developing new techniques to allow human evaluation made more easily. Gloss uniformity is of high interest.

MacGregor and Johansson (1990) pointed out that a number of important paper manufacturing problems occur in a size class of “submillimeter” region (about 1 μm to 1 mm). The conventional gloss instruments, such as a glossmeter, measure average specular reflection intensity at larger dimensions, so applying the same techniques to submillimeter dimensions is not feasible. Image analysis was therefore considered because of its potential for good resolution and its automated operation. It has been used to measure mass variation in base paper and also coating mass variation. To acquire gloss images, they used a charge coupled device (CCD) camera coupled to an image analyzer, as shown in Figure 4. This camera, with an acceptable angle of 1.5° and a 20° incidence angle, captures a 10 mm x 10 mm gloss image of the paper surface. The gloss image pixel size of about 20 μm is analogous to having ¼ million miniature gloss meters instantly measuring the specular reflection intensity from all parts of the paper surface. The relatively low 20° incidence angle is compatible with the way human view and judge prints for gloss uniformity because

low incidence angle creates greater gloss contrast sensitivity.



Figure 4. STFI gloss-variation measurement instrument (Béland and Bennett, 2000).

Another advantage of this equipment is that it can measure and compare features in images sensed in different ways, but acquired from the same reference area, which include low-angle incident light image, overhead illumination image, transmitted light image, soft X-ray mass image, Beta-ray mass image, gloss illumination image, partial gloss illumination image, etc. (MacGregor and Johansson, 1990). This group of differently sensed images, all from the same reference paper, are called “registered image stack”.

The octave band passing method developed by Johansson (1983) is used to analyze the gloss image. The gloss image is spatially band passed and the coefficient of variation of the intensity in each of the octave bands is calculated, separating the contribution from different feature sizes. Research work by MacGregor et al. (1994) showed that the coefficient of variation over the three octave bands covering wavelengths from 0.41 to 3.3 mm (feature sizes of 0.2 to 1.6 mm) agreed best with the subjective gloss uniformity ranking of the samples. Béland et al. (2000) found the

best correlation between rating and the band covering 3.3 to 6.6 mm (feature sizes of 1.6 to 3.2 mm) due to longer average viewing distance, and concluded that larger viewing distances correlate better with larger features and smaller features are better seen at smaller viewing distances.

Bernard et al. (2004) used a similar setup to measure microgloss, as shown in Figure 5. The setup is composed of three elements: a collimated light source, a digital camera, and an image analyzer. The illumination angle is 23° , and the camera is also placed at 23° in the specular direction. A length assembly mounted on the lamp housing collimates the light to ensure that the output light beam is parallel. Each pixel on the gloss map is of size $16 \mu\text{m} \times 16 \mu\text{m}$.

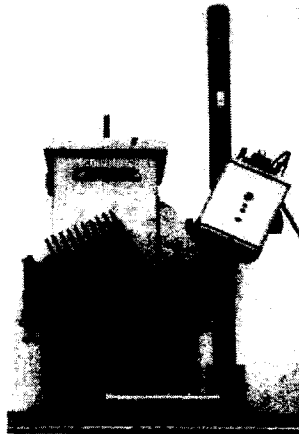


Figure 5. The setup for microgloss uniformity (Bernard et al., 2004).

The coefficient of variation of the microgloss was found to be higher for most of the samples, when compared with the coefficient of variation of the 75° standard TAPPI gloss. However, no comparison with ranking was done, so it is difficult to get any conclusion.

Relationship between Gloss and Surface Topography

Roughness

As discussed before, gloss depends on the refractive index and surface roughness. When comparing similar substrates, the refractive indices are similar, so the differences in gloss are caused largely by surface roughness.

The relation between gloss and surface topography has been outlined by Gate et al. (1973) and Oittinen (1980). Oittinen (1980) divided printed surface roughness into macroscale and microscale components. Although there is no complete agreement on the boundary between these components, the macroscale component usually stems from poor fiber dispersion, ionic destabilization or flocculation, roughness of base paper, or insufficient coating or calendaring. It consists of features larger than 10 μm . The microscale component usually stems from the ink, coating, or both, due to pigment particle size distribution, particle shape, binder type, film shrinkage, drying condition, coating holdout, and coating weight. It consists of features considerably smaller than 10 μm . As the feature size falls below half the wavelength of visible light, 0.2-0.4 μm , its individual effect on gloss diminishes.

Macroroughness. From the classical roughness measuring methods, the Parker Print-Surf (PPS) method has been widely used in the paper and printing industries because of the possibility of measuring roughness at different pressures, 490-980-1960 kPa, to mimic the conditions at a printing nip. The PPS tester uses a contact air-leak principle, measuring airflow between substrate in a 51 μm wide ring. It recalculates the airflow into a mean gap between the surface and the flat circular land pressed against it (TAPPI, 1999, and ISO, 1992).

There are some other roughness test methods utilizing air-leak principle, such

as Bendtsen (ISO, 1990), Sheffield (ISO, 2005), etc. The measurement obtained from all air-leak instruments is called macroroughness. One key disadvantage is that these instruments lack the sensitivity to measure on a scale small enough to be relevant to printing (Veenstra, 2004). For example, a half-tone dot can range from 20 to 60 μm in diameter. Various air-leak measurements can span widths ranging from 51 to 13,500 μm . Therefore, the need for measuring microroughness is growing.

Some new methods for measuring macroroughness are the stylus profilometer and laser profilometer. A stylus profilometer uses a preloaded fine cone-shaped stylus dragged across the surface. The vertical movement of the stylus compresses a piezoelectric element, which generates a fairly linear voltage response. The stylus profilometer is widely used to characterize the surface roughness of metals. When it is applied to paper, the stylus traces could be observed depending on the conditions of stylus radius and load, and the surface hardness of paper. It was found that careful selection of stylus radius and load conditions can ensure no permanent damage of paper surface (Enomae and Lepoutre, 1995). The newer laser profilometer uses a monochromatic laser light source (Zhou and Xie, 2003). It is a non-contact method so there is no damage to the paper surface.

Other reported non-contact methods include confocal laser scanning microscopy (CLSM) (Béland and Bennett, 2000), 3D sheet analyzer (Novak and Muck, 2004), and interferometric microscopy (Moreau-Tabiche, 2004). The roughness is calculated from a 3D topographic image of paper surface obtained through optical methods.

Microroughness. The development of microscopic techniques allows us to observe features in much higher resolutions than before. Scanning electron microscopy (SEM) has been widely used to study paper topography, both the coating

layer and the printed ink surface (Donigian et al., 1997, Preston et al., 2001, Dalton et al., 2002, Chinga and Helle, 2003). However, SEM has limited depth resolution, which does not enable the detection of features much less than 1 μm , especially in the height direction. In addition, the high voltage required for higher magnifications with high resolution may cause damage to the paper surface.

A newer technology is atomic force microscopy (AFM). AFM was invented by Binnig, and introduced by Binnig, Quate, and Gerber (1986), as an offshoot from the scanning tunneling microscope (STM). Since then, AFM has rapidly developed into a powerful and invaluable surface analysis technique on both micro- and nanoscale. The schematic of AFM is shown in Figure 6. The sample surface is scanned with a sharp tip mounted on a cantilever. The small deflections of the cantilever are measured using a focused laser beam, which is reflected off the cantilever to a photodiode detector. The x,y,z piezoelectric scanner located under the sample provides the precise movement of the sample. The variation in voltage signals from the photodiode detector as a function of probe position is converted into a 3D image by image processing system (Morita et al., 2002).

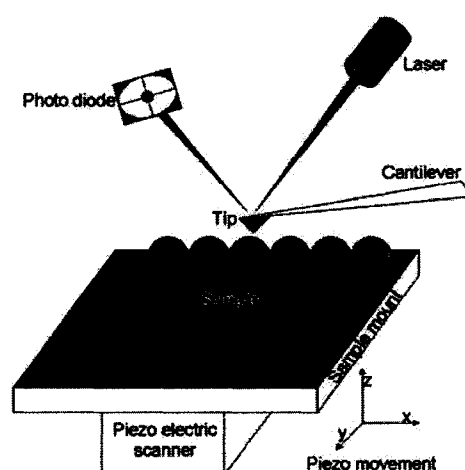


Figure 6. Schematic of AFM (Morita et al., 2002).

The tapping mode in AFM was developed especially for studying soft and fragile samples. Instead of dragging the tip across the surface in the conventional contact mode, the tapping mode is done by oscillating the cantilever with a frequency of few hundred kilohertz near its resonance. The oscillation and the force on the sample are maintained constant by a feedback loop. The tip is brought close to the surface until it begins to touch the surface by tapping it gently. While scanning the surface, the amplitude alternates depending on the topography. No lateral, shear, or friction force is applied to the sample and no sticking occurs, since the tip contacts the surface briefly during each oscillations.

AFM has been used to study paper and print topography recently (Béland and Bennett, 2000, Dalton et al., 2002, Ström et al., 2003, and Myshkin et al., 2003). Béland and Bennett (2000) combined the gloss imaging equipment with the CLSM and AFM. The AFM was used to image and measure different areas within each CLSM image for local roughness. Their results showed that the AFM measurements qualitatively supported the hypothesis that some areas on coated and printed paper samples are locally smooth but tilted, reflecting the light out of the nominal specular direction. Some areas were found to be locally flat but optically rough, causing the light to scatter diffusely and produce a local low-gloss area. They suggest that both local tilt and local roughness are important in determining how light will scatter from a given facet on a surface.

Ström et al. (2003) referred to microroughness as the root-mean-square (rms) value obtained on a $5\ \mu\text{m} \times 5\ \mu\text{m}$ AFM surface image, and “sub-macro” roughness as the rms value obtained on a $100\ \mu\text{m} \times 100\ \mu\text{m}$ image. The macroroughness was also measured by a profilometer, and was given at different wavelength intervals by Fast Fourier Transformation (FFT). The macroroughness of the coating was found to be

one of the most important factors for print gloss on heavily inked area. Features in a size of 50 to 250 μm appeared to be most detrimental. The microroughness of the coating was important in areas with low ink amounts and in particular when the coating contains coarse pigments.

Facet Angle

Although it is well accepted that gloss and roughness are to be inversely related, it has proven difficult to correlate relative gloss with quantitative determinations of specific geometric characteristics of the surface. Several groups (Lipshitz et al., 1990, MacGregor et al., 1994, and Béland et al., 2000) studying the relationship between gloss and surface profile have concluded that average facet angle is a more fundamental topographic parameter related to gloss than a generalized measures of roughness. Lipshitz et al. (1990) developed a new system to measure the heights z of closely spaced points on a surface as a function of their x,y coordinates in a reference plane. The principal is that the focusing of a narrow beam of light on a small region of the surface, inclined at a specific angle, results in a reflected diffuse image of the surface profile. Statistical distributions of a number of topographic parameters including height density, relative area, and the regional inclinations across each surface (i.e., facet angle) were determined. It was found that changes in the average facet angle and breadths of the facet angle distributions correlated with change in gloss. It was also found that measures of average roughness did not correlate with the loss of gloss when the surfaces were close in roughness.

MacGregor et al. (1994) suggested that an area that appears glossy most likely is optically smooth and lies essentially parallel to the specular reflection plane. An area that doesn't appear glossy may also be smooth but tilted too much, thus not

producing specular reflection at the viewing angle, but it will be glossy at some other angle of observation (tiled/high-gloss failure type). It could also be a macroscopically planar facet, laying parallel to the specular reflection plane, but be optically rough and scatters the light in many directions rather than specularly reflecting it (flat/low-gloss failure type). They investigated the facet angle-gloss relationship by combining digital gloss imaging with confocal laser scanning microscopy (CLSM). The CLSM, as shown in Figure 7, is a sophisticated height measuring device, and provides a high-resolution 3-dimensional topographical image of the paper surface.

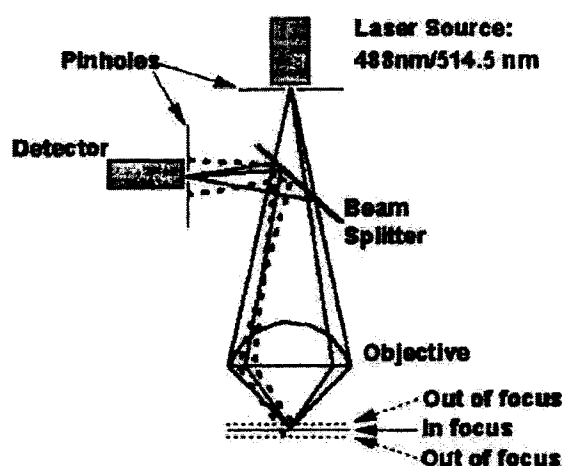


Figure 7. Principle of the CLSM (Béland and Bennett, 2000).

A direct comparison of CLSM image with the gloss image made of the same area showed all places where the facet angle-gloss hypothesis succeeded and failed. A 78% match between the gloss and facet angle images was found, and the Chi-squared significance test established a statistically significant dependence between gloss and facet angle. About half of the 22% unmatched area was due to the “flat/low-gloss” failure type. A “flat” area that had less than 1.5° slope could appear non-glossy if that area was rough on the micro scale (optically rough). However, none of the

measurement mentioned in the previous section addressed microscale roughness of near 1 μm or below.

Factors Affecting Print Gloss

Print gloss is one of the most important quality properties of printed products and papermakers strive to improve the paper surface to gain higher and more even print gloss. Studies on the relation between print gloss and paper surface properties is consequently of high relevancy for the paper industry.

The above discussion about the relationship between gloss and surface topography also applies to print gloss. Because most inks have similar refractive indices, gloss is determined by the final surface roughness of the ink film, which depends on a number of characteristics such as substrate roughness, pore size, printing conditions, ink setting rate, leveling, etc. There have been some attempts to separate the effects of these different characteristics on print gloss, but a clear understanding is still lacking. As Zang and Aspler (1994) pointed out, some researchers are concerned only with the gloss of the substrate (roughness), while others are concerned with the rate of ink setting as a factor that determines print gloss.

Borchers (1958) reported that paper gloss has a greater effect on printed gloss than ink absorptivity in lithographic printing. As ink film thickness approaches zero, the printed gloss would naturally approach the paper gloss. Fetsko and Zettlemyer (1962) found that print gloss decreases with increasing paper absorbency. Zang and Aspler (1994) suggested that this contradiction may be caused by the difference in ink amount. Their study shows that offset print gloss increases with increasing substrate gloss at low ink levels, but at high ink levels, the print gloss is primarily influenced by microroughness, or gloss, of the ink film, which in turn depends on filament patterns

produced during ink splitting and on absorbency of the coating. They also suggested that high absorbency may cause low print gloss due to reduced time for the inks to flow and level on the coating surface before setting.

Donigian et al. (1997) also studied the coating pore structure and offset print gloss. Their finding is that the coating absorbency profoundly influences printed gloss. In their experiments with fine to very fine pigments, large changes in coating absorbency completely overwhelmed the changes in paper gloss. Very fine coating particles produce high pigment surface area and very fine coating pores that can greatly reduce printed gloss. Fewer pores and larger pores led to higher print gloss. They found that printed gloss also correlated strongly with the print and ink (P&I) slope obtained by Paper and Ink Stability Test (Sandreuter, 1994), which measures the rate of the increase of ink tack after application to a paper surface and the rate of tack increase is a common measure of ink solvent removal by the paper. Lower P&I slope, i.e. slower ink tack increase after printing, corresponds to higher print gloss. They proposed hypothetical mechanisms for print gloss reduction that rapid solvent removal either prevents the ink film split pattern from leveling or causes the ink film to shrink forcing the coated surface to buckle in response.

Glatter and Bousfield (1997) proposed a model for leveling of a fluid layer in response to surface-tension forces on a level surface. It is assumed that ink is a Newtonian fluid, there is no drying or absorption of ink solvents, and the ink acts as a continuous fluid. Figure 8 shows the initial film profile and substrate roughness. h_s is the substrate profile; h is the ink film profile; h_0 is the ink film thickness; λ is the wavelength of the substrate roughness.

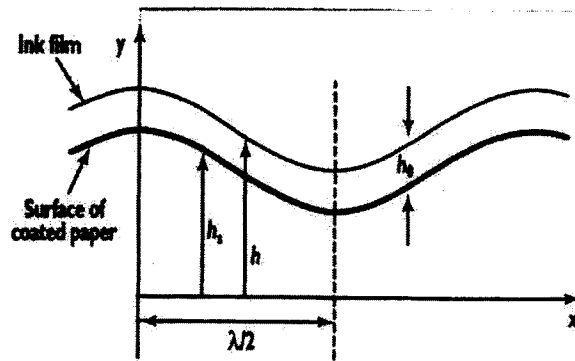


Figure 8. Thin film leveling on a rough surface (Glatter and Bousfield, 1997).

The working equation of the model is

$$\partial h / \partial t = (-\gamma / 3\mu) \{ [(\partial^4 h / \partial x^4)(h - h_s)^3] + [(3\partial^3 h / \partial x^3)(h - h_s)^2(\partial h / \partial x)] \} \quad (8)$$

where γ is surface tension of the ink, and μ is ink viscosity.

Linear analysis of equation (8) gives

$$h = h_0 + [\varepsilon \cos(2\pi x / \lambda) \exp(-\alpha t)] \quad (9)$$

where the exponent factor, α , is

$$\alpha = (16/3)\gamma\pi^4(h_0^3/\mu\lambda^4) \quad (10)$$

This shows that the leveling rate should be of an exponential form, with the rate constant proportional to the surface tension divided by viscosity. The leveling rate also depends on the third power of film thickness and the fourth power of the wavelength.

Figure 9 shows the predicted ink film profiles using the proposed model for a substrate with roughness amplitude of $1.5 \mu\text{m}$ and roughness wavelength of $50 \mu\text{m}$. The ink viscosity and surface tensions are $50 \text{ Pa}\cdot\text{s}$ and 40 mN/m , respectively. The final ink profile is nearly horizontal after 20 s of leveling. When the curvatures of the film are high, there is rapid leveling. As the film becomes uniform, the leveling rate slows down.

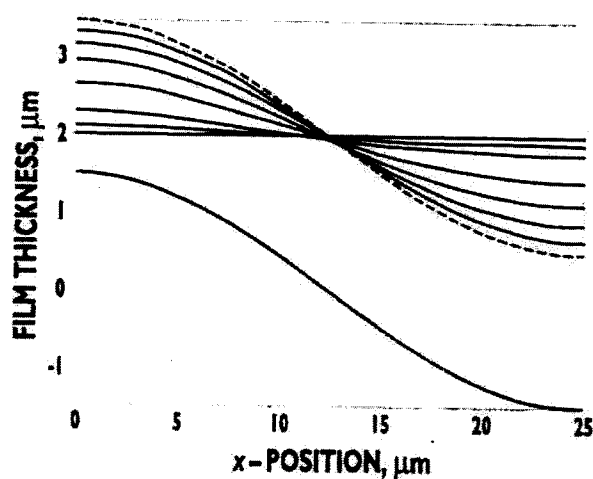


Figure 9. Model results showing predicted profile of a 2 μm ink film on a rough substrate at time = 0 (dashed line) and after 0.2, 0.5, 1, 2, 5, 10, 20 s (the thick curve at the bottom is the substrate surface) (Glatter and Bousfield, 1997).

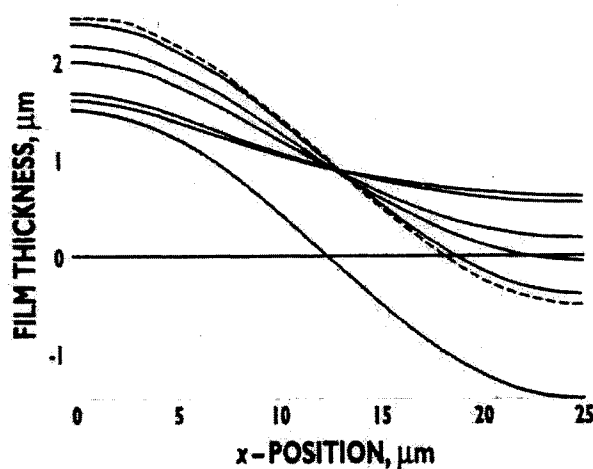


Figure 10. Model results showing predicted profile of a 1 μm ink film on a rough substrate at time = 0 (dashed line) and after 1, 5, 10, 50, 100 s (Glatter and Bousfield, 1997).

The results predicted by using this model also show that the thicker film levels more rapidly. However, at low film thickness, the film thinning rate slows more than expected. This behavior is caused by surface roughness. The film can never become

uniform because there is not enough ink to fill the void. This behavior is illustrated in Figure 10. Ink leveling is inhibited by the thin layer formed on the high region of the substrate.

One important point is that the leveling rate exponential factor is a function of wavelength to the fourth power. This indicates that film nonuniformities that occur on a short-wavelength scale will level quickly. Defects with long wavelengths will take much more time to level. Thus, it is critical to avoid defects of long wavelengths during the printing process. Figure 11 shows the short-wavelength disturbances quickly level. This demonstrates the importance of disturbance wavelength on leveling rate.

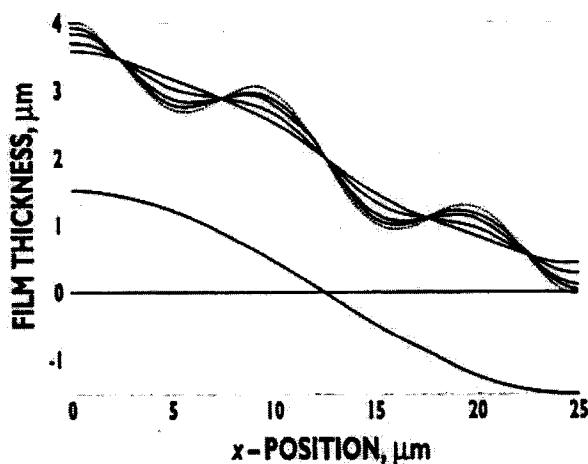


Figure 11. Model results showing predicted profile of a 2 μm ink film on a rough substrate at time = 0 (dashed line) and after 0.01, 0.02, 0.05, 0.1 s (Glatter and Bousfield, 1997).

Even though the model has a number of assumptions that are not valid, such as constant ink viscosity after printing, the model does provide a starting point for future work and accounts for the influence of different variables such as defect wavelength.

An experimental setup was used to record changes in printed gloss right after printing nip, as shown in Figure 12. A laser light source and detector are mounted at a 75° angle at the end of a laboratory print tester. The light reflects from a mirror to the sample and then back to a light detector. A video camera was also set up to view the ink film at short time.

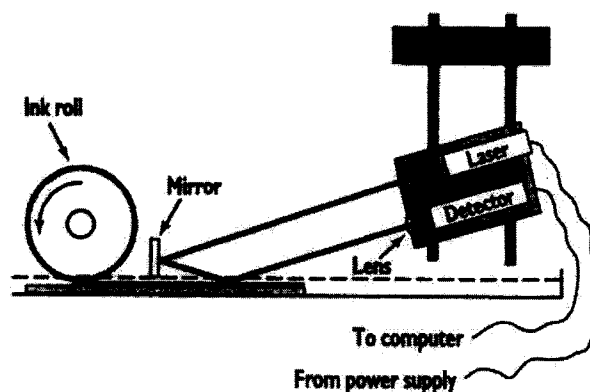


Figure 12. Schematic of experimental setup to record changes in printed gloss right after printing nip (Glatter and Bousfield, 1997).

A quick-set offset ink was used to print at different printing speeds and ink film thicknesses. The results show that print gloss generally increases in time after printing. The increase in print gloss occurs as defects in the ink layer level out in response to the effects of surface tension. The length scale of the initial defects was found to be a critical parameter in the extent of leveling achieved over time. High printing speeds and high ink film thicknesses produce many defects with a wide range of length scales. The fine-scale defects level rapidly, while the large-scale defects level slowly. This leads to a rapid increase in gloss at short times, but a lower gloss at long times, if compared with the gloss obtained at slower speeds with thinner ink films. The experimental results qualitatively agree with the prediction obtained from the proposed model.

Preston et al. (2001, 2002) pointed out that the balance between the microroughness of the coating and the pore size in the coating is essential to achieve a good offset print gloss. In this study, steep and broad particle size distribution clays were assessed over a range of binder levels and compared at constant coating strength. There is an excellent correlation between pore size, ink tack generation and print snap (difference between paper and print gloss), with larger pore size yielding slower ink setting rates, greater ink film leveling and higher print gloss. These results can be attributed to the increase in the capillary pressure or driving force for imbibition of ink vehicle into the coating with decreased pore size. However, the final print gloss is also dictated by the roughness of the coating which is not completely masked by the ink film.

Experiments carried out with different ink loadings indicated that differences in pigment types and coating structures do not affect the amount of ink transferred to the paper. However, print snap was found to be low at low ink loadings, but it increased quickly once ink loading was increased. The low print snap at low ink loadings was found to correlate with an increased refractive index of the print. For a given surface roughness, a higher refractive index should yield a higher gloss. This unexpected observation can only be explained by surface roughness. Ink pigments have a much higher refractive index than other components in the ink. If pigment particles are concentrated at the surface of the ink film, the surface must be more micro-rough, leading to lower gloss. When the ink films are thicker, there is a great proportion of ink resin surrounding the particles, so the surfaces are smoother and have a lower refractive index. This concept is illustrated in Figure 13. Capillary imbibition of ink vehicle and resin can be cited as the mechanism for this effect. SEM micrographs showed that fine pores lead to greater print roughness at low ink

loadings.

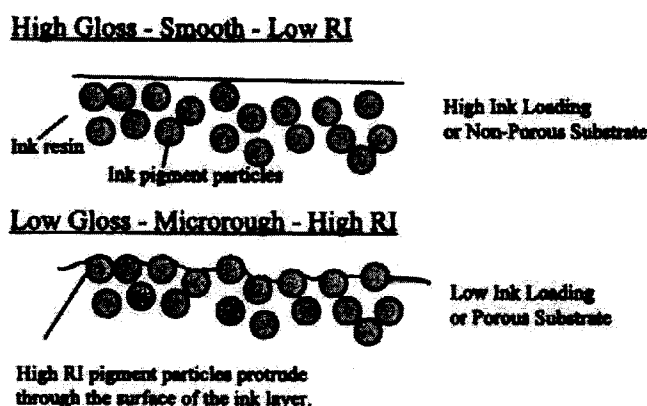


Figure 13. Pictorial representation of gloss, roughness and refractive index (Preston et al., 2002).

Further work was done by Dalton et al. (2002) using X-ray photoelectron spectroscopy (XPS) and secondary ion mass spectroscopy (SIMS) to analyze the chemical composition through an ink film printed onto kaolin coated paper. This is done by analyzing certain key atoms representing the various molecules in the ink formulation. Both XPS and SIMS showed the presence of resin at the very surface of the ink film, which was formed by cross-linking of unsaturated hydrocarbons moieties present in the ink formulation. The concentration of pigment throughout the film was approximately constant until the kaolin coating was reached, at which point the concentration fell at a rate that was determined by the roughness of the kaolin-ink interface. XPS results showed that a more microporous kaolin coating with a lower ink loading had a thinner surface resin than a higher ink loading with a less porous coating. This differing in surface resin content is in agreement with the refractive index measurements. The higher resin content appears to give a higher gloss.

Work published in this area has mainly been carried out with laboratory coated substrates, printed with laboratory printers such as IGT and Prüfbau. There are a few

significant differences between laboratory printing and full-scale offset printing. First, laboratory printing is done at low speed and fountain solution is normally not used. Second, full-scale printing applies the ink from several print units, each of which applies roughly 0.6-0.7 g ink per square meter full tone area (Ström et al., 2000). A heavily inked area consists of three to four ink layers on top of each other. Thus, the ink amount may reach 2.5-3 g/m². In laboratory printing the whole ink layer is applied in one single step. This is an important difference since leveling is affected by the thickness of the liquid film (Zang and Aspler, 1994, Glatter and Bousfield, 1997, Preston et al., 2001 and 2002).

Ström et al. (2000) studied the relations between print gloss and coating structure after full-scale sheet-fed offset printing of commercially and pilot manufactured fine papers. It was confirmed that print gloss decreases with increasing ink setting rate, as has been found in laboratory printing. The strong decrease in print gloss found at high ink amount in laboratory printing was not found in full-scale printing.

Ink Mileage

Definition

First, what is ink mileage? We all heard about gas mileage a lot. With gas price rocketing, more auto makers put high gas mileage in their advertisements to attract buyers. Gas mileage is how many miles a vehicle can run with a gallon of gas. The higher the gas mileage, the better the performance of the vehicle. The printing industry borrowed this concept. Ink mileage is defined as the number of square meters covered by a kilogram of ink to give a specific level of relative print density (Oittinen and Saarelma, 1998). The higher the ink mileage, the better the performance of the

ink. The last part of its definition is very important, because more ink is needed to get a higher print density so ink mileage is lower. It's the same as gas mileage is lower in local than on highway.

Ink mileage is a very important factor for printers because it has major effect on printing cost. Printers always want to use as little ink as possible to achieve the same printing quality. Therefore, it has been the subject of research for many years. In order to study the ink mileage behavior, it is important to understand some ink film optics first.

Ink Film Optics

In a color-reproduction process, the purpose of the ink is to absorb light of various colors selectively. For example, yellow ink absorbs blue light, and reflects red and green light, so it appears yellow. The function of the paper is to reflect the incident light diffusely. The incident light passes through the ink layer, is reflected in all directions by the paper, passes through the ink layer again, and emerges from the surface of the ink. The observer only sees that portion of it in the direction of his eyes (Figure 14). During the two passages through the ink film, some of the light is absorbed, depending on the absorption coefficient at each wavelength and on the thickness of the ink layer (Yule, 1967).

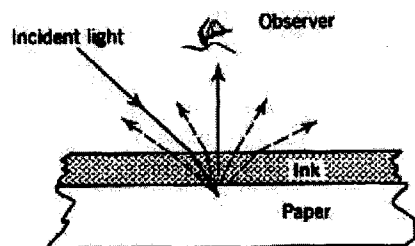


Figure 14. Major paths of light in ink and paper (Yule, 1967).

The light-absorbing ability of the ink can be evaluated by reflectance or reflection density. Reflectance R is defined as

$$R = (\text{Reflected light}) / (\text{Incident light}) \quad (11)$$

Reflection density D is defined as

$$D = \log (1/R) = - \log R \quad (12)$$

The more light the ink absorbs, the lower the reflectance, hence the higher the reflection density. The standard geometry to measure reflection density is 45 degree of incident light angle and 0 degree of observer's angle, or vice versa.

There are, however, other factors to be taken into account, such as first-surface reflection and multiple internal reflections. Figures 15 and 16 show how some of the light is reflected from the ink surface instead of penetrating the ink layer. With an angle of incidence of 45° , the first-surface reflection is about 4%. When the ink layer is glossy, the light will be reflected at 45° and will not reach the eyes (Figure 15), so it will not affect the reflection density. With a matte surface, however, the specular reflections are in all directions, and some of them will reach the eyes (Figure 16), which will increase the reflectance and lower the reflection density.

The other factor is multiple internal reflections, as shown in Figure 17. After the light passes through the ink film twice, a considerable proportion of it fails to escape and is internally reflected by the ink surface. It passes through the ink film a third time, to be again reflected by the paper, and this can be repeated several times before it finally either emerges from the surface or is absorbed. These multiple internal reflections cause an increase in the reflection density, since some of the light is absorbed each time it passes through the ink film. The reflection density increases with increasing ink film thickness until the saturation density is achieved. The saturation density results from the minimum reflectance, which comes from the first-

surface reflection.

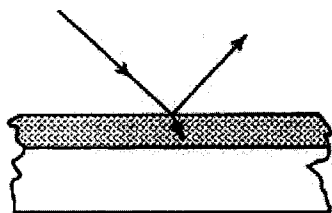


Figure 15. First-surface reflection of glossy surface (Yule, 1967).

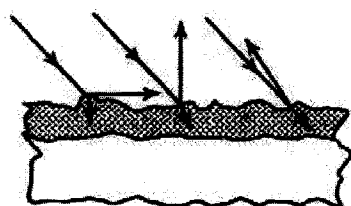


Figure 16. First-surface reflection of matte surface (Yule, 1967).

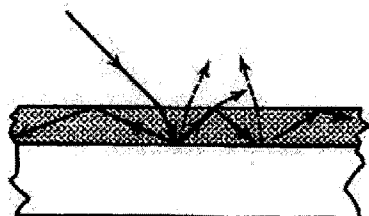


Figure 17. Multiple internal reflections in the ink layer (Yule, 1967).

Ink Mileage Curve

Definition

The relationship between the reflection density and ink film thickness is shown in Figure 18. As discussed in last section, the reflection density increases with increasing ink film thickness until the saturation density is achieved. The ink film

thickness needed to achieve a desired print density can easily be found from the curve. In practice, the ink film thickness is difficult to measure, so the weight of ink per unit print area is used to represent ink film thickness, and it is called ink film coat weight in this study. Its unit is gsm, which means gram per square meter. Remember the unit of ink mileage is square meter per gram, so the reciprocal of ink film coat weight is the ink mileage. This is the reason why this curve is called ink mileage curve. Ink mileage curve makes it possible to predict how much ink is needed to produce a desired print density.

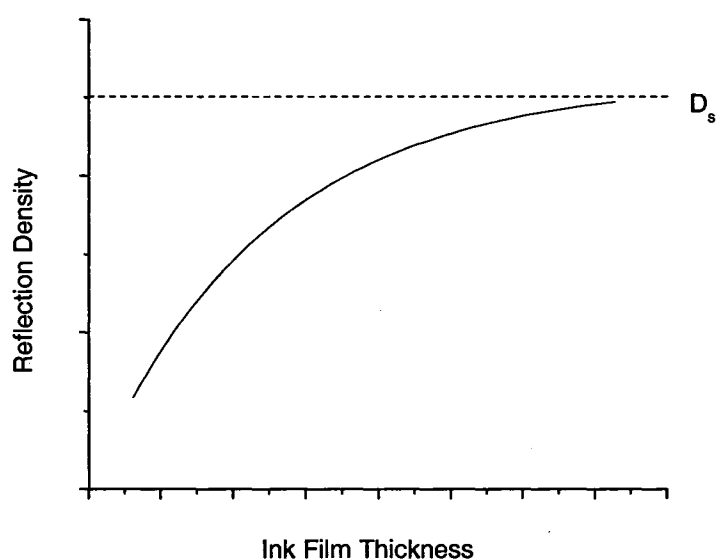


Figure 18. Ink mileage curve.

An ink mileage curve provides only qualitative information about the ink mileage characteristics of the ink. In order to describe it quantitatively, it is essential to fit an equation to the experimental data (Chou and Harbin, 1991). The regression coefficients derived from curve fitting are very useful to compare different inks. The coefficients can also be related to some basic properties of ink and paper, in some cases, the printing conditions. However, the empirical model must fit the

experimental data well so the regression coefficients can be useful in characterizing the interactions (Blom and Conner, 1990).

Mathematic Models

Tollenaar-Ernst Model. Several models for curve fitting have been reported by different researchers. One of the most used models is attributed to Tollenaar and Ernst (1962). Their equation was based upon the shape of the ink mileage curve

$$D = D_s (1 - e^{-mw}) \quad (13)$$

where D is the reflection density, and w is the coat weight of ink film on the substrate. D_s and m are two regression coefficients. D_s represents the saturation density of the solid at infinite ink film coat weight under specified printing conditions. The parameter m determines how fast the reflection density D approaches its saturation density D_s by the increase of ink film coat weight.

For low values of w the equation becomes

$$D = D_s m w \quad (14)$$

The factor m represents the increase of relative density D/D_s per unit increase of ink film coat weight at low values of w . It determines the steepness of the ink mileage curve in the region of very thin ink films.

The parameter m was reported to correlate with the degree of contact between the ink film and the paper, so it was also called "density smoothness".

The effect of printing speed and pressure on regression coefficients D_s and m was studied. The authors found that m was very little affected by printing speed, and increased with higher printing pressure. D_s was strongly influenced by both of the variables. It increased with pressure and decreased with speed, especially at low printing pressure.

Oittinen Model. Oittinen (1972) developed an improved equation by introducing a power index n to the ink film coat weight

$$D = D_s (1 - e^{-mw^n}) \quad (15)$$

It is a common practice in mathematics to add an exponent to independent variable in order to get a better curve fitting. The author found that this three-parameter model gave better fit to experimental data than its two-parameter correspondent.

Calabro-Mercatucci Model. Calabro and Mercatucci (1974) pointed out that exponential equation in general was only approximately true, so the obtained saturation density D_s and smoothness density m depended on the range of reflection density in which the experimental data was carried out. Therefore, they presented another empirical expression

$$\frac{1}{D} = \frac{1}{D_s} + \frac{m}{w} \quad (16)$$

By plotting, instead of the reflection density values as a function of the ink film coat weight, the inverse of such values, one a function of another, the experimental data would result contemporaneously and equally significantly, and the deduced parameters would not depend exclusively on a particular zone of the curve itself.

The authors found that saturation density D_s would depend on the characteristics of the ink as well as those of the paper. The m parameter represented the reciprocal of an inking, and its magnitude indicated the quantity of ink required to produce a density equal to $0.5 D_s$.

They also pointed out that the equation was completely satisfactory for newsprint, but it didn't fit the experimental ink mileage curve obtained for papers

showing a higher steepness in the first zone and also a sudden inflexion toward the density limit value. With matte coated papers, which were particularly absorbent, the method was applicable, while it was not applicable for glossy coated papers.

Calabro-Savagnone Model. Calabro and Savagnone (1983) later developed an improved equation to extend the validity of previous equation to other kinds of paper and ink, and to divide the influence of paper and ink characteristic on the parameter, through introduction of a third parameter n

$$\frac{1}{D} = \frac{1}{D_s} + \left(\frac{m}{w}\right)^n \quad (17)$$

They found that the parameter m was correlated mainly with the smoothness, gloss and absorption values, and at a less significant level, with the scattering coefficient and opacity. The ink film coat weight exponent n was found to have a better correlation with ink's rheological variables, such as viscosity, yield value and tack, and its optical properties, such as the absorption coefficient and the fineness of grind of the pigment. Saturation density D_s showed very poor correlation with measured ink characteristics.

The authors recommended the use of the parameter $1/m$ for the determination of paper printability and the use of both the parameters n and D_s for the determination of ink printability.

Kornerup-Fink-Jensen-Rosted Model. Another empirical expression was given by Kornerup et al. (1969)

$$\frac{R_p - R_s}{R - R_s} = 1 + (mw)^n \quad (18)$$

where R is the reflectance of the print, R_p is the reflectance of paper, and R_s is the reflectance of an infinitely thick ink film. This equation originates from Bouguer's

law with some assumptions and simplifications.

The authors determined R_s experimentally by measurement of very thick film as opposed to treating it as another regression coefficient. Therefore, only m and n were regression coefficients. They found it necessary to restrict the data range to $w = 1 - 4 \text{ g/m}^2$ to improve the curve fitting. They also included the residuals, which was the difference between predicted and experimental data.

The authors found that m was related to ink's absorption of light and its value decreased with decreasing pigment concentration. The ink film coat weight exponent n was found to be affected by the spectral properties of the pigment.

Blom Model. Another empirical expression, found (Blom and Conner, 1990) useful for newsprint, is

$$\frac{R}{R_p} = \frac{R_s}{R_p} + \frac{m}{w} \quad (19)$$

This expression is a simplified version of equation (18). The term "1" on the right hand side of equation (18) was included to insure that the reflectance approached a limiting value with increasing ink film coat weight. Omission of this term in their derivation and setting of the exponent "n" equal to 1 allows the expression to be transformed into equation (19). The authors, using black ink on newsprint, found this equation useful for ink film coat weight greater than 1 g/m^2 or relative reflectance (R/R_s) less than 0.35.

Comparison of Models

Blom and Conner (1990) reviewed Tollenaar-Ernst model, Calabro-Mercatucci model, Calabro-Savagnone model, Kornerup-Fink-Jensen-Rosted model, and Blom model. They examined these models for their applicability to black ink on

uncoated paper. Test prints were made on a Prüfbau Printability Tester with various ink viscosity, printing speed and printing pressure. They found that Calabro-Mercatucci model, Calabro-Savagnone model, and Kornerup-Fink-Jensen-Rosted model fitted the experimental data quite well, and were used to study the effect of printing variables on their respective regression coefficients. Ink viscosity, over the limited range studied, was not found to be significant in its effect on any of the regression coefficients. Analysis of variance showed that paper roughness and printing pressure were the most significant factors affecting the coefficients for all models. However, low printing pressure and rough paper led to large errors in the estimation of regression coefficients, due to poor ink transfer. Small effects could sometimes be seen, e.g. only looking at calendered paper under certain operating conditions, exclusion of ink weights less than 1 g/m^2 , etc. These effects could become more significant with smoother papers.

Chou and Harbin (1991) also reviewed Tollenaar-Ernst model, Oittinen model, Calabro-Mercatucci model, Calabro-Savagnone model, Kornerup-Fink-Jensen-Rosted model, and Blom model. Several inks were printed on a Prüfbau and an IGT Printability Tester under various conditions of printing speed and printing force. The substrate was a standard 30-lb newsprint. It was found that three-parameter equations fitted the experimental data much better than their two-parameter correspondents and the Calabro-Savagnone model was the best model. Their experimental results showed that printing force and printing speed had minimal influence on the characteristics of ink mileage behavior, while their effect on ink transfer characteristics was significant. A logical conclusion would be that the reflection density of a printed image was primarily determined by the ink film coat weight on the substrate rather than by how the ink was placed there. However, any

change in the printing conditions would in fact alter the reflection density of printed images because the amount of ink being transferred to the substrate would change.

Recently MacPhee and Lind (2002) pointed out that Tollenaar-Ernst model did not provide a good fit to measurements of reflection density versus printed ink film coat weight and the widely accepted theory used to explain the same relationship could not be substantiated. Nevertheless, the Tollenaar-Ernst model is still useful for characterizing data taken over the ranges of ink film coat weight normally used in practice. They also found that the shape of the ink mileage curve was strongly affected by the bandwidth of densitometer filter that was used. The shape of the curve resulted from Status T and Status I density readings differed a lot. Interestingly, this effect was only applicable to coated paper and the prints on uncoated paper did not show similar behavior. Kubelka and Munk (1931) have derived certain equations concerning the reflection of light by a colorant layer of known absorption and scattering properties, applied to a substrate having a known reflectance. A series of calculation of Kubelka's formulae for the reflectance of a printed film and for the transmittance, were carried out and the results converted to reflection densities. This model provided good correlation with Status I curves of reflection density versus ink film coat weight.

Limitations of Previous Models

The major disadvantage of these models is that they were based on the experimental data of prints made on IGT and/or Prüfbau printability tester using offset inks. The weight of the printing disc was measured before and after printing and the difference determined the quantity of transferred ink and hence the amount of ink on paper. Therefore, these models may not be applied to the ink mileage behavior

of other ink types, nor on commercial printing presses.

Ink Film Coat Weight Measurement

Weight Difference Method

There is no standard method to measure ink mileage on commercial printing presses. Ink estimating charts have been used for many years to make the calculation of ink consumption (Silver, 1984). These charts are based on the approximate number of thousand square inches that can be printed with a pound of a particular type of ink on a particular type of paper.

In offset printing, the amount of ink transferred to paper can be determined by weighing the amount of ink in ink pan before and after printing a minimum of between 1,000 and 5,000 impressions of a form having an accurately known image area, which provides a measure of the total area of ink printed during the run. The weight of ink consumed during the press run is used in conjunction with total area to calculate average ink film coat weight in grams per meter (MacPhee and Lind, 1991). The corresponding reflection density is measured. Reflection density versus the amount of ink is then plotted in a graph, from which the ink requirement at any give point can be determined.

For gravure printing, a similar technique is not applicable. Solids content in solvent-based gravure ink is about 30% of the weight, thus the weight of the ink film compared to variation of substrate grammage is too small to achieve reliable results. Currently, the method for measuring ink mileage on a gravure press is weighing the amount of the ink in the ink fountain before and after a printing job. This method is inaccurate, and inconvenient, because of the large uncertainty in the amount of evaporated solvent. Therefore, a new method is needed for gravure printing to

measure ink mileage accurately.

Internal Tracer Method

A new internal tracer method has been studied recently (Anonym, 2002). The principle is to dope the ink with a tracer not originally present in the ink and paper, which can be measured analytically. Metal carboxylates, used as sheet-fed ink drying additives, were found to be conveniently available. Metal ions can be easily detected analytically using inductively coupled plasma (ICP) atomic emission spectroscopy (AES) (Boumans, 1987). Of course, the concentration of the tracer in the ink must be low enough not to affect ink performance characteristics, such as viscosity, particle size, or color shade.

One of the advantages of this new internal tracer method is that it can be used for all ink types. Not only offset inks, but also solvent-based gravure and flexo inks. Another advantage is that it can be applied to high-speed commercial presses.

CHAPTER III

EXPERIMENTAL

Substrates

Inkjet Printing

Three commercial Epson inkjet photo papers, Premium Glossy Photo Paper (simplified as Epson Glossy), Premium Luster Photo Paper (Epson Luster), and Archival Matte Paper (Epson Matte), along with two Kodak inkjet premium picture papers, High Gloss Picture Paper (Kodak Gloss) and Satin Picture Paper (Kodak Satin) were used in all experiments. The Epson papers used are known to be of the microporous type, while the Kodak papers used are the resinous type (Eastman Kodak, 2004).

Gravure Printing Trial One

The papers used were five commercial LWC coated papers for rotogravure with basis weight of 53.9 g/m². No information about their coating formulations was available.

Gravure Printing Trial Two

Five trial coated papers for rotogravure, of about the same grammage, were used in the second trial. The grammage was measured according to TAPPI standards (TAPPI, 2002).

Paper Physical Properties

Roughness

The paper surface roughness was measured using the following three methods:

Parker Print-Surf (PPS)

The PPS roughness was measured according to TAPPI standard (1999). A PPS Model 90 from Messmer Instrument Ltd. (UK) was employed. The inkjet papers were measured at pressure of 1960 kPa with hard backing. The gravure LWC papers were measured at 490 kPa with soft backing. The roughness was calculated as the mean of 10 readings at different locations.

Stylus Profilometer

An Electronic Microgauge Model 210 from EMVECO Inc. (Newburg, OR, now Lorentzen & Wettre USA, Inc.) with the spherical steel stylus having a radius of 0.001 inch was used. The test conditions were 500 readings per group, 0.1 mm reading space, and 0.5 mm/s scanning speed. The roughness R was calculated using equation (20)

$$R = \sum (Z_{i+1} - Z_i) / 499; \quad i = 1, 2, \dots, 499 \quad (20)$$

where Z is the vertical position of the stylus.

Atomic Force Microscopy (AFM)

The AFM measurements were carried out using a Model Autoprobe CP, Scanning Probe Microscopy from Park Scientific Instruments Inc. (Sunnyvale, CA, now ThermoSpectra Corp.), with Proscan version 1.3 software. The tapping mode

was used with a silicon tip (radius of the tip end curvature ~ 10 nm). Topographic data were obtained over a $70 \mu\text{m} \times 70 \mu\text{m}$ area for inkjet papers and a $20 \mu\text{m} \times 20 \mu\text{m}$ area for gravure papers, with a typical scanning rate of 0.5 Hz.

All images were “flattened”, i.e., the mean plane of the height distribution was subtracted from each image. The roughness values were reported as the root-mean-square (RMS) deviation of the surface heights from the mean surface plane, expressed by equation (21)

$$\text{RMS Roughness} = \sqrt{\frac{1}{n} \sum_i^n (Z_i - \bar{Z})^2} \quad (21)$$

where Z is the vertical position of the tip.

The surface was observed after all measurements to monitor changes produced by scanning. There were no visible scratches on the paper surface and therefore it can be concluded that the pressure on the profilometer and AFM was not too high to damage the paper surface.

Air Permeability

The Parker Print-Surf instrument was used to measure air permeability (PPS porosity) of the papers at a clamping pressure of 490 kPa. The PPS porosity can be used to determine the actual air permeability of a paper sample (Pal et al., 2005 and 2006). The PPS porosity was calculated as the mean of 10 readings at different locations.

Pore Size Distribution

Pore size distributions were determined by mercury intrusion porosimetry (Yamauchi and Murakami, 2002). Measurements were carried out using an Autopore IV 9500 from Micromeritics Instrument Corp. (Norcross, GA). A known mass of

paper sample, approximately 10 cm², was placed in a penetrometer and evacuated at 50 µm Hg for 5 minutes immediately before measurement.

Printing Processes

Inkjet Printing

Three different inkjet printers were used: the Epson Stylus[®] Pro 5000 inkjet printer with a dye-based ink set, the Epson Stylus[®] Pro 5500 inkjet printer employing Archival ink technology, and the Epson Stylus[®] Photo 2200 inkjet printer with 7-color UltraChrome™ ink. Archival ink and UltraChrome™ ink are both pigment-based inks (Chovancova, 2004 and 2005).

Gravure Printing Trial One

The papers were printed on a four-color rotogravure web press Model 118 from Cerutti Group (Italy), located at Western Michigan University (WMU) Printing Pilot Plant. Commercial toluene-based coated yellow, magenta, cyan, and black inks for rotogravure from Flint Group (Ann Arbor, MI) were used. Magenta, cyan, and black inks were doped with selected tracers. The ink efflux time with Shell cup #2 was kept at 22±0.5 seconds for yellow, magenta, and cyan inks and 20±0.5 seconds for black ink, by frequent addition (every 10 minutes) of toluene during the printing process. Liquid ink samples were collected in the beginning, middle and end of the trial.

The electromechanically engraved cylinders have different cell types and screen values, as shown in Table 1.

Table 1
Cylinder engraving information

Cylinder	Cell Type	Screen (lpi)
Yellow	Normal	175
Magenta	Elongated	175
Cyan	Compressed	175
Black	Normal	225

Both sides of the papers were printed, but not at the same time in order to avoid sidedness effects of the press. Printing was done at 1000 ft/min with electrostatic assist (ESA) on. The target print densities were 1.0 for yellow, 1.3 for magenta, 1.25 for cyan, and 1.50 for black, which was achieved for the first printed substrate, and then the same printing condition was maintained during the printing process of the rest of the substrates.

Gravure Printing Trial Two

The print layout used in the first trial does not have tone areas big enough to perform chemical analysis; therefore, it is not possible to plot the ink mileage curve. When planning the second trial, another set of cylinders with large tone areas were selected for printing. Unfortunately, the second layout only contained tone areas of magenta and cyan colors.

The magenta cylinder has elongated cells, while the cyan cylinder has compressed cells. The print layout contains different magenta and cyan tone areas from 25% to 100 %, which means from low to high ink film coat weight.

The papers were printed the same way as in the first trial. Only the smooth

sides of the papers were printed. The target print densities were 0.95 for yellow, 1.35 for magenta, and 1.2 for cyan. Liquid ink samples were collected during the printing process of each substrate.

The particle size distributions of cyan and magenta inks were measured by a Particle Sizer Submicron 370 NICOMP analyzer from Particle Sizing Systems, Inc. (Santa Barbara, CA). This instrument is based on dynamic light scattering. The measuring period time used was 20 minutes.

Paper and Print Gloss

Paper gloss at both 60° and 75° was measured using a Novo-Gloss™ Glossmeter from Paul N. Gardner Company, Inc. (Pompano Beach, FL), according to TAPPI standard (1992). The gloss of printed samples was tested on CMYK solid colors using the same geometries. The gloss value was calculated as the mean of 10 readings at different locations.

Gravure Ink Mileage

Gravure Printing Trial One

Ink Film Coat Weight Analysis

Both collected liquid ink samples and solid areas of printed samples were analyzed using ICP-AES at Chemisar Laboratories (Guelph, ON). By knowing the amount of tracer metal in both the liquid ink and printed ink film, the ink film coat weight can be calculated by using

$$\text{Ink film coat weight (gsm)} = \frac{\text{Tracer in ink film (gsm)}}{\text{Tracer in liquid ink (wt\%)}} \quad (22)$$

Reflection Density Measurement

The reflection densities at solid CMYK areas were measured with reference to the reflection density of unprinted paper using a 530 SpectroDensitometer with Status T filter from X-Rite, Inc. (Grandville, MI). The density value was calculated as the mean of 10 readings at different locations.

Gravure Printing Trial Two

Ink Film Coat Weight Analysis

The ink film coat weights at different tone areas of cyan and magenta ink films were analyzed the same way as in the first trial.

Reflection Density Measurement

The relative reflection densities at different tone areas of cyan and magenta ink films were measured the same way as in the first trial.

Curve Fitting

The ink film coat weight and reflection density data was plotted and analyzed using appropriate OriginPro 7.5 non-linear curve fitting routines. Tollenaar-Ernst model, Oittinen model, Calabro-Mercatucci model, Calabro-Savagnone model, Kornerup-Fink-Jensen-Rosted model, and Blom model were examined. Saturation density D_s or saturation reflectance R_s , parameter m , and ink film coat weight exponent n were treated as regression variables.

CHAPTER IV

RESULTS AND DISCUSSION

Inkjet Printing

AFM Images of Paper Topography

Atomic force microscopic (AFM) images of topography of Epson Glossy, Epson Luster, Kodak Gloss, and Kodak Satin papers are shown in Figure 19.

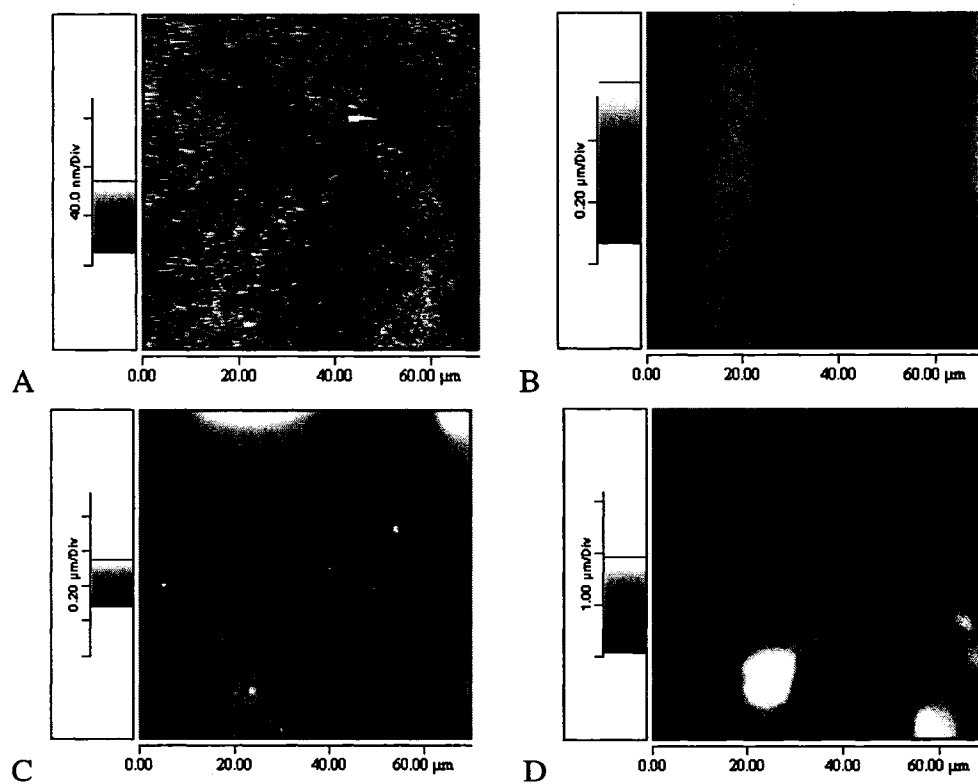


Figure 19. AFM images of topography of the inkjet papers (A: Epson Glossy, B: Epson Luster, C: Kodak Gloss, D: Kodak Satin).

The surface of Epson Glossy paper is the smoothest among all substrates, averaging 9.71 nm. The surface of Epson Luster (22.39 nm) and Kodak Gloss paper (18.11 nm) were considerably rougher than Epson Glossy paper, mainly due to the surface waviness. Kodak Satin paper has very rough surface, reaching 312.1 nm. The surface of Epson Matte paper was too rough for current settings of AFM. The maximum vertical depth the tip can reach was 6 μm , so the AFM could not be used when the distance between the highest peak and the lowest valley of the surface exceeded 6 μm . This method can only be applied on relatively smooth surfaces.

Relationships between Roughness and Paper Gloss

The comparison of the results of the three roughness testing methods as well as the results of paper gloss at 60° and 75° are presented in Table 2. A good correlation exists between the PPS and stylus profilometer test methods (93.7%). A little lower correlation was obtained between PPS and AFM (90.3%) and between profilometer and AFM (89.3%), which is surprising, because it was expected that the two profilometric techniques would correlate better, while PPS, measuring at a pressure, would include compressibility and thus, give a lower correlation. However, AFM roughness is microroughness, while PPS roughness and profilometer roughness are both macroroughness, so it is still not surprising that these two have a better correlation.

Epson Glossy paper was the smoothest, while Epson Matte paper was the roughest according to all three methods. Epson Luster, Kodak Gloss and Kodak Satin three papers have close PPS roughness values, but Epson Luster paper has much higher profilometer roughness, and Kodak Satin paper has much higher AFM roughness. This probably means that the surface of the Epson Luster paper is rough

on a microscale, but smooth on nanoscale. On the contrary, the surface of the Kodak Satin paper is smooth at the microscale, but rough on nanoscale.

Table 2
Correlation coefficients between surface roughness and paper gloss

Sample	PPS	Profilometer	AFM	Paper Gloss	
	(μm)	(μm)	(nm)	(60°, %)	(75°, %)
Epson Glossy	1.04	0.36	9.71	34.64	62.92
Epson Luster	3.23	2.30	22.39	17.06	50.84
Epson Matte	6.78	4.40	-	2.60	6.80
Kodak Gloss	3.22	0.94	18.11	77.80	95.00
Kodak Satin	3.11	1.07	312.1	27.04	67.54

	PPS	Profilometer	AFM	60° Gloss	75° Gloss
PPS	1				
Profilometer	0.937	1			
AFM	0.903	0.893	1		
60° Gloss	-0.468	-0.676	-0.598	1	
75° Gloss	-0.722	-0.880	-0.864	0.896	1

Some gloss values were out of the measurement range at one or the other angles, but are presented here for comparison purposes. The 75° angle appears more suitable for comparison of all the substrates in this experiment. The correlation of PPS roughness and paper gloss is low, only 72.2%. Profilometer and AFM roughness showed higher correlations (88.0% and 86.4%, respectively) with paper gloss. Interestingly, both Kodak papers are rougher than Epson Glossy paper, but have much higher gloss values, especially Kodak Gloss paper. According to Fresnel theory (Casey, 1981), the gloss of paper is determined by the incident angle of light, incident

light wavelength, and refractive index and the surface roughness of the paper. For an instrument of defined incident angle of light and wavelength, the gloss is determined by the refractive index and surface roughness of the paper. In this experiment, the wavelength and angle of incident light was the same for all the samples. Therefore, the reason probably was that Kodak papers have coating layers with higher refractive index than Epson papers.

Relationships between Roughness and Print Gloss

The correlation coefficients between paper roughness and print gloss at 60° and 75° for all three printers are listed in Tables 3 – 5.

Table 3

Correlation coefficients between paper roughness and print gloss
for Photo 2200 Inkjet Printer

	PPS	Profilometer	AFM	60° Paper Gloss	60° Print Gloss			
					C	M	Y	K
C	-0.914	-0.953	-0.897	0.782	1			
M	-0.910	-0.946	-0.892	0.785	1.000	1		
Y	-0.934	-0.908	-0.828	0.665	0.970	0.973	1	
K	-0.943	-0.905	-0.854	0.653	0.971	0.974	0.998	1
	PPS	Profilometer	AFM	75° Paper Gloss	75° Print Gloss			
					C	M	Y	K
C	-0.908	-0.935	-0.990	0.916	1			
M	-0.939	-0.941	-0.992	0.880	0.996	1		
Y	-0.947	-0.927	-0.992	0.855	0.990	0.998	1	
K	-0.928	-0.941	-0.977	0.905	0.992	0.991	0.989	1

Table 4

Correlation coefficients between paper roughness and print gloss
for Pro 5000 Inkjet Printer

	PPS	Profilometer	AFM	60° Paper Gloss	60° Print Gloss			
					C	M	Y	K
C	-0.666	-0.863	-0.745	0.943	1			
M	-0.695	-0.879	-0.745	0.939	0.997	1		
Y	-0.696	-0.875	-0.747	0.943	0.996	1.000	1	
K	-0.656	-0.827	-0.740	0.973	0.985	0.987	0.990	1
	PPS	Profilometer	AFM	75° Paper Gloss	75° Print Gloss			
					C	M	Y	K
C	-0.798	-0.926	-0.920	0.975	1			
M	-0.823	-0.942	-0.928	0.972	0.999	1		
Y	-0.786	-0.926	-0.900	0.989	0.996	0.996	1	
K	-0.846	-0.955	-0.927	0.978	0.989	0.994	0.993	1

The correlations of roughness to print gloss are higher than to paper gloss with all three methods. Inkjet printing is non-impact printing, not like the classical printing processes with contact pressure, so the ink film surface topography mainly depends on paper surface. Since the ink is the same for the same printer, the refractive index of each ink film is the same for all the samples. Therefore, the print gloss value is more determined by the surface roughness.

The test method with the highest correlation of nearly 100% to print gloss is AFM roughness with the Photo 2200 printer. AFM roughness and profilometer roughness both have high correlation with print gloss for all three printers, and PPS roughness has a low correlation with the Pro 5000 printer, which uses a dye-based ink set.

Table 5

Correlation coefficients between paper roughness and print gloss
for Pro 5500 Inkjet Printer

	PPS	Profilometer	AFM	60° Paper Gloss (60°)	60° Print Gloss			
					C	M	Y	K
C	-0.938	-0.927	-0.850	0.693	1			
M	-0.918	-0.769	-0.731	0.357	0.912	1		
Y	-0.939	-0.821	-0.794	0.460	0.951	0.992	1	
K	-0.927	-0.930	-0.837	0.713	0.999	0.898	0.939	1
	PPS	Profilometer	AFM	75° Paper Gloss	75° Print Gloss			
					C	M	Y	K
C	-0.961	-0.947	-0.984	0.857	1			
M	-0.970	-0.894	-0.964	0.761	0.983	1		
Y	-0.963	-0.901	-0.970	0.793	0.988	0.998	1	
K	-0.942	-0.971	-0.974	0.897	0.991	0.952	0.959	1

The ink also has effect on the print gloss, which can be seen by comparing the three different printers. Paper gloss and print gloss correlate much better for the Pro 5000 printer (>97%) than the other two. The Pro 5000 printer uses dye-based inks, unlike other two printers using pigment-based inks. Dyes are made of single molecules, while pigments are composed of much larger particles around 100 nm (Chovancova et al., 2004 and 2005).

The 60° and 75 ° print gloss by three printers are compared in Figure 20 for all five papers, with dotted line indicating paper gloss value.

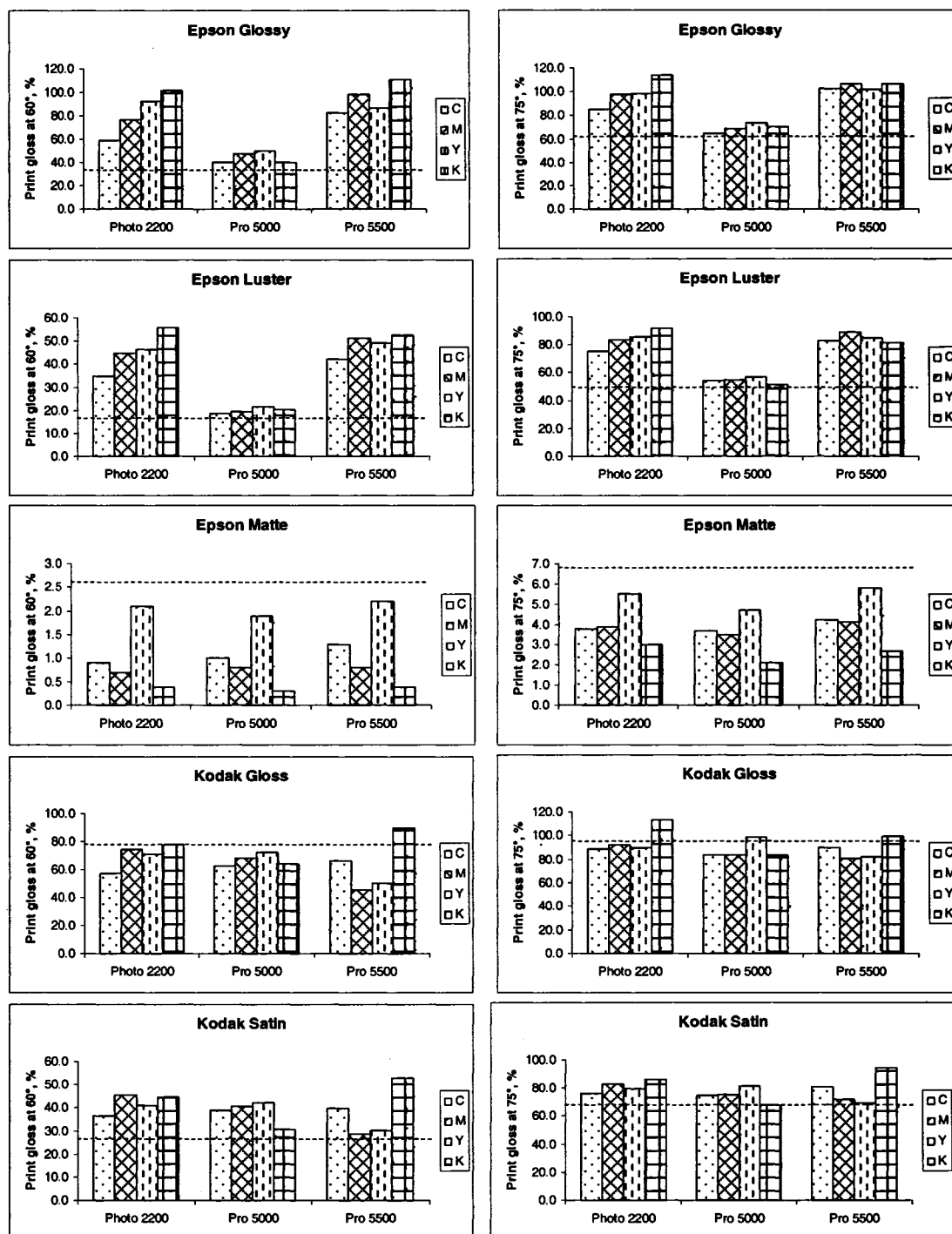


Figure 20. Comparisons of print gloss at 60° (left) and 75° (right) between three printers for all five papers, with dotted line indicating paper gloss value (print gloss lower than the paper gloss results in negative delta gloss).

It is found that for microporous Epson papers, higher print gloss was obtained with the Pro 5500 and Photo 2200 printers using pigment-based inks than Pro 5000 printer using dye-based inks. Pigment-based inks can achieve very high positive delta gloss (Delta gloss is the difference between print and paper gloss), because of packing of ink particles with coating pigment particles. Paper coating gloss depends on packing of different size coating pigment particles (Lee et al., 2004 and 2005a, b). Dye-based inks cannot improve upon the paper because the dye molecules are too small to efficiently fill the low spots in the coating. However, the Epson Matte paper was too rough that even pigment-based inks couldn't achieve positive delta gloss. For resinous Kodak papers, a different effect was observed. The Pro 5000 printer with dye-based inks achieved as high print gloss as obtained by Pro 5500 and Photo 2200 printers, even higher print gloss of yellow color. Colorant type is not a dominant factor to print gloss in the case of resinous inkjet papers. It was also found that negative delta gloss values were obtained for Kodak Gloss paper, most likely because the water based inks can swell the coating, creating a rougher surface, resulting in lower print gloss and ultimately negative delta gloss (Figure 20).

AFM Images of Ink Film Topography

Figure 21 shows AFM images of black ink film surface on Epson Glossy paper printed by all three printers. Ink droplets can be observed clearly in the images of the Pro 5500 and Photo 2200 printers. Dyes were distributed very evenly in the image of Pro 5000 printer. Their RMS roughness values are 31.77 nm, 36.09 nm and 27.7 nm respectively (from A to C). The Pro 5000 printer uses dye-based inks; therefore the ink film surface is smoother than using pigment-based inks because dyes have smaller particle sizes than pigments. This ink film roughness is, however, about

three times larger than the corresponding paper roughness.

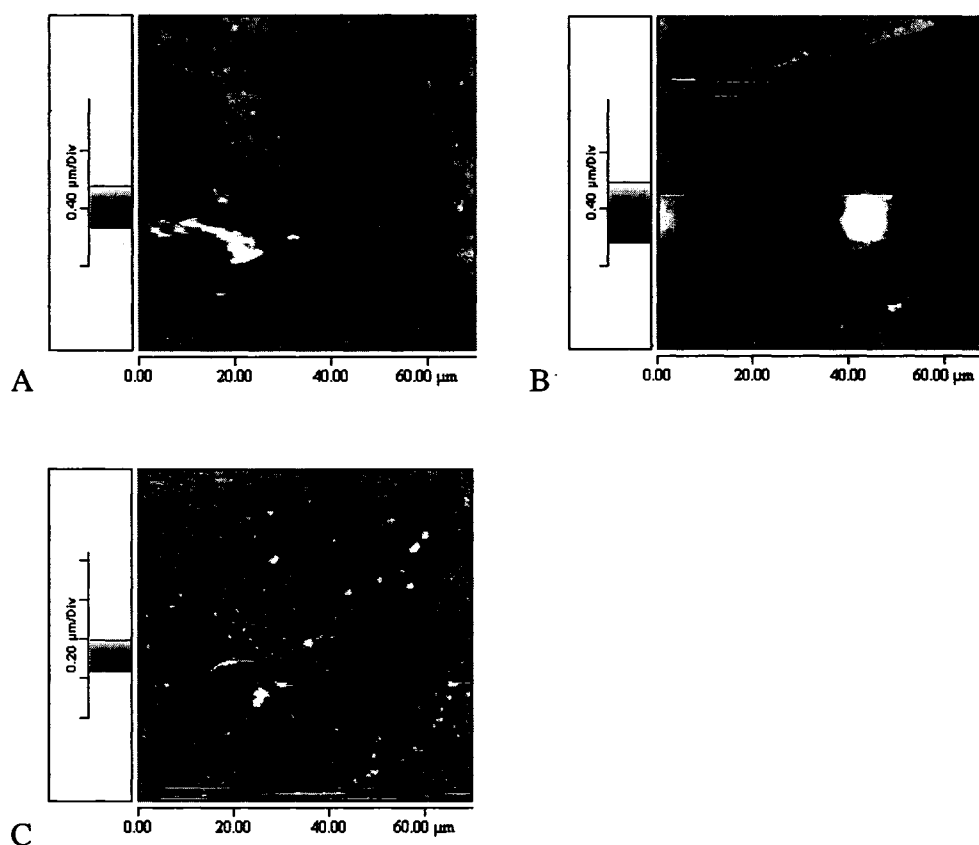


Figure 21. AFM images of black ink film topography on Epson Glossy paper printed by all three printers (A: Pro 5500 Printer, B: Photo 2200 Printer, C: Pro 5000 Printer).

Ink Film Thickness

Ink film thickness measurements were also tried using AFM. The scale of AFM is very small (100 μm by 100 μm maximum), so only the film thickness at the border can be measured. The AFM image of cyan ink printed on Kodak Gloss paper by Pro 5500 printer is shown in Figure 22. The darker (lower) area is the paper substrate, and the brighter (higher) area is the ink film. As seen there, the ink film is

not uniform at the border. For example, the top green line crosses two droplets, and its height profile shows the ink film thickness is about 150 nm. Based on the ink pigment size, this corresponds to approximately a monolayer of ink pigment particles. This needs further investigation, with other sampling methods.

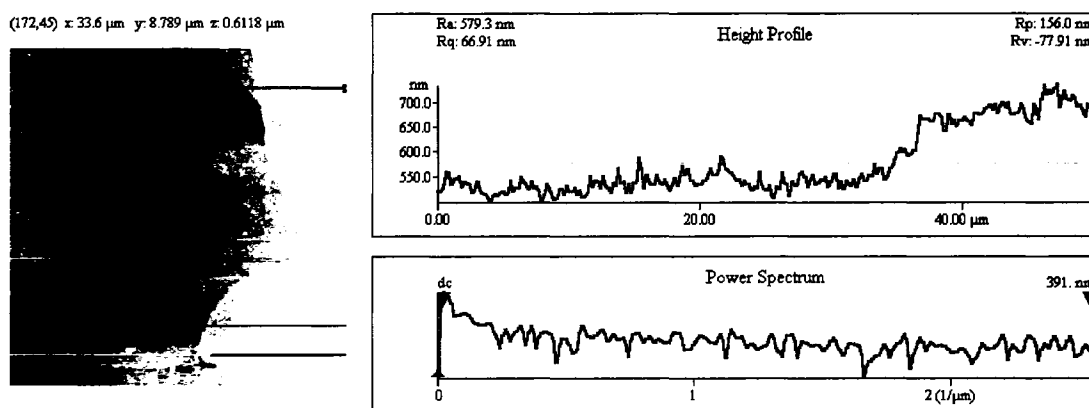


Figure 22. Ink film thickness measurement using AFM.

Gravure Printing Trial One

Paper Physical Properties

Roughness

Five LWC papers were printed on both sides, totaling 10 samples. They were designated as No. 1-10. The results of paper surface roughness are listed in Table 6. Sample No. 5 is the smoothest for all three methods, while sample No. 1 has highest PPS roughness, sample No. 8 has highest profilometer roughness, and sample No. 10 has highest AFM roughness.

AFM images of the smoothest and roughest sample, sample No. 5 and No. 10, are shown in Figure 23. The image on the right (No. 10) looks much rougher than the

left (No. 5) even at larger scale, which is confirmed by its AFM roughness value more than two times higher than the other.

Table 6

Surface roughness measured by different methods

Paper	No.	PPS S5 (μm)	Profilometer (μm)	AFM (nm)
LWC#1	1	2.45	1.51	40.16
	2	2.22	1.57	44.83
LWC#2	3	1.95	1.43	31.95
	4	1.98	1.39	44.11
LWC#3	5	1.79	1.25	29.89
	6	1.93	1.39	35.05
LWC#4	7	1.90	1.56	34.90
	8	1.98	1.63	40.43
LWC#5	9	1.99	1.62	74.49
	10	1.99	1.57	76.49

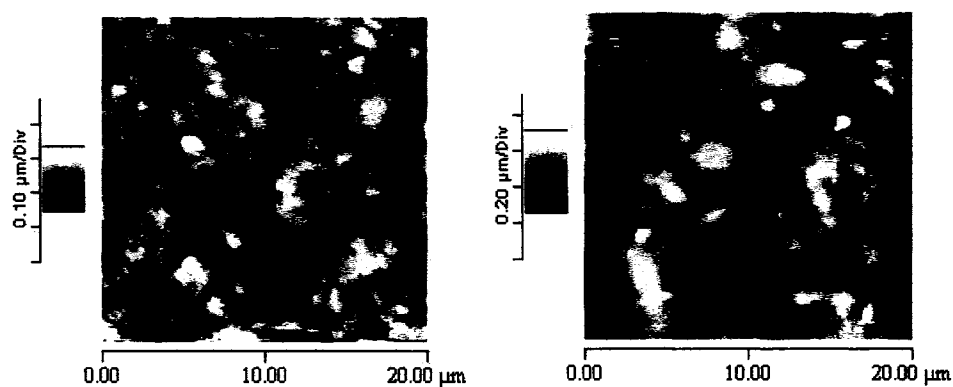


Figure 23. AFM images of sample No. 5 (left) and No. 10 (right).

Air Permeability

The resistance to flow through a porous medium must be controlled by the neck pores such as openings of the packed spheres type of pores because they are paths of flow. Further, air cannot pass through dead-end pores; it passes only through interconnected pores (Dullien, 1979). For paper, sheet grammage has effect on permeability. The permeability coefficient of paper sheet decreases with an increase in its grammage due to completion of the internal pore structure. Papers with low grammage tend to have more interconnected pores.

The results of PPS porosity are listed in Table 7. LWC#5 and LWC#4 have higher PPS porosity, which means they have more interconnected pores than other substrates.

Table 7

Comparison of PPS porosity

Paper	PPS Porosity (ml/min)
LWC#1	8.08
LWC#2	7.18
LWC#3	7.37
LWC#4	11.32
LWC#5	13.76

Pore Size Distribution

Mercury porosimetry curves in Figure 24 show the pore size distributions of all the substrates. The x,y axes were chosen so that the area under the curve is equal to the pore volume. Papers LWC#1 to LWC#4 all have peaks of pore sizes at about 1 μm . LWC#5 has smaller pores between 1 μm to 100 nm. LWC#4 has some large pores with size of several tens of microns, as seen in Figure 24. Large pores were also found in the AFM image of sample LWC#4 (Figure 25), in which the size of the pore is in the range of microns.

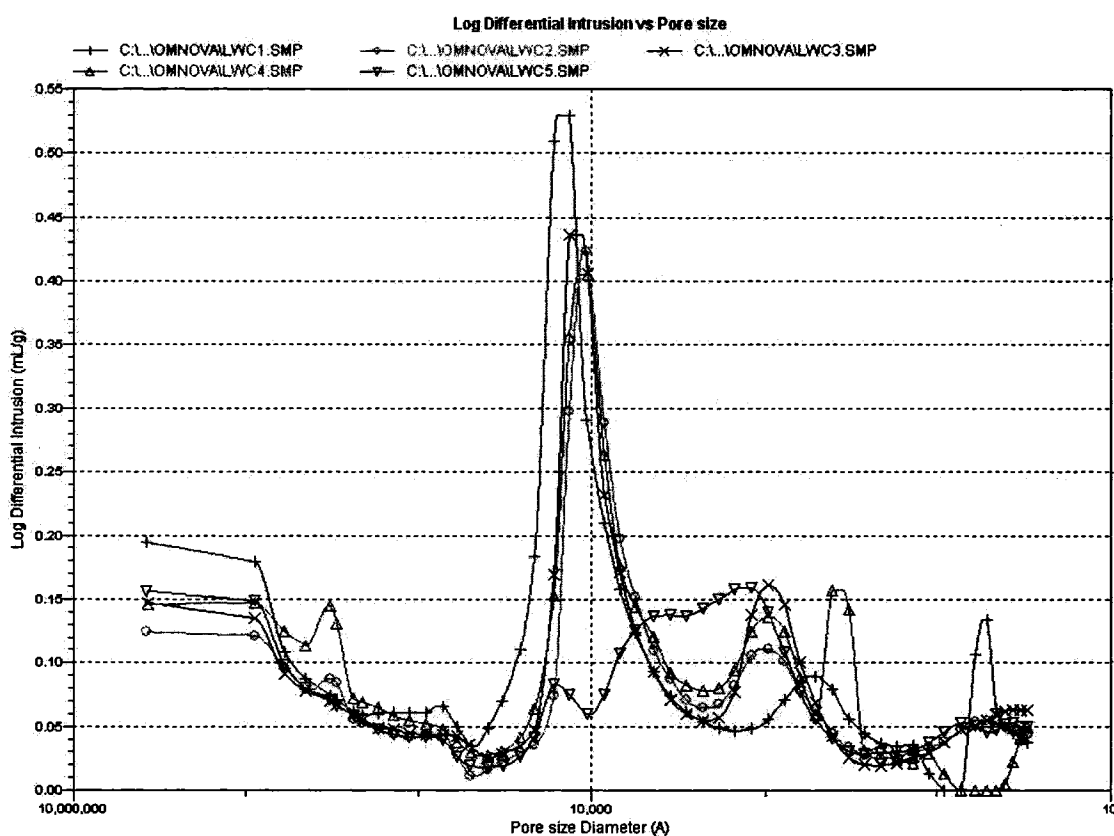


Figure 24. Pore size distributions from mercury porosimetry curves.

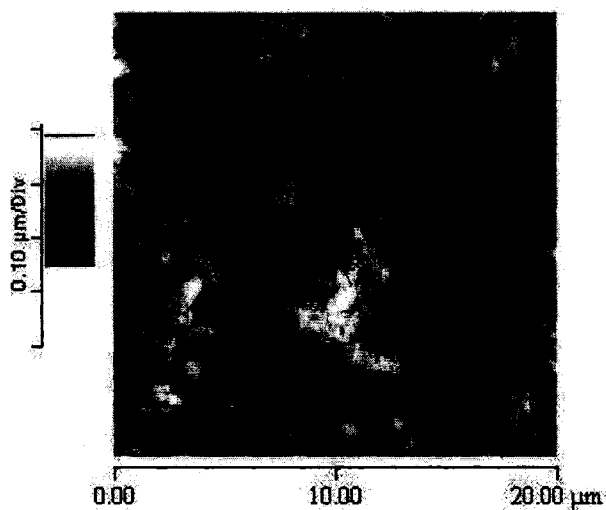


Figure 25. AFM image of LWC#4.

Average pore diameters can be calculated from mercury porosimetry curves, which are shown in Table 8. As discussed above, both LWC#5 and LWC#4 have higher PPS porosity and thus more interconnected pores, but LWC#4 has the largest average pore size, while LWC#5 has the smallest one. Therefore, their internal pore structures are expected to be totally different.

Table 8

Comparison of pore sizes

Sample	Average Pore Diameter (nm)
LWC#1	74.4
LWC#2	65.0
LWC#3	63.7
LWC#4	135.2
LWC#5	59.1

Paper and Print Gloss

The results of paper and print gloss at 60° and 75° are listed in Table 9 and Table 10, respectively. The correlation coefficients between paper roughness and paper and print gloss are list in Table 11 and Table 12. AFM roughness has the best correlation with both 60° and 75° paper and print gloss, while PPS roughness the worst. As seen in Figure 26, the size of a black half-tone dot is only about 30 μm . Therefore, microroughness measured by AFM correlates better with print gloss than macroroughness measured by PPS and profilometer.

Table 9
Paper and print gloss at 60°

Sample No.	Paper Gloss (60°, %)	Print Gloss (60°, %)			
		C	M	Y	K
1	18.70	27.0	25.2	26.4	24.0
2	18.38	25.4	22.8	24.9	22.0
3	21.28	31.1	32.2	29.0	30.5
4	22.38	35.1	31.1	34.3	29.1
5	24.34	40.1	35.2	35.5	35.3
6	23.28	33.8	30.3	31.5	30.0
7	21.66	35.7	32.1	34.1	32.0
8	22.02	31.8	31.3	32.3	30.5
9	17.38	24.1	23.0	23.3	21.7
10	18.04	23.2	22.0	23.0	21.8

Table 10
Paper and print gloss at 75°

Sample No.	Paper Gloss (75°, %)	Print Gloss (75°, %)			
		C	M	Y	K
1	55.74	68.7	58.4	65.8	59.7
2	52.72	64.4	59.8	61.8	61.5
3	61.82	73.5	68.9	69.1	65.3
4	63.78	70.2	62.0	70.0	68.3
5	65.52	75.3	70.5	68.1	68.3
6	63.46	71.1	70.8	68.5	68.0
7	62.32	71.7	69.4	70.5	67.6
8	59.38	67.1	64.1	69.1	66.5
9	51.38	63.4	61.2	65.4	58.3
10	53.20	59.5	56.6	58.1	55.5

Table 11
Correlation matrix of paper and print gloss at 60°

	PPS	Profil.	AFM	Paper Gloss (60°)	C	M	Y	K
PPS	1							
Profil.	0.387	1						
AFM	0.100	0.563	1					
Paper Gloss	-0.613	-0.734	-0.759	1				
C	-0.587	-0.729	-0.768	0.955	1			
M	-0.605	-0.651	-0.793	0.940	0.951	1		
Y	-0.536	-0.607	-0.753	0.939	0.976	0.936	1	
K	-0.634	-0.642	-0.783	0.947	0.960	0.990	0.936	1

Table 12
Correlation matrix of paper and print gloss at 75°

	PPS	Profil.	AFM	Paper Gloss (75°)	C	M	Y	K
PPS	1							
Profil.	0.387	1						
AFM	0.100	0.563	1					
Paper Gloss	-0.568	-0.769	-0.776	1				
C	-0.348	-0.750	-0.889	0.885	1			
M	-0.669	-0.575	-0.710	0.810	0.834	1		
Y	-0.364	-0.391	-0.712	0.782	0.823	0.733	1	
K	-0.514	-0.589	-0.822	0.918	0.841	0.813	0.864	1

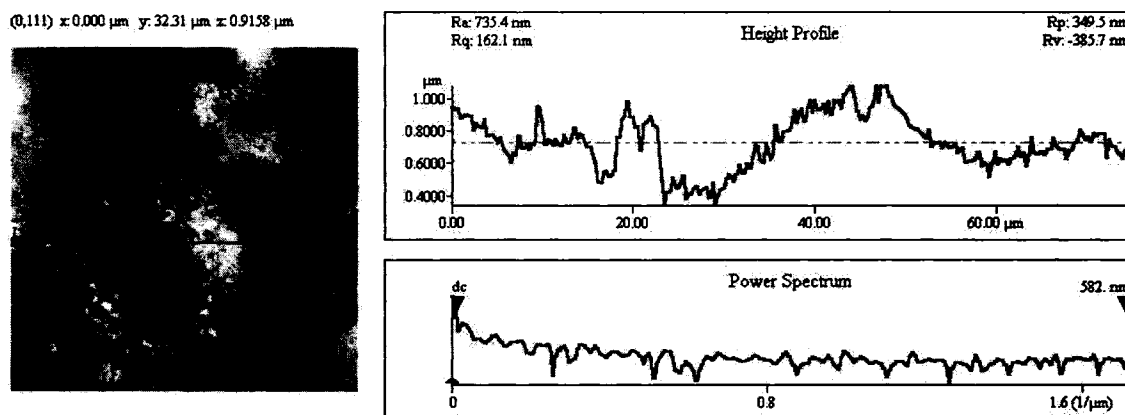


Figure 26. AFM image of a black half-tone dot.

Reflection Density

The reflection density values of all samples are compared in Figure 27. Because the printing conditions remained the same after the first printed substrate achieved the target densities, the densities of the following printed substrates had different degrees of variation due to the effects of paper properties. However, the densities are still in an acceptable range.

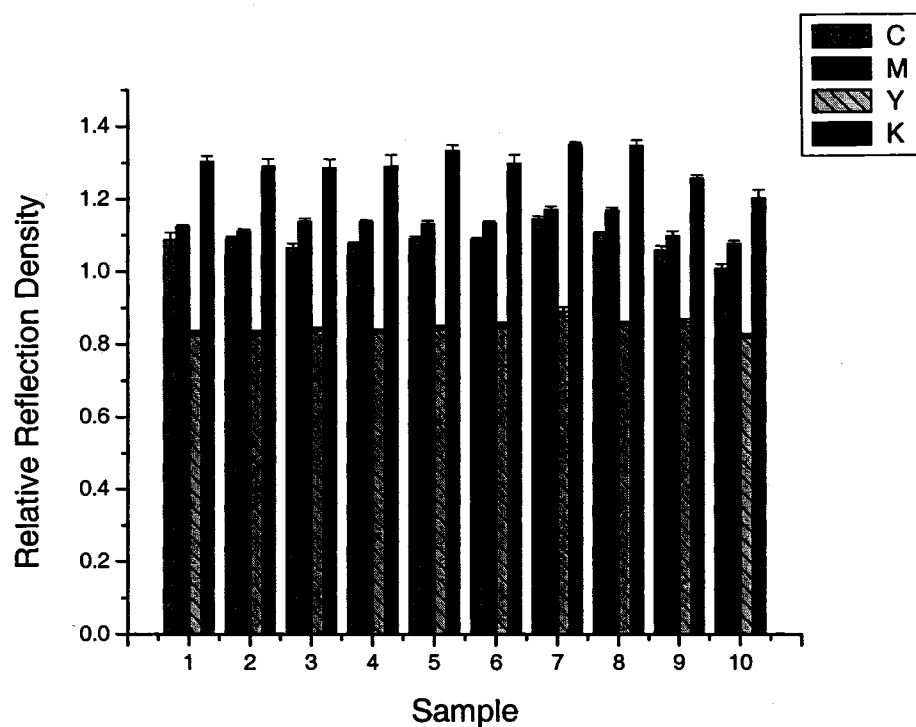


Figure 27. Comparison of relative reflection density.

Ink Film Coat Weight

The average value of tracing metal concentration in three collected liquid inks for each color was used for calculation of ink film coat weight according to equation

(22). The calculated ink film coat weight for each color is shown in Table 13. The error comes from the standard deviation of tracer concentration in liquid ink.

Table 13
Ink film coat weight results

Paper	No.	Magenta		Cyan		Black	
		g/m ²	error	g/m ²	error	g/m ²	error
LWC#1	1	4.053	0.128	3.405	0.068	2.562	0.180
	2	3.634	0.114	3.739	0.075	2.521	0.178
LWC#2	3	4.121	0.130	3.546	0.071	2.381	0.168
	4	3.678	0.116	3.781	0.075	2.531	0.178
LWC#3	5	3.829	0.120	3.484	0.069	2.540	0.179
	6	3.731	0.117	3.788	0.076	2.372	0.167
LWC#4	7	3.775	0.119	3.519	0.070	2.378	0.167
	8	3.768	0.119	3.388	0.068	2.396	0.169
LWC#5	9	3.887	0.122	3.478	0.069	2.453	0.173
	10	4.002	0.126	3.554	0.071	2.400	0.169

The ink amounts transferred onto LWC papers for three different inks and three different cell geometries are shown in Figure 28. It is very clear that ink requirement of black ink is much less than cyan and magenta inks, because black ink films have lower ink film coat weights than cyan and magenta ink films but higher reflection densities. It is difficult to tell the difference between magenta and cyan ink films, since magenta ink films have higher reflection densities than cyan ink films but they have close ink film coat weights.

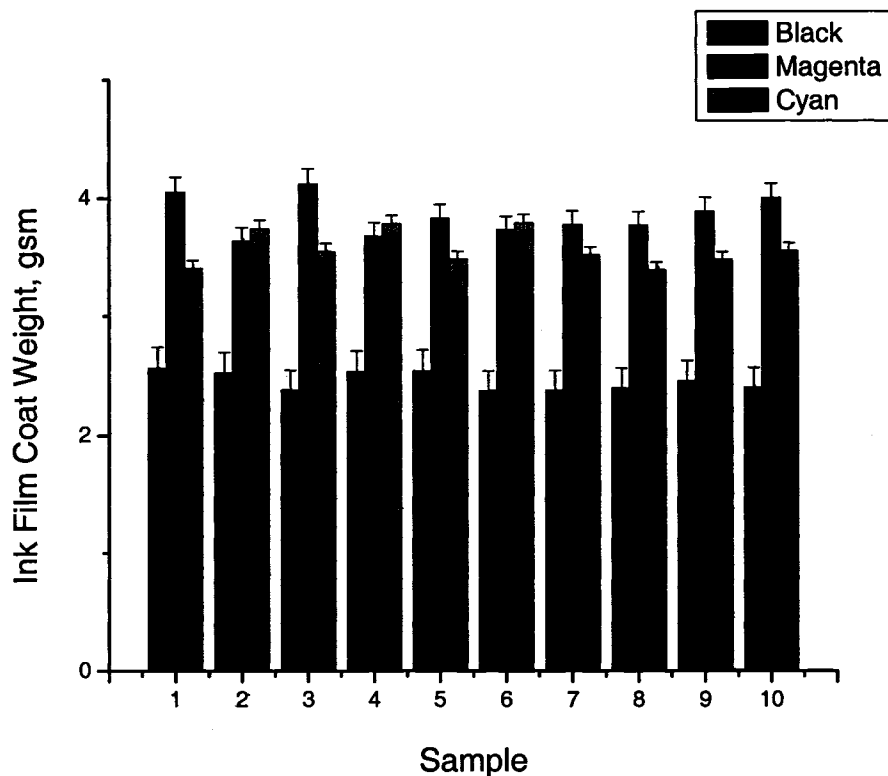


Figure 28. Comparison of ink film coat weight.

Relationships between Paper Physical Properties and Ink Film Coat Weight

The correlations between paper physical properties and ink film coat weight are listed in Table 14. There were no strong correlations found. The reason is probably that the reflection densities vary between different substrates, so it is not appropriate to compare their corresponding ink film coat weights. Therefore, a better way is to print all the papers with the same densities. However, the best way is to compare the ink mileage curves.

Table 14
Correlation matrix of ink film coat weight

	Ink Film Coat Weight		
	M	C	K
PPS Roughness	0.198	-0.110	0.485
Profil. Roughness	0.042	-0.330	-0.301
AFM Roughness	0.170	-0.081	-0.071
PPS Porosity	0.151	-0.437	-0.394
Pore Size	-0.267	-0.390	-0.357

Gravure Printing Trial Two

Paper Physical Properties

The physical properties of the papers are reported in Table 15.

Table 15
Paper physical properties

Sample No.	Grammage (g/m ²)	PPS Roughness (μ m)	Profilometer Roughness (μ m)	AFM Roughness (nm)	PPS Porosity (ml/min)	Pore Size (nm)
1	50.05	1.69	1.51	34.3	10.58	101.5
2	48.95	1.60	1.62	76.5	10.67	113.0
3	50.06	1.57	1.61	36.9	7.97	100.3
4	49.58	1.52	1.65	65.0	11.93	233.1
5	50.62	1.54	1.58	65.8	10.46	146.5

It is surprising that the correlation coefficients between PPS roughness and other two are negative (as shown in Table 17). Very low correlation (57.9%) exists between profilometer and AFM roughness. Sample 3 has lower PPS porosity than other four samples. Sample 1, 2, and 3 have similar average pore size, while Sample 4 much larger.

Paper and Print Gloss

The results of paper and print gloss at both 60° and 75° are listed in Table 16. Their correlation matrices are shown in Table 17 and Table 18. AFM roughness was found to correlate well with paper gloss (80.6% and 93.6%), but not with print gloss. PPS roughness and profilometer roughness have very poor correlations with both paper and print gloss.

Table 16
Paper and print gloss at 60° and 75°

Sample No.	Paper Gloss (60°, %)	Print Gloss (60°, %)		Paper Gloss (75°, %)	Print Gloss (75°, %)	
		C	M		C	M
1	20.94	33.8	35.6	58.02	71.0	70.5
2	18.14	33.9	34.4	51.76	70.7	70.8
3	25.48	43.0	44.0	61.38	72.4	74.1
4	16.96	33.0	32.2	53.46	66.9	66.6
5	17.90	33.7	37.1	52.86	70.4	72.1

Table 17

Correlation matrix of paper and print gloss at 60°

	PPS	Profil.	AFM	Paper Gloss (60°)	Print Gloss (60°) C	M
PPS	1					
Profil.	-0.857	1				
AFM	-0.539	0.579	1			
Paper Gloss	0.304	-0.211	-0.806	1		
C	-0.069	0.166	-0.559	0.920	1	
M	0.016	-0.061	-0.590	0.904	0.935	1

Table 18

Correlation matrix of paper and print gloss at 75°

	PPS	Profil.	AFM	Paper Gloss (75°)	Print Gloss (75°) C	M
PPS	1					
Profil.	-0.857	1				
AFM	-0.539	0.579	1			
Paper Gloss	0.344	-0.308	-0.936	1		
C	0.498	-0.454	-0.499	0.580	1	
M	0.173	-0.245	-0.387	0.527	0.933	1

Ink Mileage Curves

The calculated ink film coat weight and relative reflection density at different tone areas for all samples are listed in Table 19.

Table 19

Ink film coat weights and relative reflection densities at different tones

Sample No.	Tone (%)	Cyan		Magenta	
		Ink Film Coat Weight (g/m ²)	Relative Reflection Density (%)	Ink Film Coat Weight (g/m ²)	Relative Reflection Density (%)
1	25	0.63	0.198	1.03	0.291
	50	1.33	0.405	1.91	0.578
	75	2.51	0.652	2.90	0.9
	85	3.53	0.873	3.93	1.066
	100	4.90	1.07	4.48	1.208
2	25	0.71	0.208	1.01	0.305
	50	1.33	0.411	1.87	0.599
	75	2.56	0.653	2.94	0.903
	85	3.81	0.874	4.03	1.075
	100	5.06	1.06	4.79	1.225
3	25	0.67	0.207	1.10	0.297
	50	1.31	0.403	1.83	0.59
	75	2.61	0.641	3.09	0.897
	85	3.71	0.856	3.84	1.053
	100	4.92	1.04	4.83	1.171
4	25	0.73	0.199	1.07	0.288
	50	1.33	0.41	2.06	0.572
	75	2.53	0.66	3.35	0.898
	85	3.91	0.88	4.01	1.061
	100	5.33	1.08	4.72	1.191
5	25	0.58	0.203	1.12	0.296
	50	1.29	0.409	1.92	0.592
	75	2.40	0.649	3.14	0.912
	85	3.62	0.871	3.87	1.074
	100	4.93	1.064	4.71	1.215

Ink film coat weight versus relative reflection density was then plotted and curve fitting was performed using all six models. All of the curve fitting results are listed in the Appendix. An example is given in Figure 29. The solid dots are experimental data of cyan ink on paper sample No. 1. The solid line is the non-linear fitting result using Oittinen model. The hollow dots are residual values. The residual is equal to the experimental value minus the value calculated from the fitting model. Residual values can be used to tell how good the fit is. The smaller the absolute values of the residuals are, the better the curve fit is.

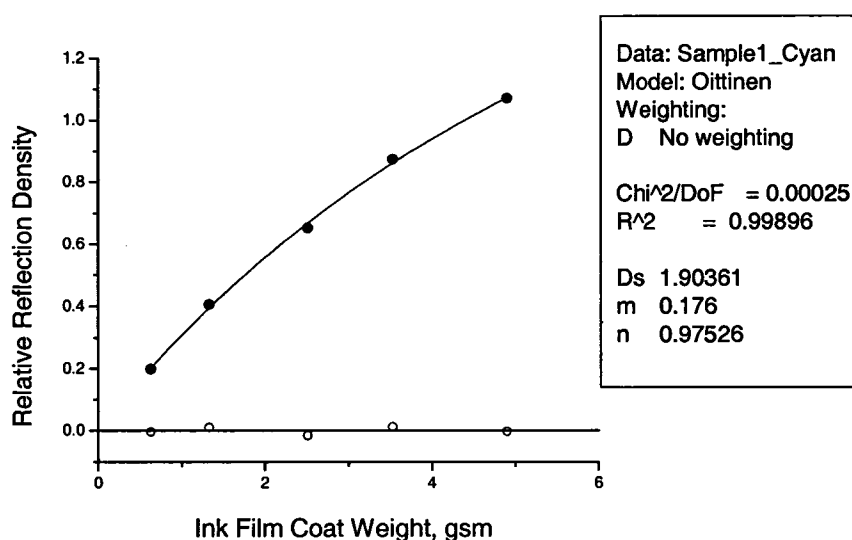
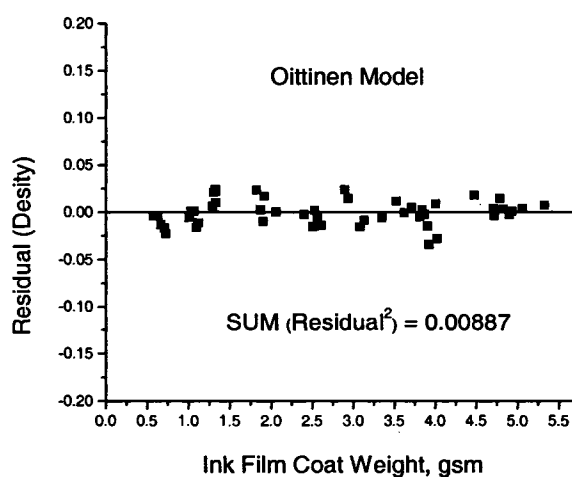
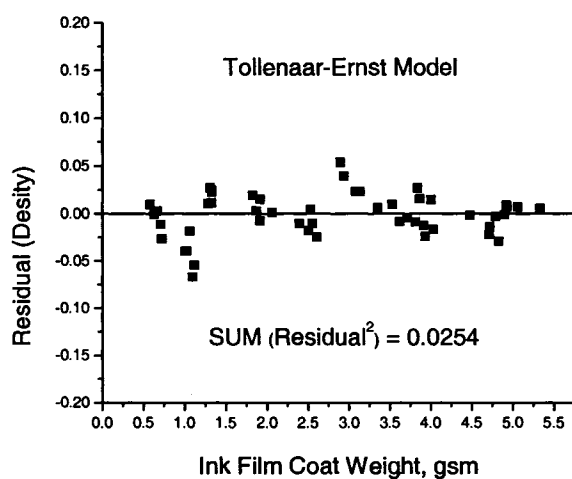
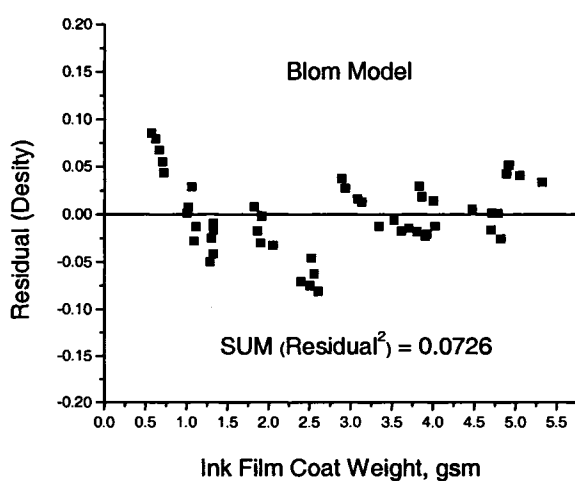
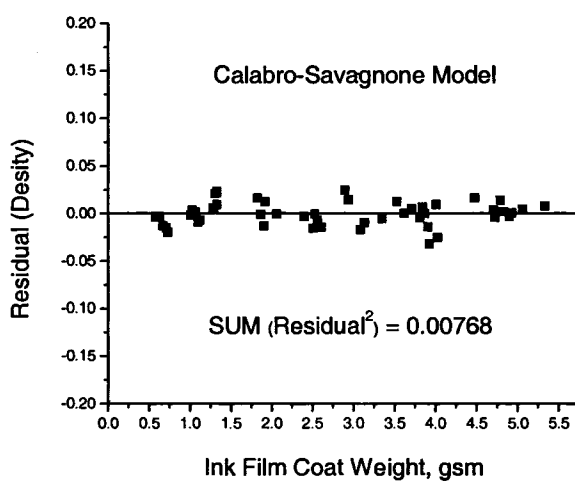
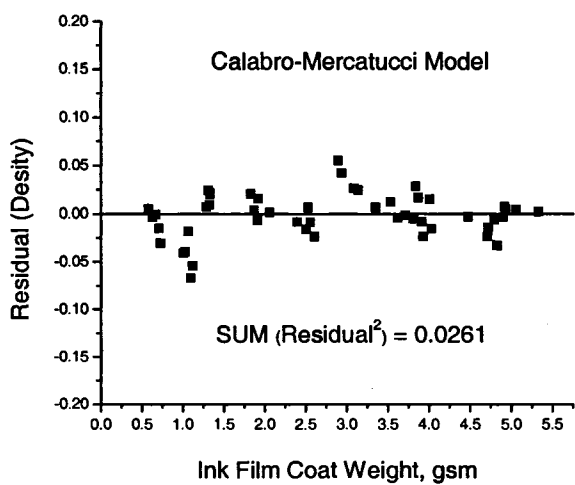


Figure 29. Curve fitting results of cyan ink film on sample 1 using Oittinen model.

The residual values obtained from curve fitting of all paper samples were plotted against ink film coat weight. The degree of fit of an equation to the experimental data can be determined by the sum of the square of residuals and the distribution of residuals around zero. A small sum of the square of residuals and an even distribution indicate a good fit. The residual plots of all six models are compared in Figure 30. The comparison indicates that three-parameter models Oittinen model,

Calabro-Savagnone model, and Kornerup-Fink-Jensen-Rosted model fit, as expected, the experimental data much better than their two-parameter correspondents Tollenaar-Ernst model, Calabro-Mercatucci model, and Blom model. Both Oittinen model and Calabro-Savagnone model have minimal sum of the square of residuals (0.00887 and 0.00768, respectively) and even distribution of residuals around zero, which means they fit the experimental data better than the other four models. Therefore, these two models were used to study the effects of paper physical properties on ink mileage characteristics. The Oittinen model was found not good enough in previous studies (Chou and Harbin, 1991), but it appears a good fit here.





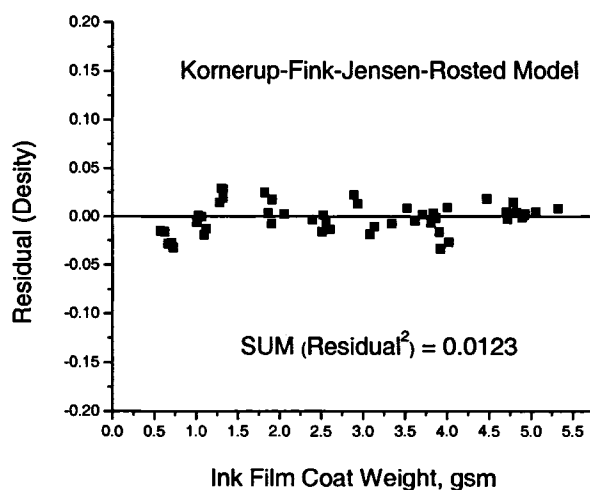


Figure 30. Sum of the square of reflection density residuals and their distributions for various models.

Effects of Paper Physical Properties on Ink Mileage Characteristics

The Oittinen model and Calabro-Savagnone model were used to further study the effects of paper physical properties on ink mileage characteristics. The ink mileage curves of five samples obtained by non-linear fitting using these two models are shown in Figure 31 – 34. These curves have close initial slopes at low ink film coat weight, and the slopes change differently as ink film coat weight increases for different samples.

The regression coefficients, D_s , m , n , derived from curve fitting for Oittinen model and Calabro-Savagnone models are listed in Table 20 and Table 21. Saturation density D_s values derived from Calabro-Savagnone model are higher than those from Oittinen model. D_s values of cyan ink films are higher than those of magenta ink films. Since these two inks have different rheological and other properties, as well as different cell geometries on gravure cylinders (compressed for cyan and elongated for

magenta), it is not practical to conclude based on one printing trial. More experimental results are needed to compare these two inks.

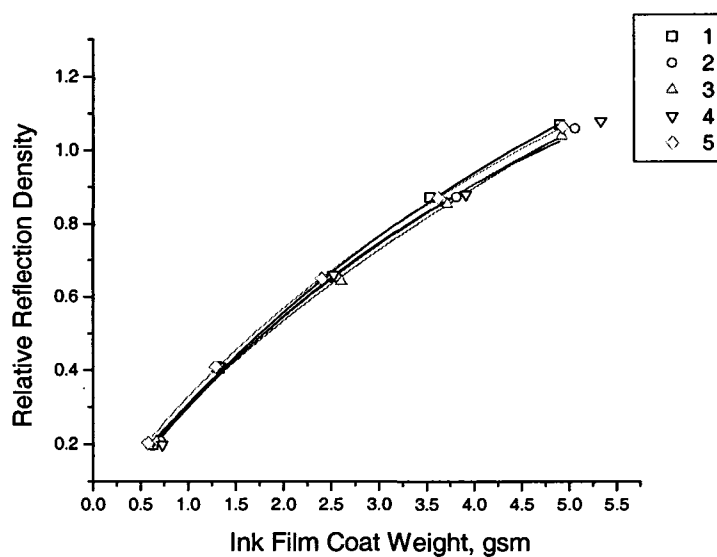


Figure 31. Ink mileage curves of cyan ink film using Oittinen model.

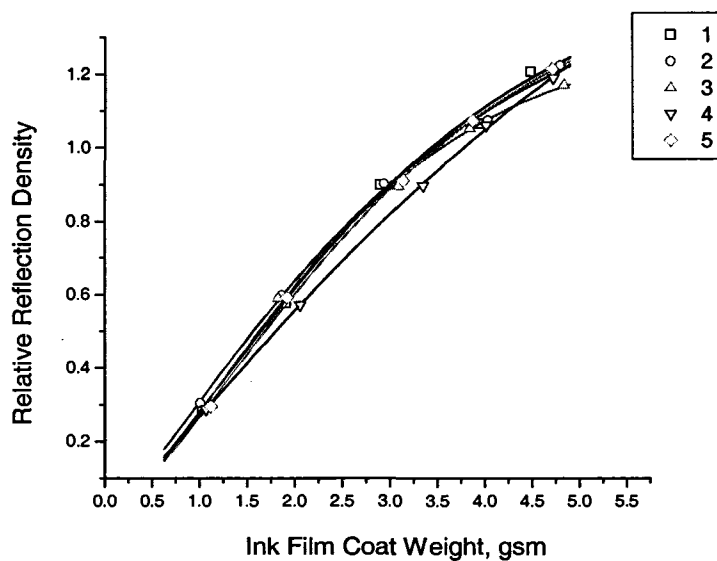


Figure 32. Ink mileage curves of magenta ink film using Oittinen model.

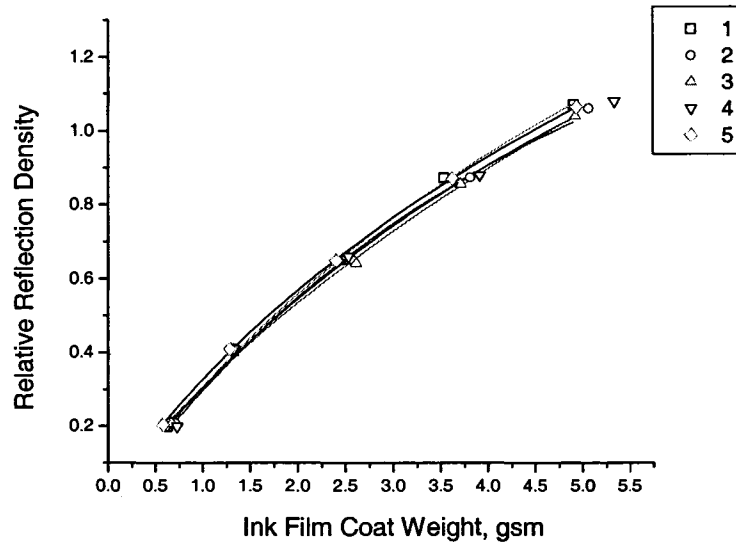


Figure 33. Ink mileage curves of cyan ink film using Calabro-Savagnone model.

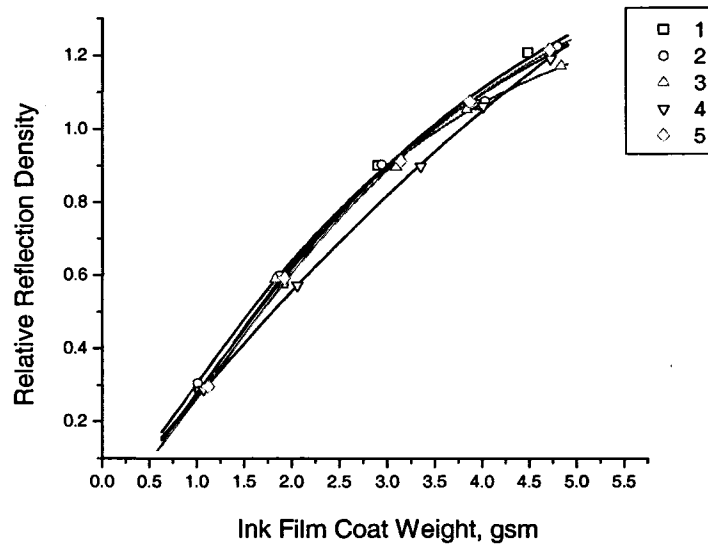


Figure 34. Ink mileage curves of magenta ink film using Calabro-Savagnone model.

Table 20
Regression coefficients of Oittinen model

Paper		Cyan			Magenta		
Sample No.	D _s	m	n	D _s	m	n	
1	1.904	0.176	0.975	1.491	0.208	1.361	
2	1.872	0.177	0.952	1.478	0.233	1.271	
3	2.981	0.109	0.862	1.296	0.241	1.435	
4	1.524	0.218	1.029	2.075	0.138	1.179	
5	2.044	0.175	0.901	1.477	0.199	1.388	

Table 21
Regression coefficients of Calabro-Savagnone model

Paper		Cyan			Magenta		
Sample No.	D _s	m	n	D _s	m	n	
1	2.957	2.910	1.001	1.979	2.143	1.488	
2	2.785	2.960	0.991	1.904	2.052	1.419	
3	4.985	3.601	0.873	1.547	1.931	1.709	
4	2.080	2.604	1.108	3.184	2.767	1.215	
5	3.207	2.981	0.923	1.888	2.153	1.558	

The correlations between paper characteristics and regression coefficients for both models are shown in Table 22 and Table 23.

Table 22

Correlation matrix of regression coefficients of Oittinen model

	Cyan			Magenta		
	D_s	m	n	D_s	m	n
PPS Roughness	0.017	-0.156	0.061	-0.432	0.440	0.293
Profil. Roughness	-0.006	0.111	0.058	0.433	-0.285	-0.483
AFM Roughness	-0.556	0.563	0.283	0.386	-0.271	-0.606
PPS Porosity	-0.994	0.998	0.892	0.811	-0.780	-0.840
Pore Size	-0.617	0.738	0.652	0.945	-0.944	-0.765

Table 23

Correlation matrix of regression coefficients of Calabro-Savagnone model

	Cyan			Magenta		
	D_s	m	n	D_s	m	n
PPS Roughness	0.049	0.079	-0.076	-0.408	-0.450	0.210
Profil. Roughness	-0.054	-0.028	0.195	0.414	0.395	-0.319
AFM Roughness	-0.579	-0.512	0.356	0.355	0.326	-0.539
PPS Porosity	-0.995	-0.997	0.894	0.804	0.786	-0.927
Pore Size	-0.640	-0.693	0.740	0.936	0.957	-0.784

It is apparent that for both cyan and magenta inks, permeability and pore size have more effects on the D_s , m, and n parameters than roughness. Pauler (1988) pointed out the importance of ink penetration to the shape of the ink mileage curve and proposed a model to study the effect of different paper structures on ink

penetration. Permeability and pore size are the main factors for ink penetration, therefore, have effects on ink mileage characteristics.

It should be noticed that the effects of paper characteristics on ink mileage parameters of cyan and magenta inks are reverse to each other. The particle size distributions of ink pigments were measured and shown in Figure 35. The mean diameter of magenta ink pigments is 227.0 nm, while that of cyan is 306.5 nm. The average pore sizes of coating layer of five samples are between 100.3 nm to 233.1 nm. For magenta ink film, larger pore size resulted in lower density smoothness, which is parameter m , since more ink pigments entered the pores. For cyan ink film, larger pore size resulted in higher density smoothness, because of more close packing of ink pigments with coating pigments. However, the pore size can not be too big for cyan ink pigments to enter.

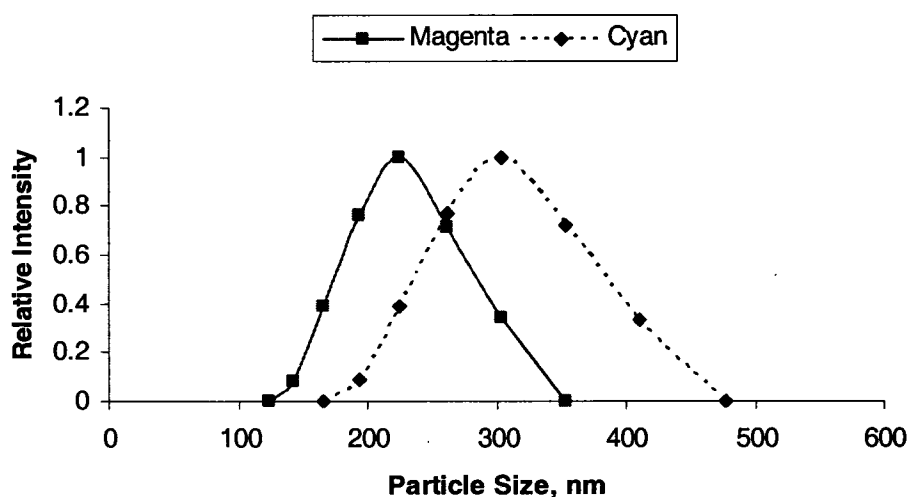


Figure 35. Particle size distributions of magenta and cyan ink pigments.

Comparison of Cyan and Magenta Ink Mileage Curves

The ink mileages curves of both cyan and magenta inks for sample 1 using Oittinen model are compared in Figure 36. The density of magenta ink film approached saturation density faster than that of cyan ink film. Magenta ink has higher ink mileage than cyan ink in mid to high ink film thickness region. Magenta ink pigments are smaller than cyan ink pigments. At low ink film coat weights, more magenta ink pigments were lost in the pores of coating layer than cyan ink pigments, so the reflection density of magenta ink film was lower than that of cyan ink film.

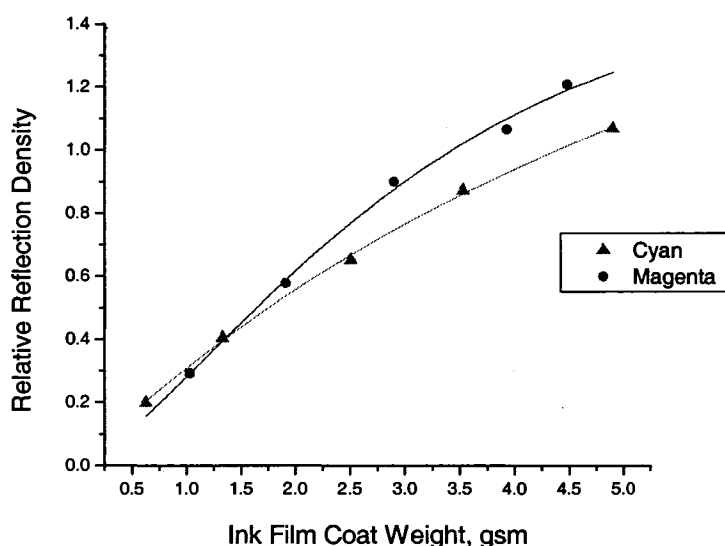


Figure 36. Cyan and magenta ink mileage curves of sample 1.

CHAPTER V

CONCLUSIONS

Inkjet printing is non-impact printing, not like the classical printing processes with contact pressure, so the ink film surface topography mainly depends on the substrate surface. Among the three roughness measurement methods used for inkjet papers, AFM roughness and profilometer roughness showed higher correlations with paper gloss. AFM roughness and profilometer roughness also have high correlation with print gloss at both 60° and 75° for all three printers. The highest correlation of nearly 100% to print gloss is with AFM roughness printed by the Photo 2200 printer.

Pigment-based and dye-based inks have different effects on print gloss of microporous Epson papers and resinous Kodak papers. Higher print gloss was found with the Pro 5500 and Photo 2200 printers using pigment-based inks than the Pro 5000 printer using dye-based inks for Epson papers. On the contrary, the ink types had less effect on print gloss for Kodak papers. However, higher correlation exists between paper gloss and print gloss printed by Pro 5000 printer.

The black ink film surface printed on Epson Glossy paper was studied using AFM. Dyed ink films resulted in smoother ink film surface than pigmented ones. The attempt to measure ink film thickness using AFM did not succeed, due to the wide boundary between paper substrate and ink film. The ink film thickness is roughly around 150 nm.

In gravure printing, AFM roughness also showed the best correlation with both 60° and 75° paper and print gloss, while PPS roughness the worst. The size of a black half-tone dot is only about 30 μm . Therefore, microroughness measured by

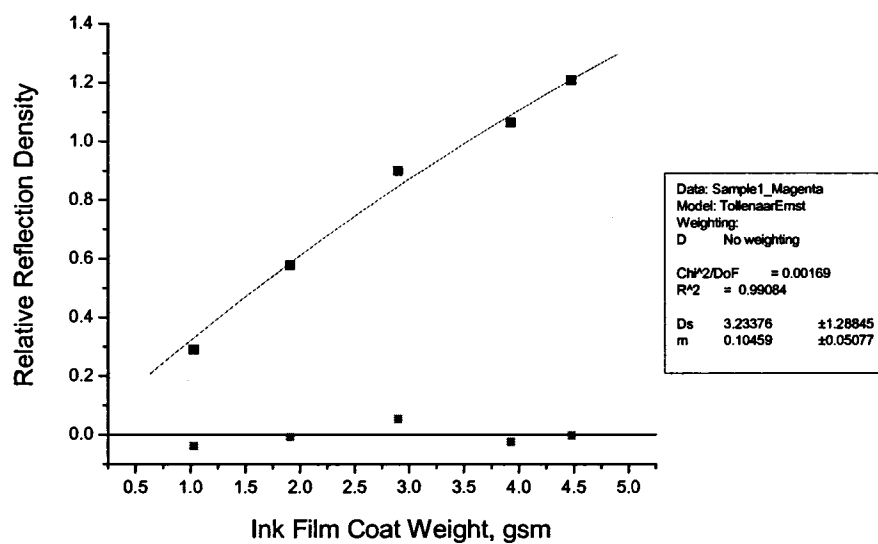
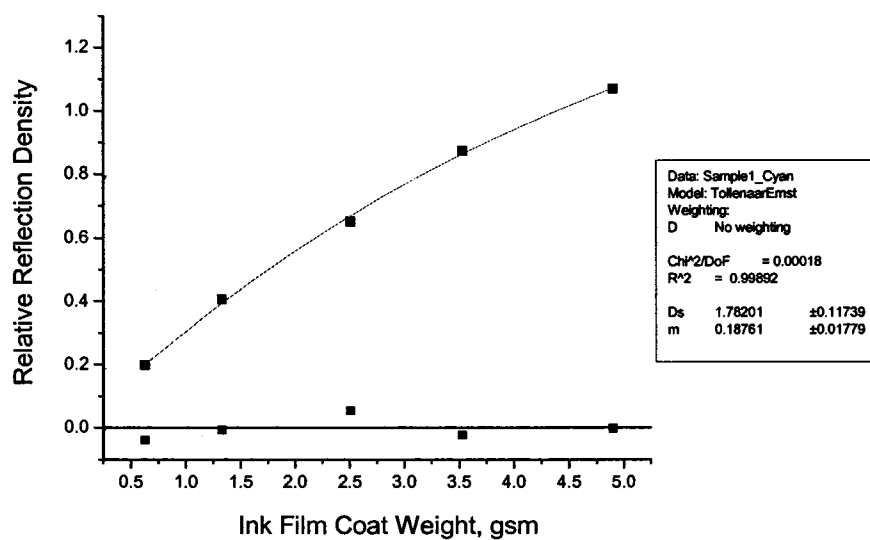
AFM correlates better with print gloss than macroroughness measured by PPS and profilometer.

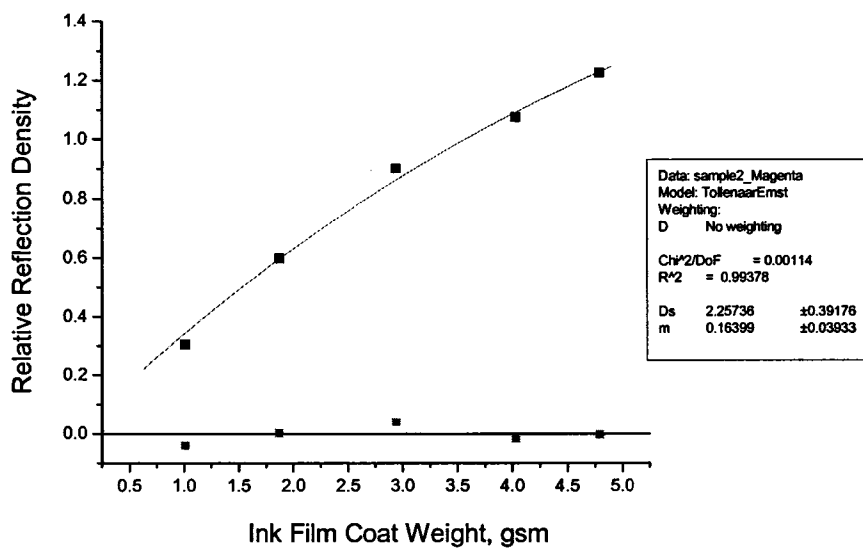
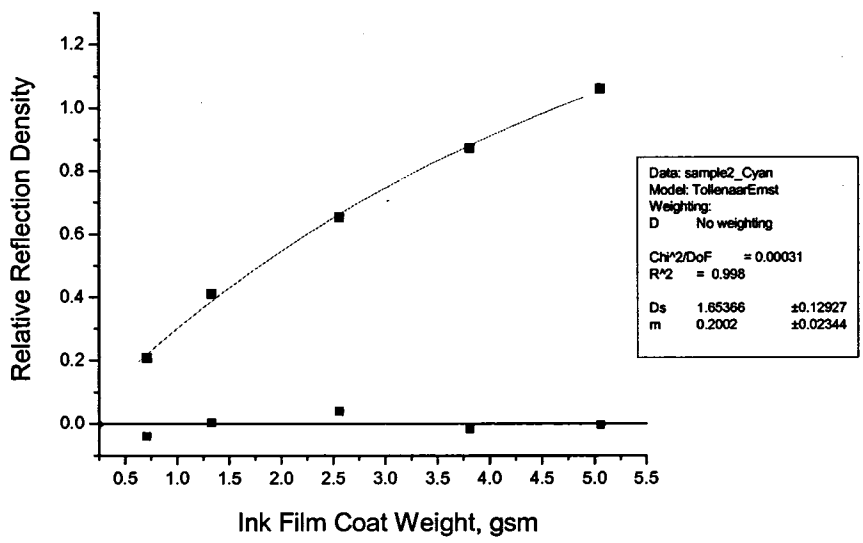
The internal tracer method has proven to be a convenient analytical method to measure ink film coat weight after gravure printing. Ink requirement of black ink is much less than those of cyan and magenta inks.

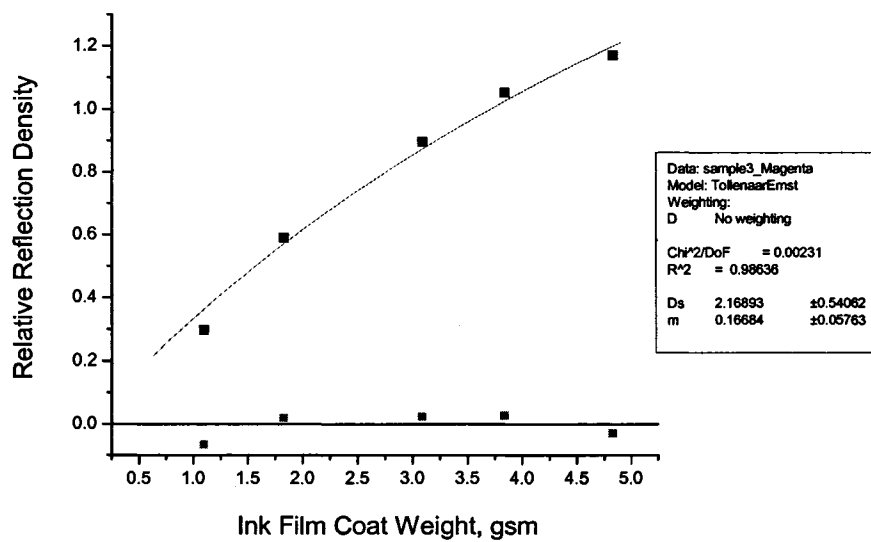
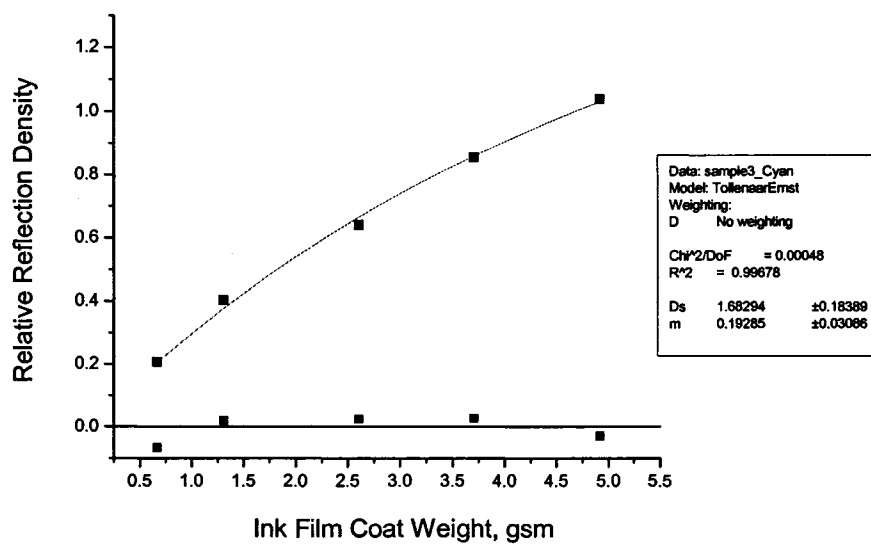
The models for ink mileage curve that were used to fit laboratory results were also found useful to fit pilot plant press results. It was found that Oittinen model and Calabro-Savagnone model fitted the experimental data much better than the other four models, which was evidenced by minimal sum of the square of residuals and their even distribution around zero point. These two models were used to study ink mileage characteristics. The regression coefficients derived from curve fitting were compared and related to paper physical properties. Good correlations were found with permeability and pore size. Magenta ink had higher ink mileage than cyan ink except at very low coat weight.

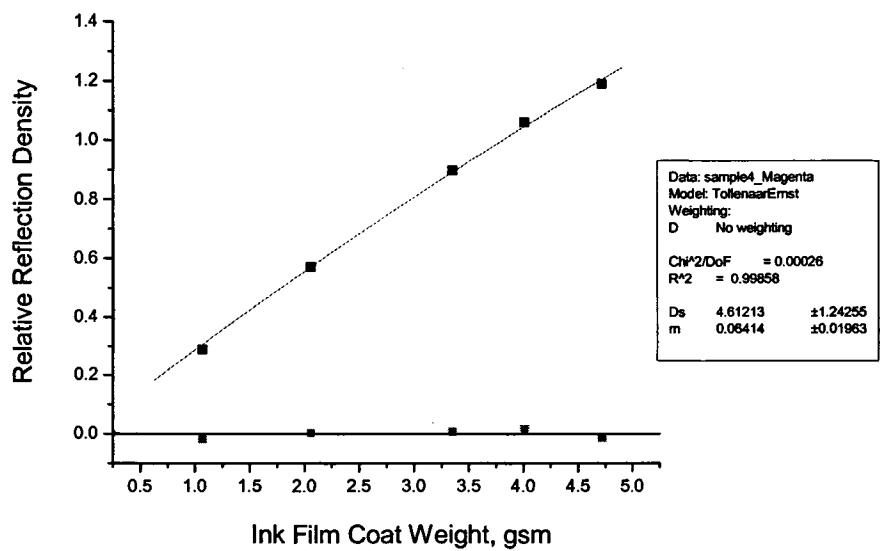
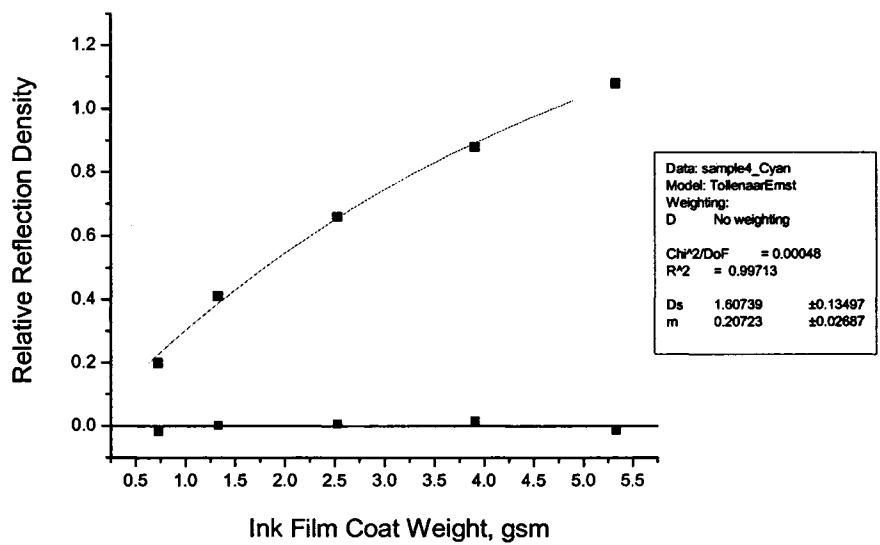
Ink characteristics and printing conditions are also important to ink mileage curves. However, they were not investigated at this step. A clearer understanding will be achieved after more studies. The ultimate goal is that an ink mileage curve can be programmed for the press to adjust ink input as the printing conditions change.

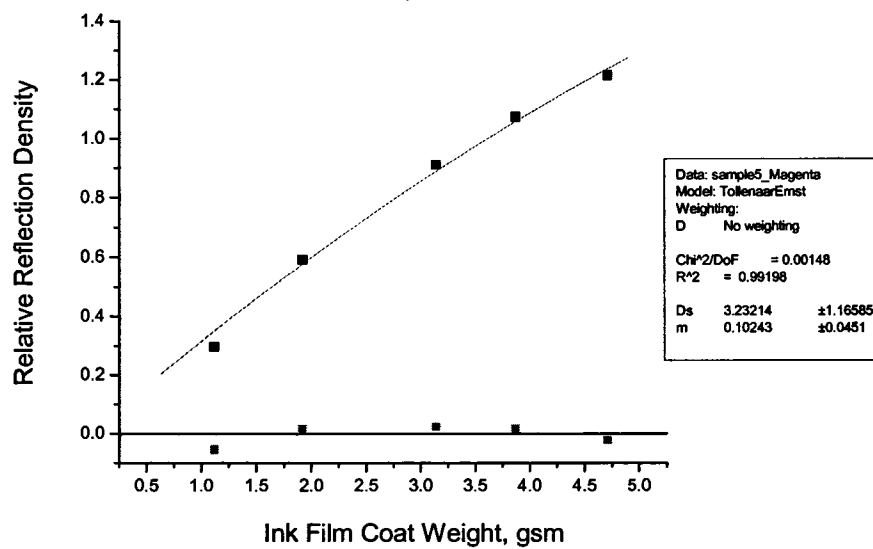
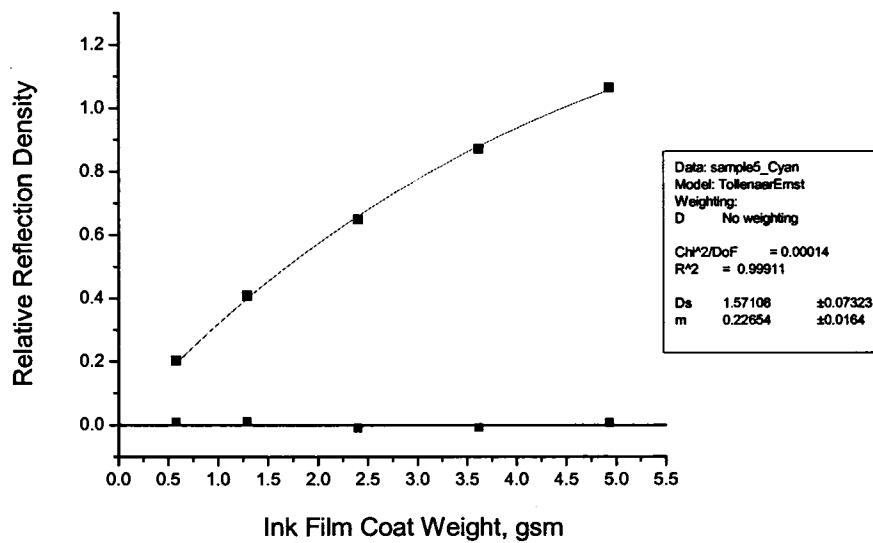
Appendix
Ink Mileage Curve Fitting Results

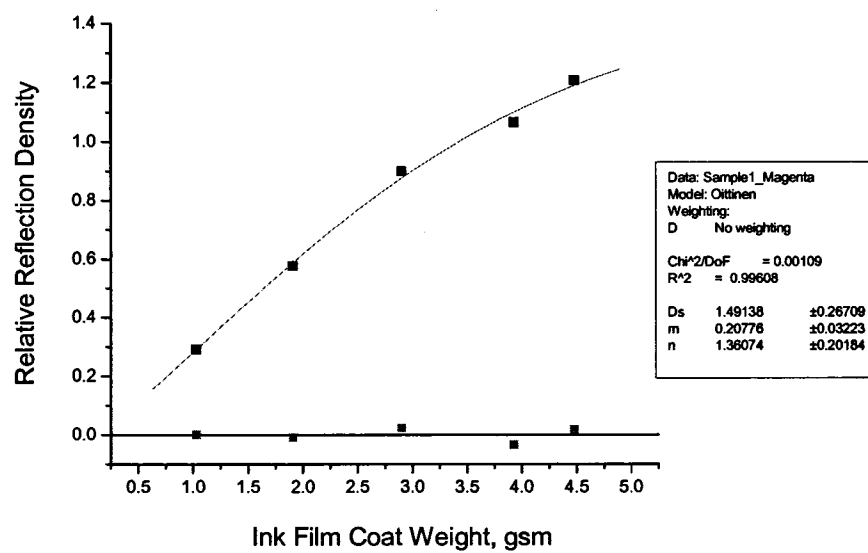
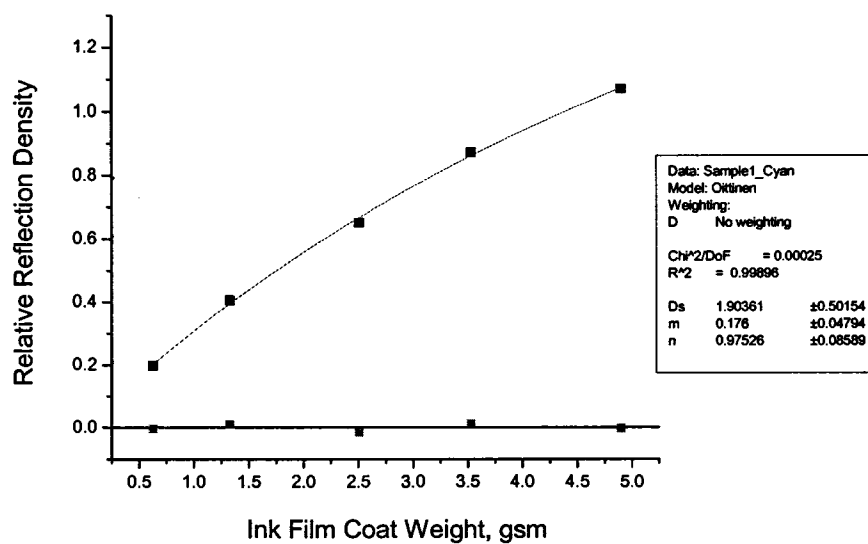


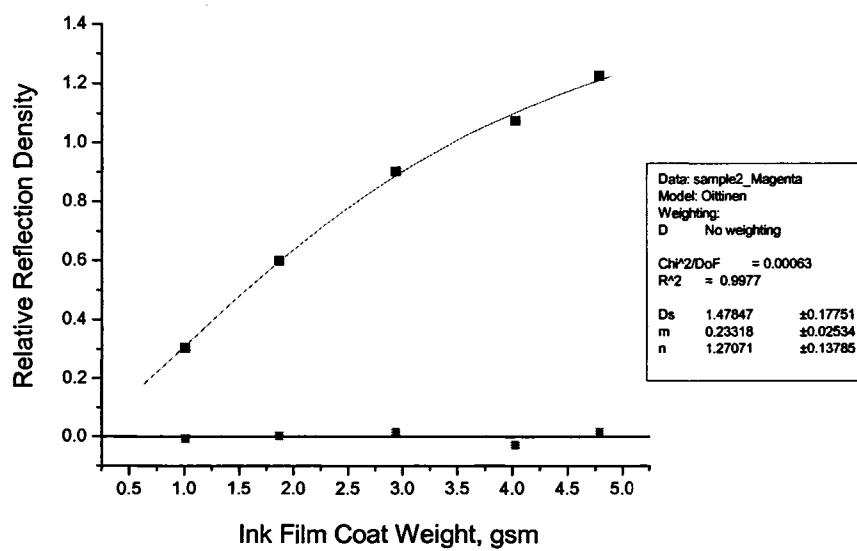
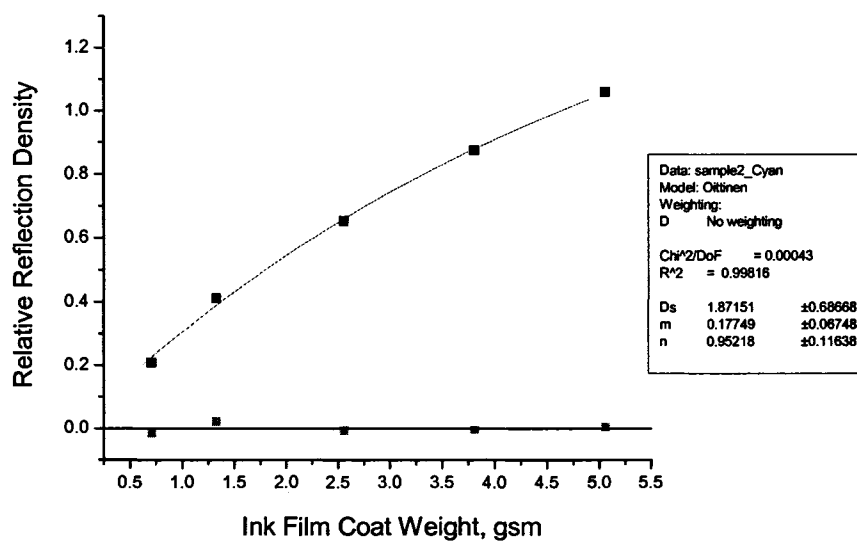


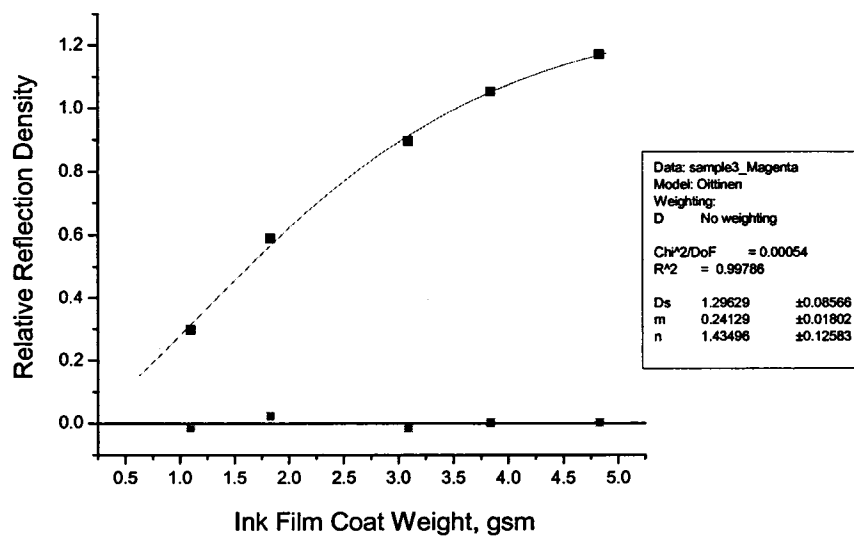
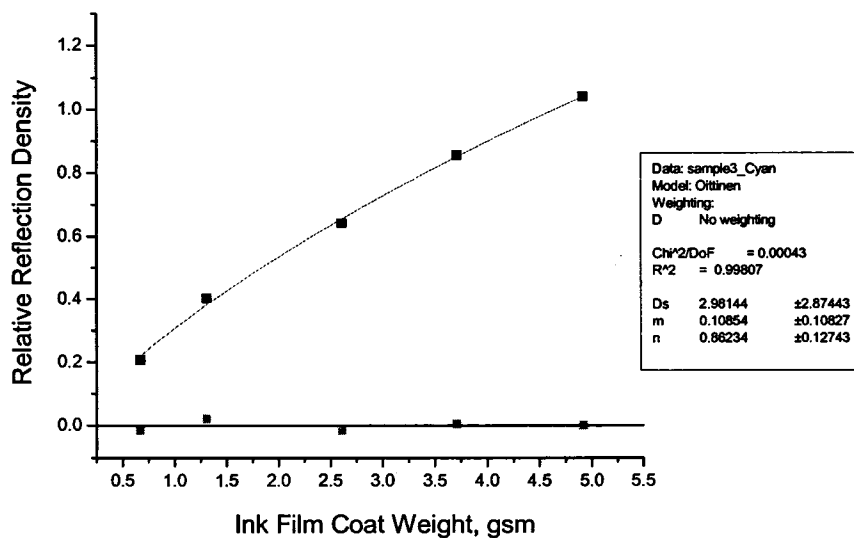


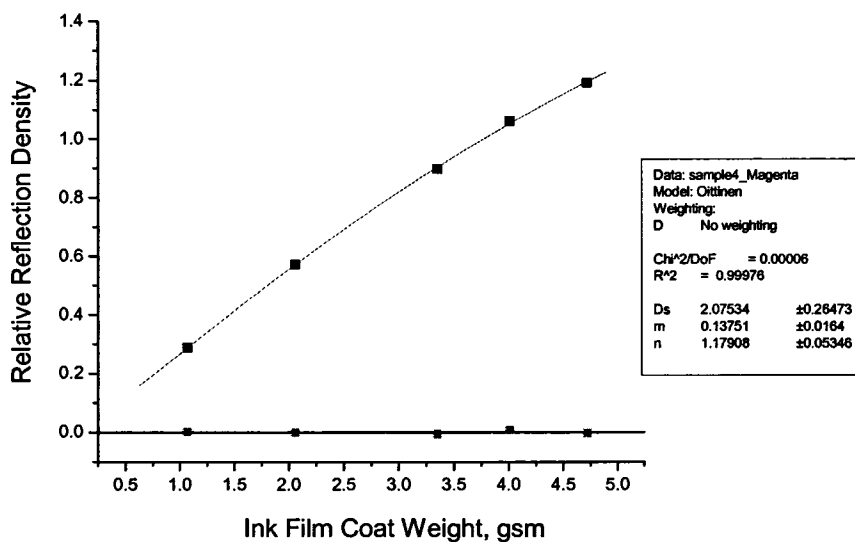
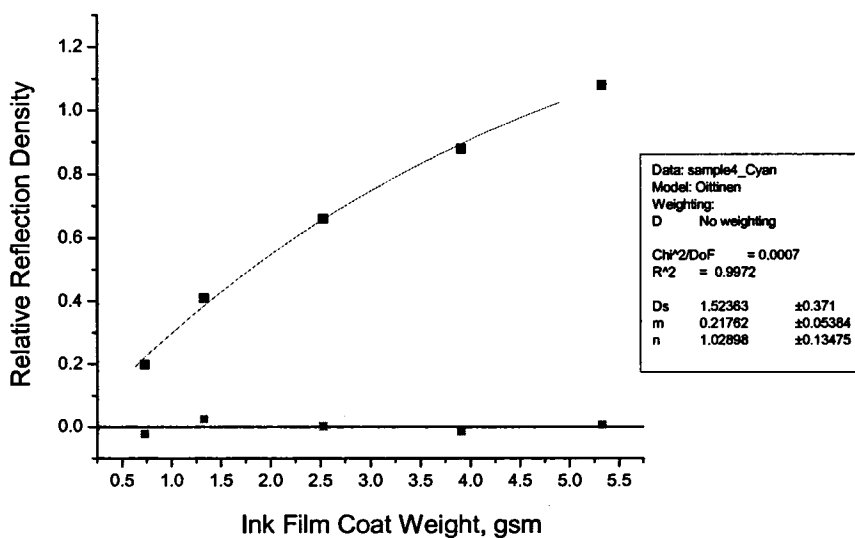


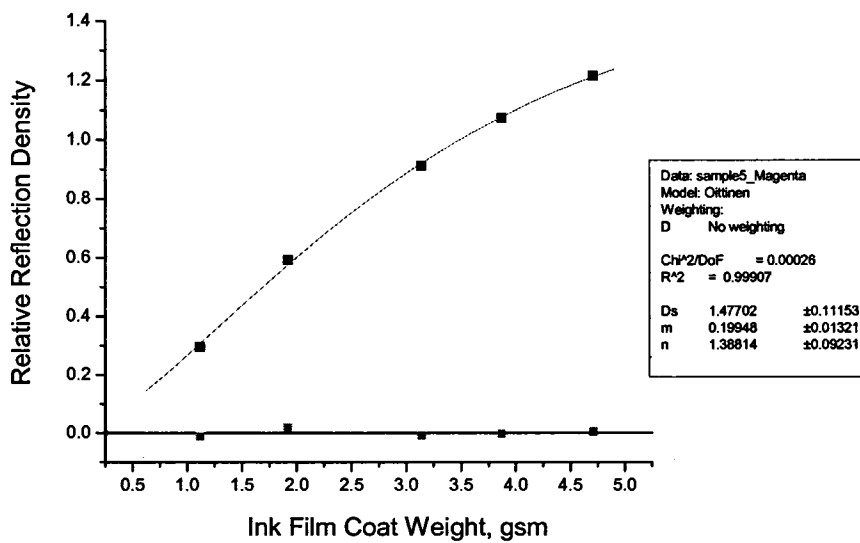
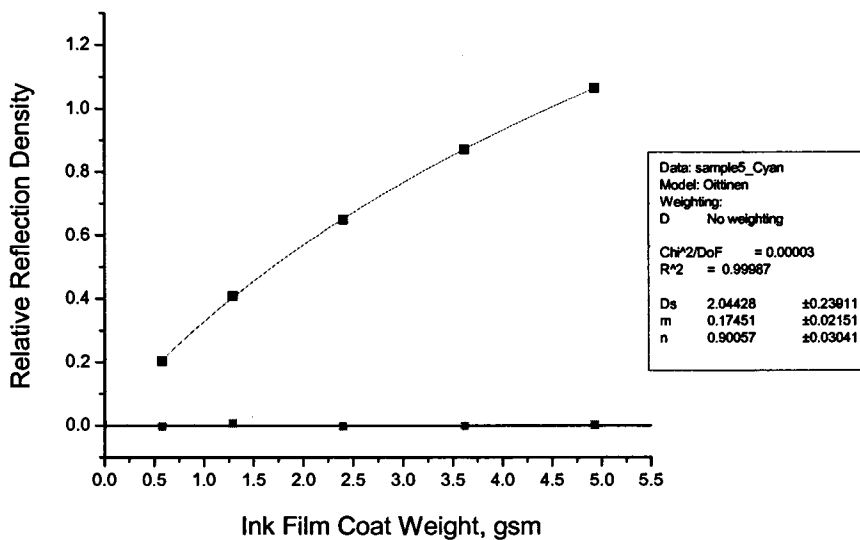


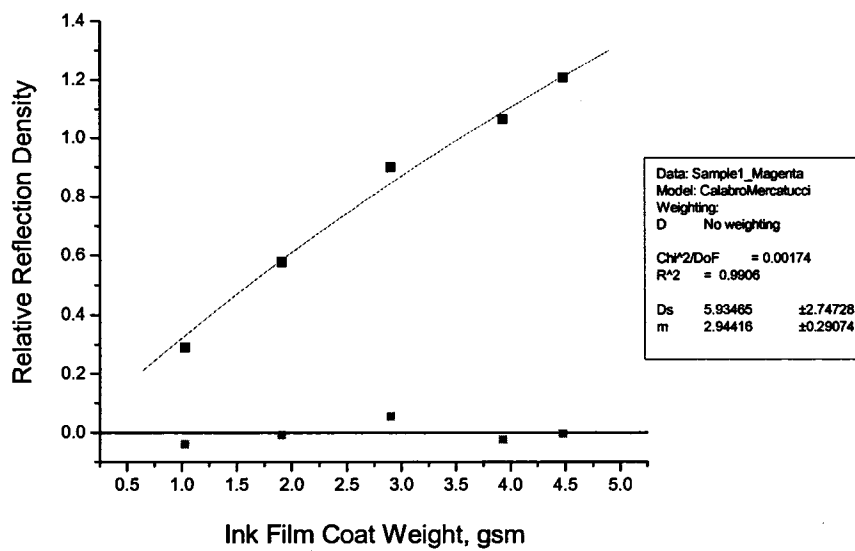
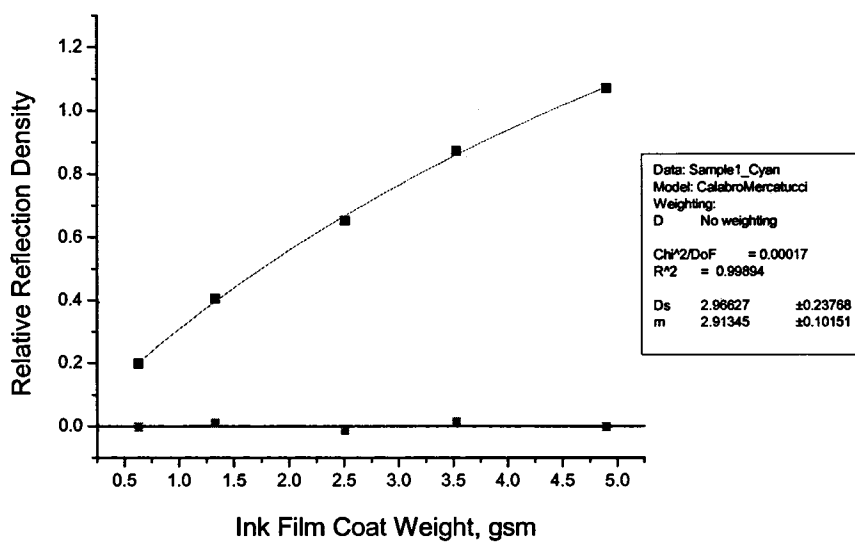


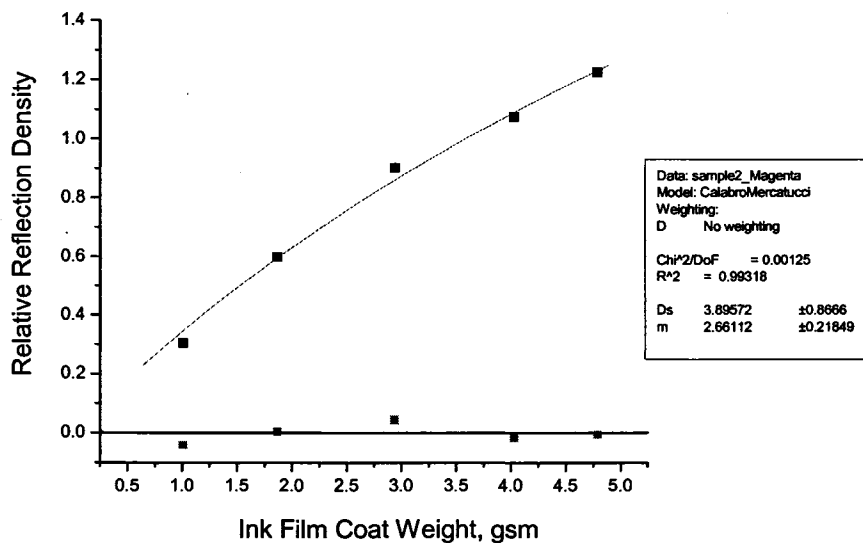
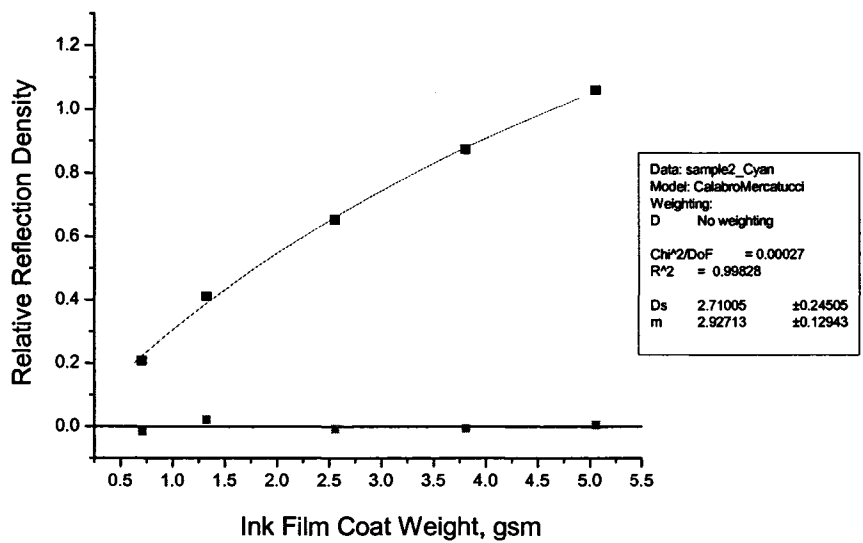


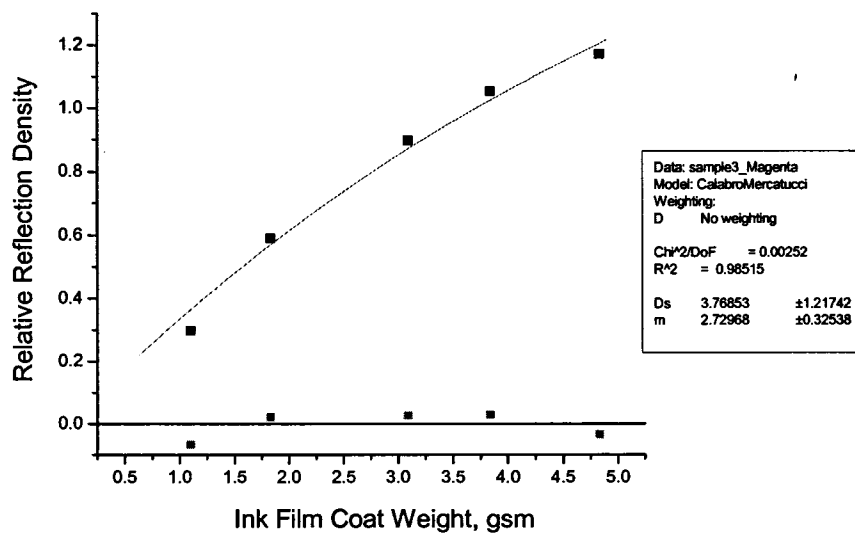
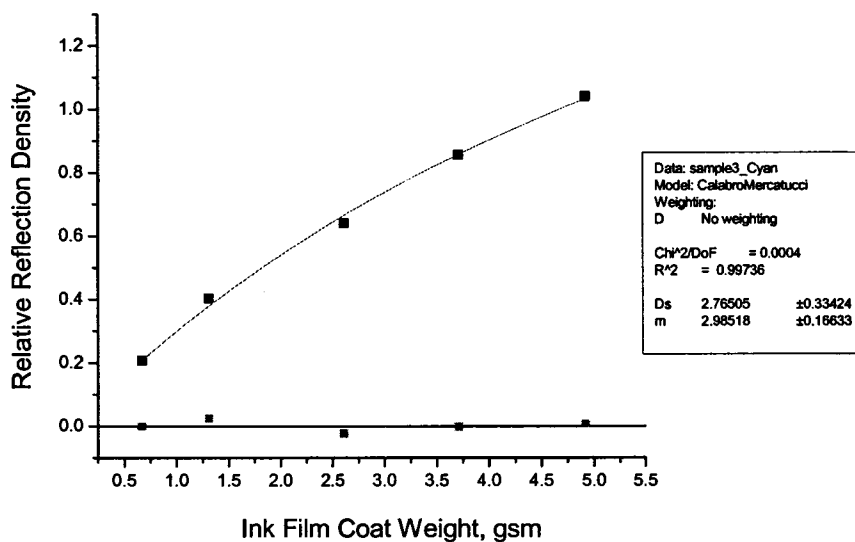


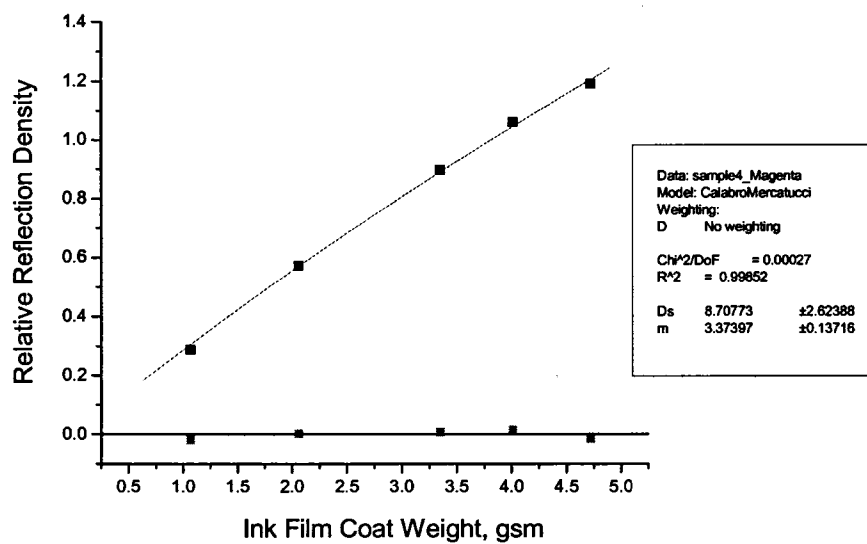
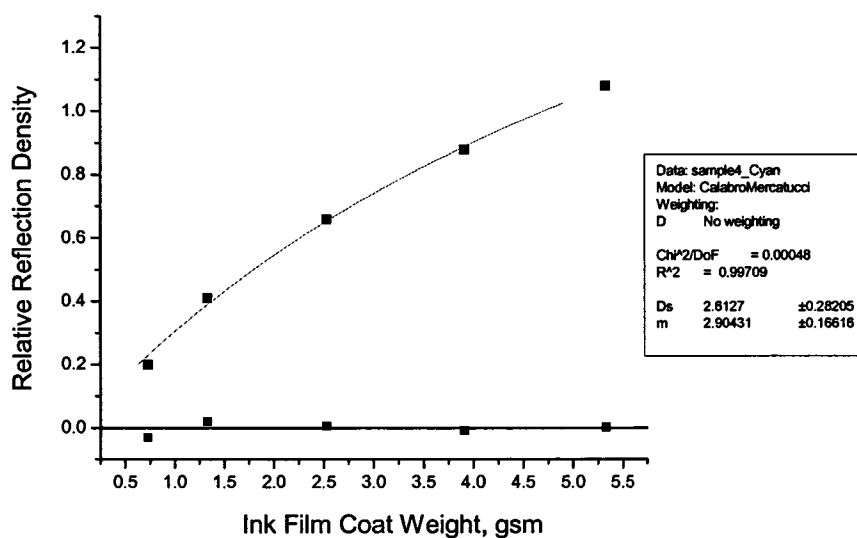


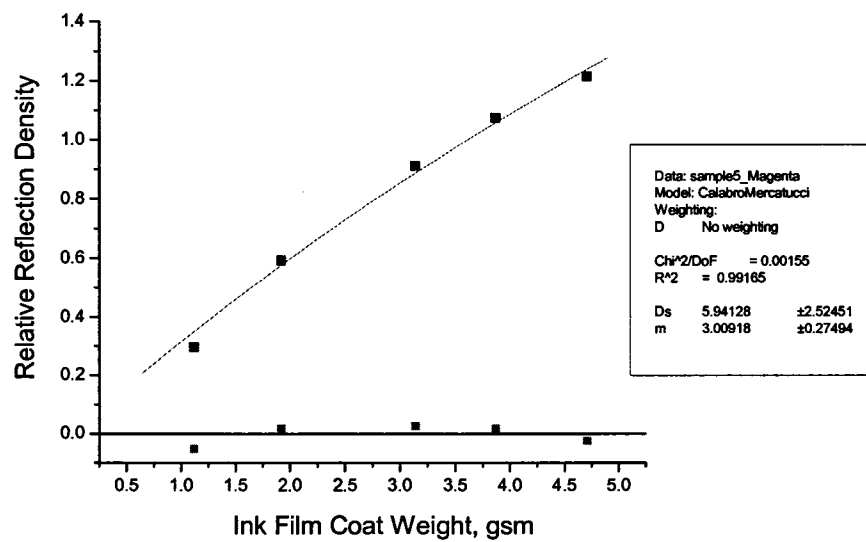
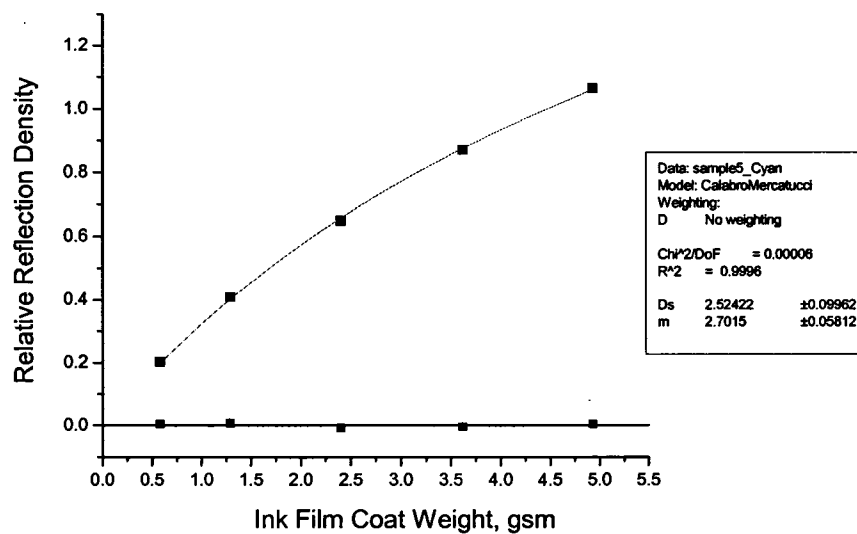


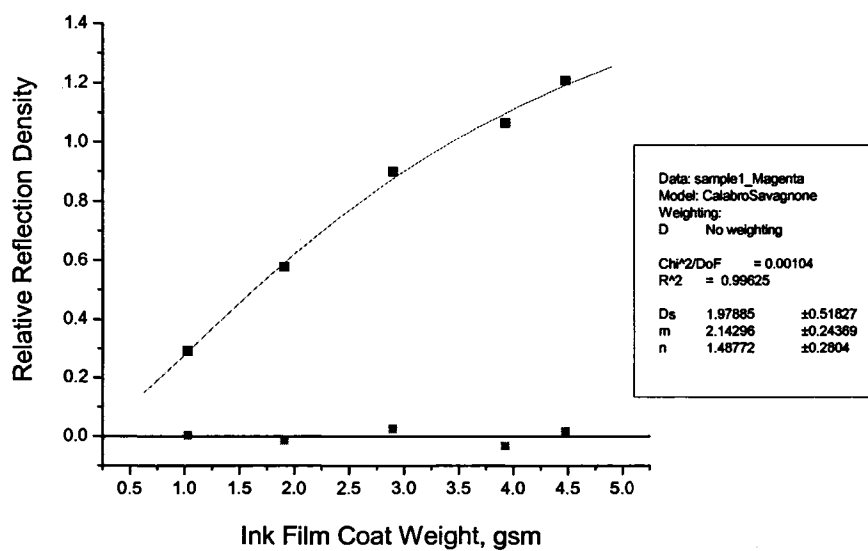
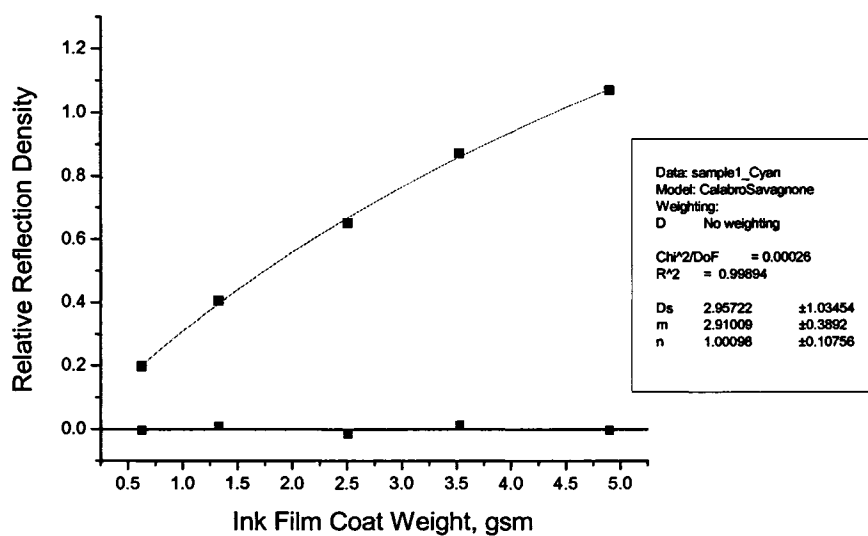


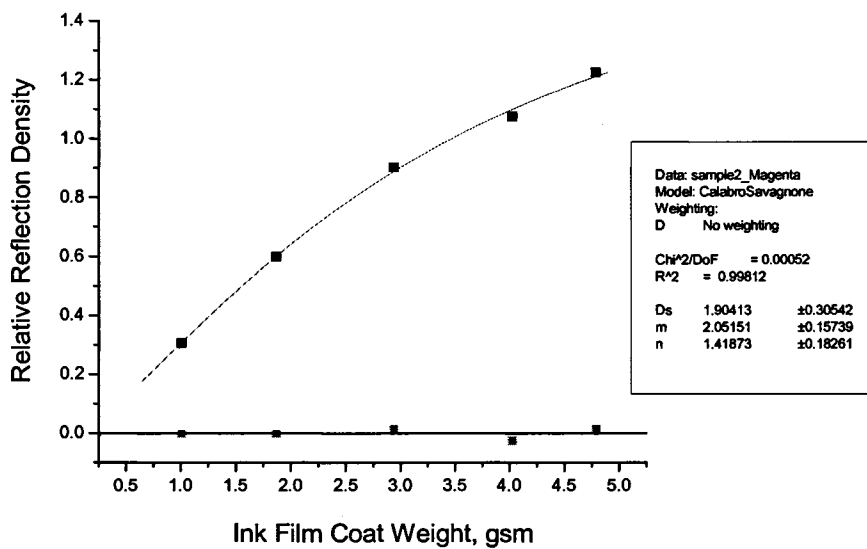
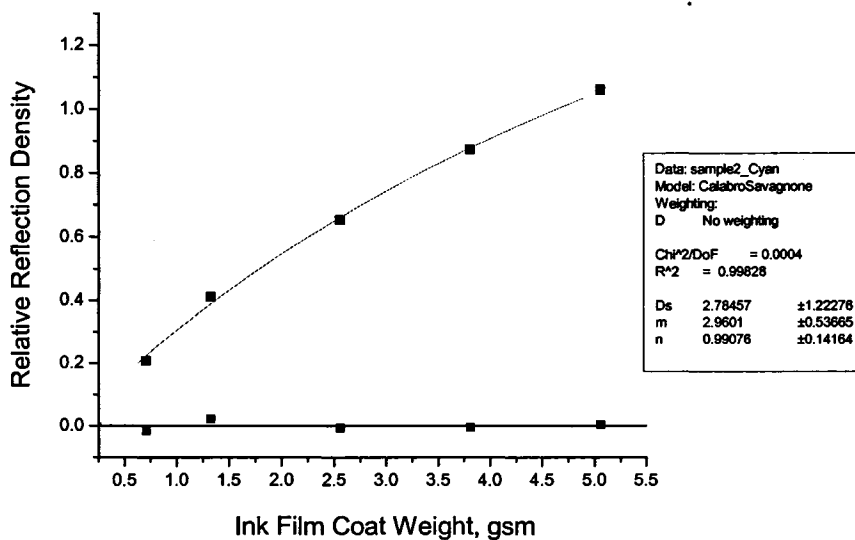


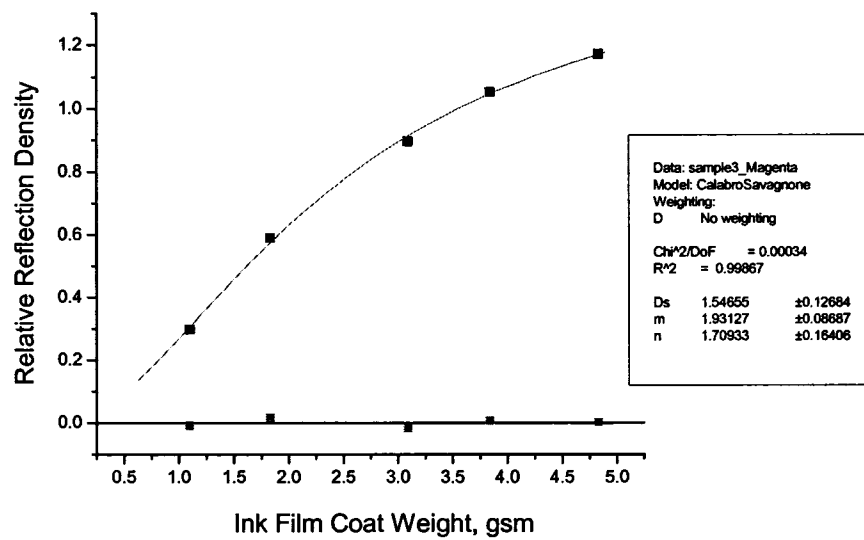
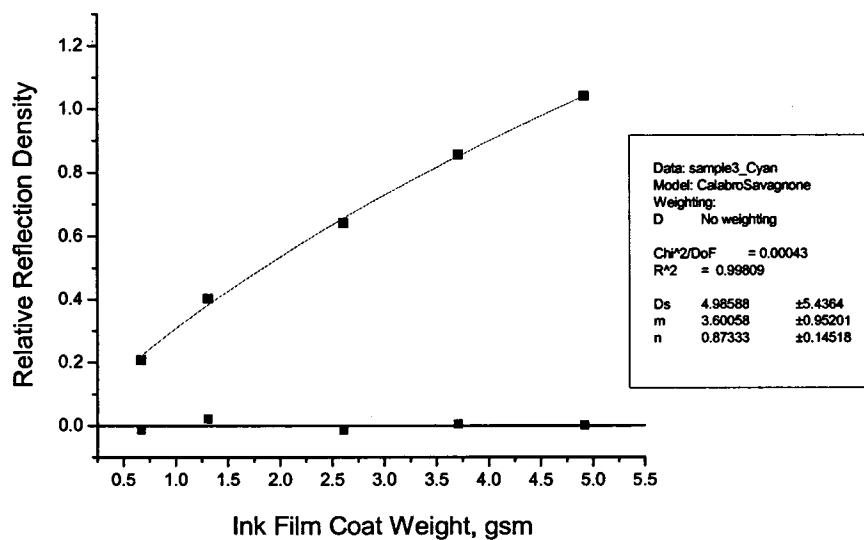


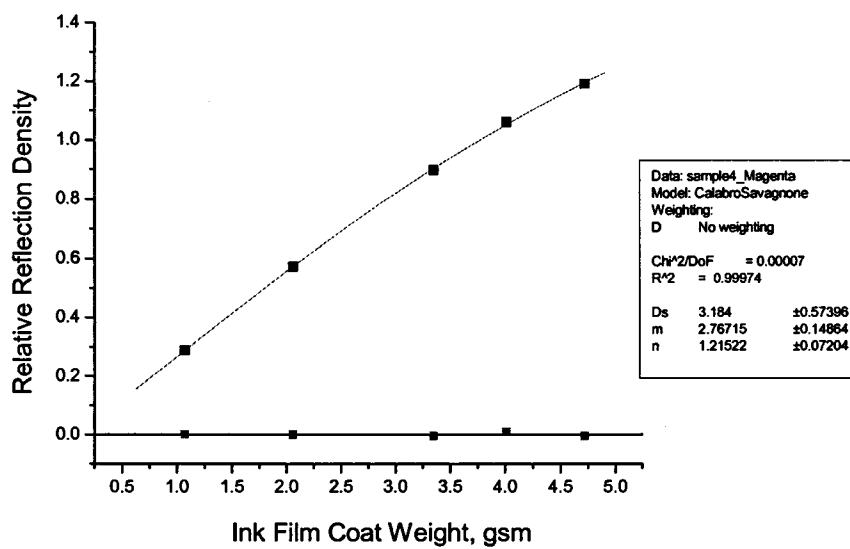
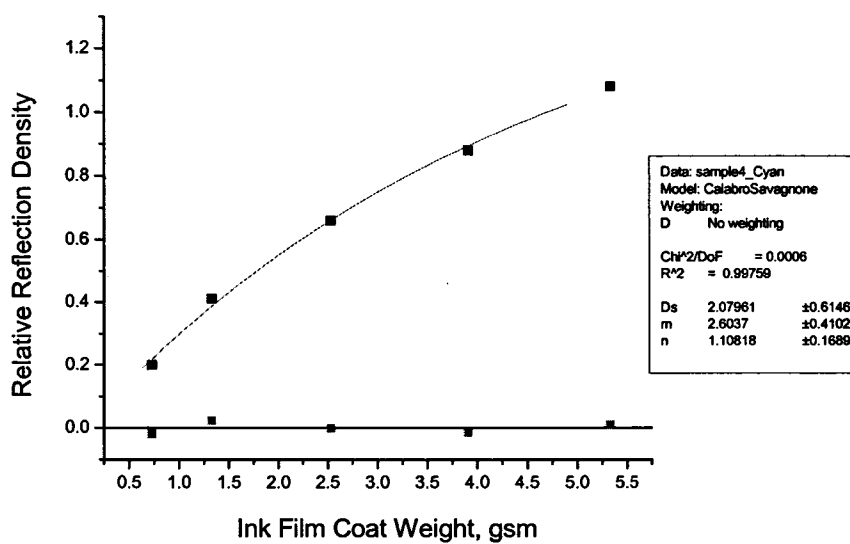


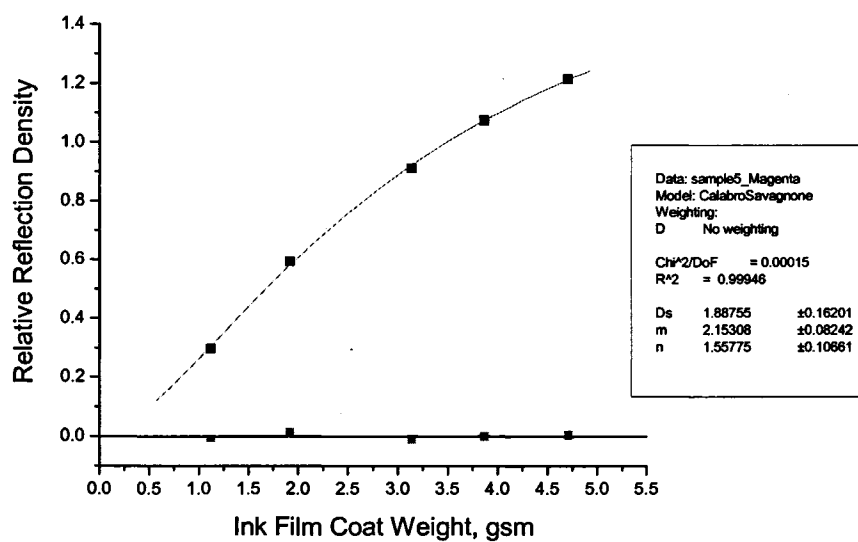
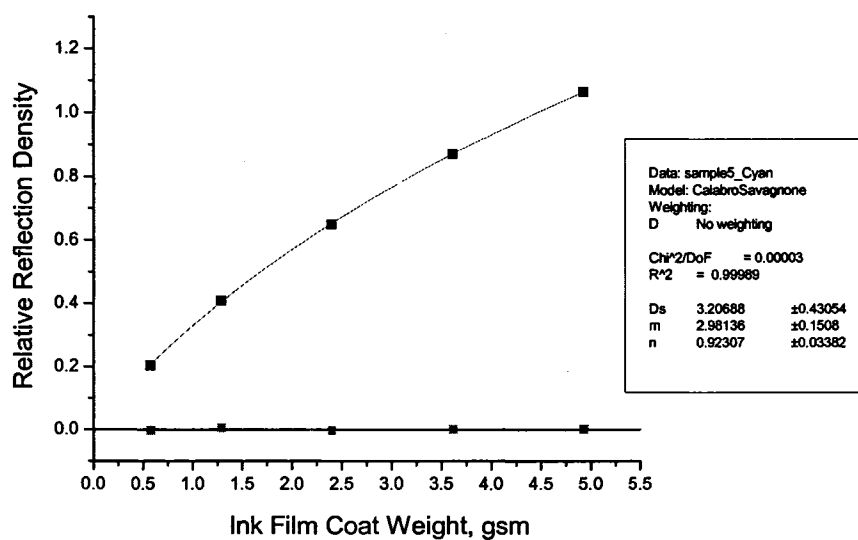


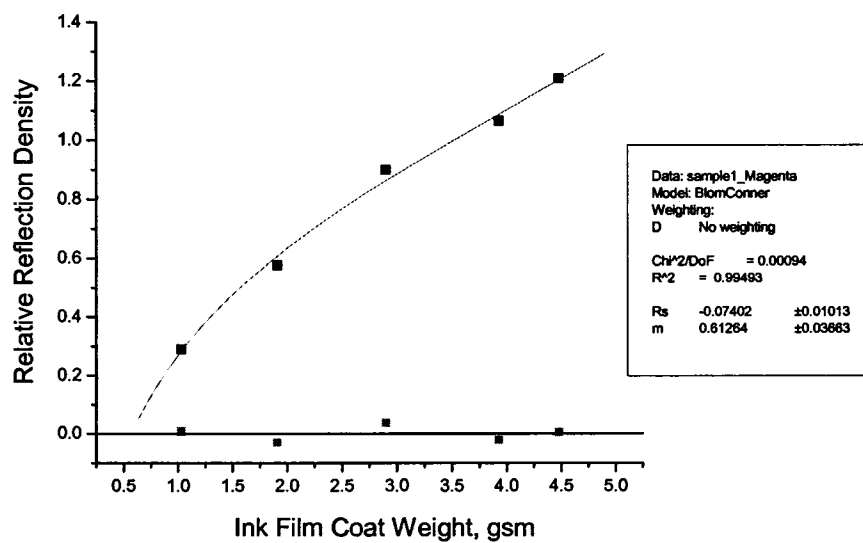
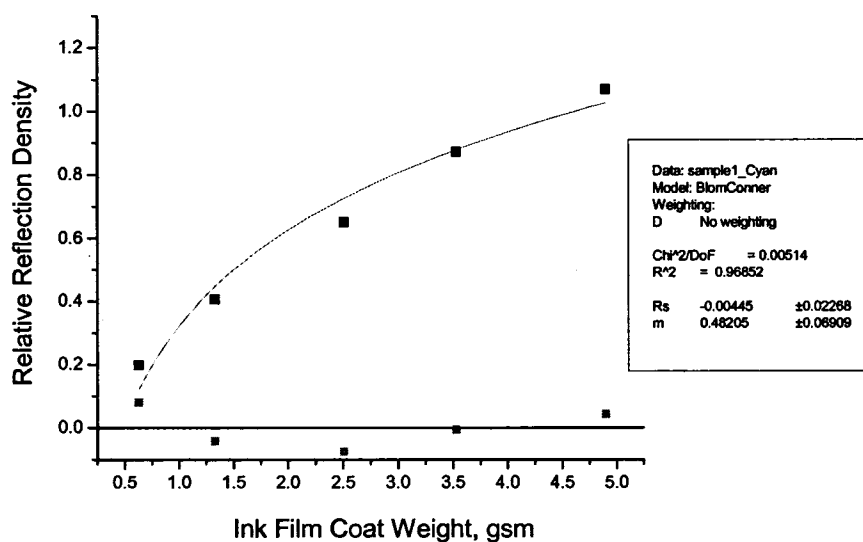


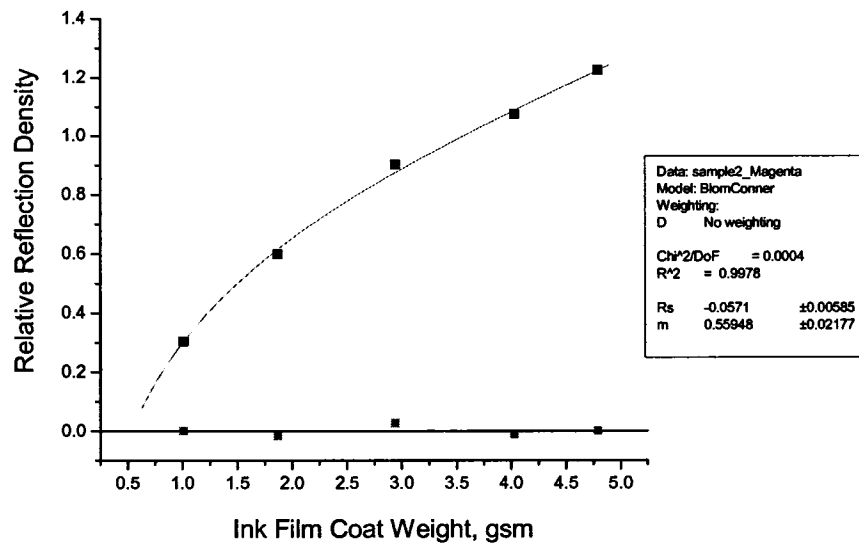
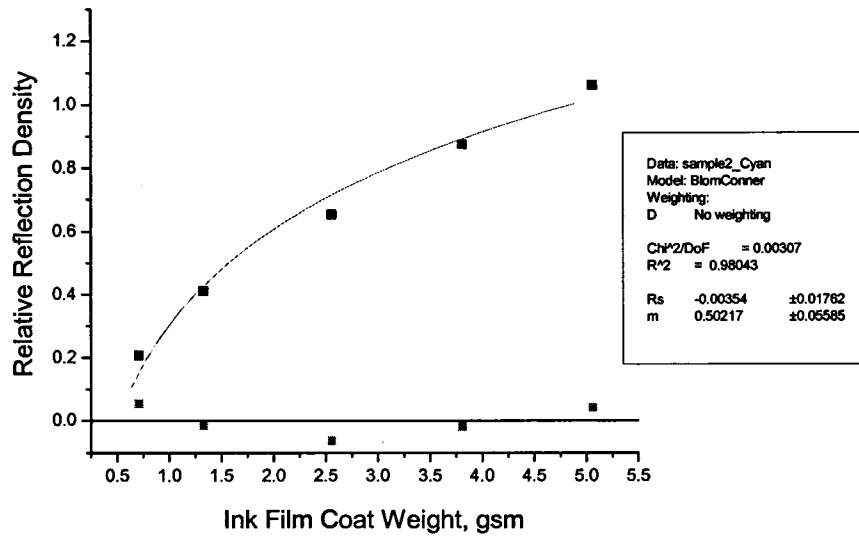


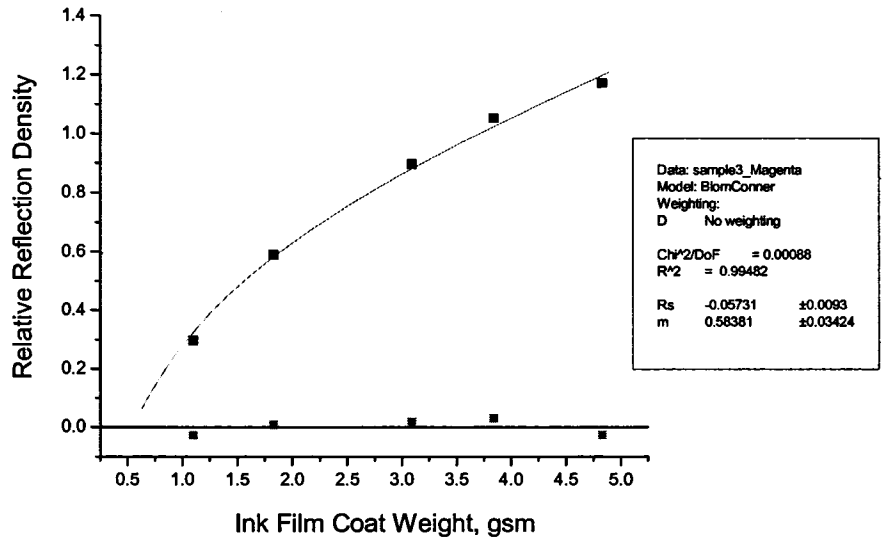
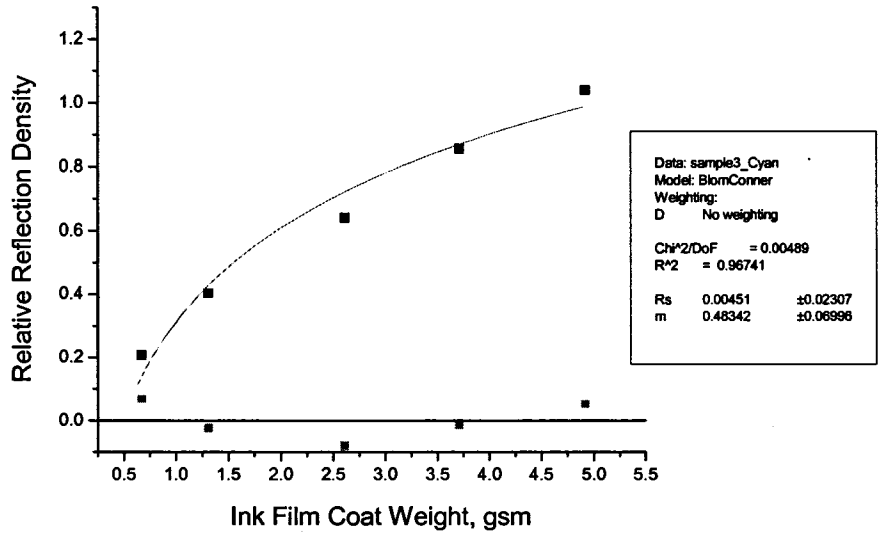


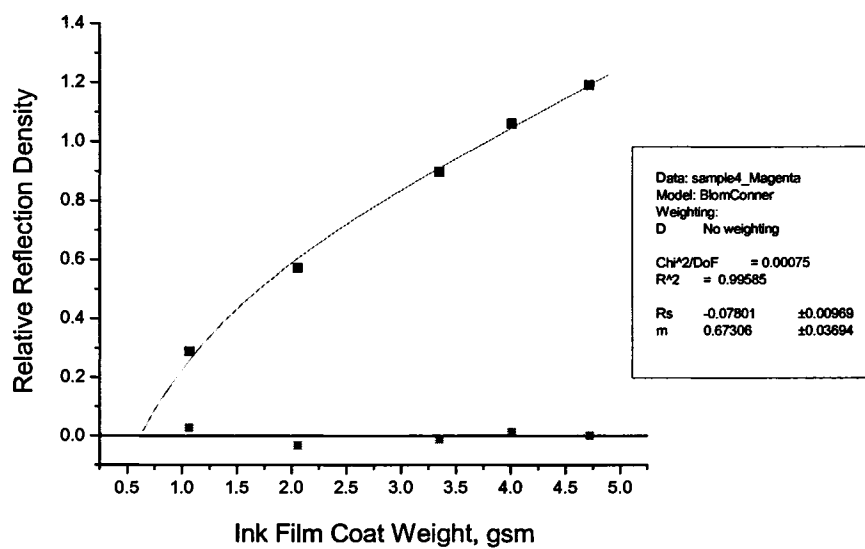
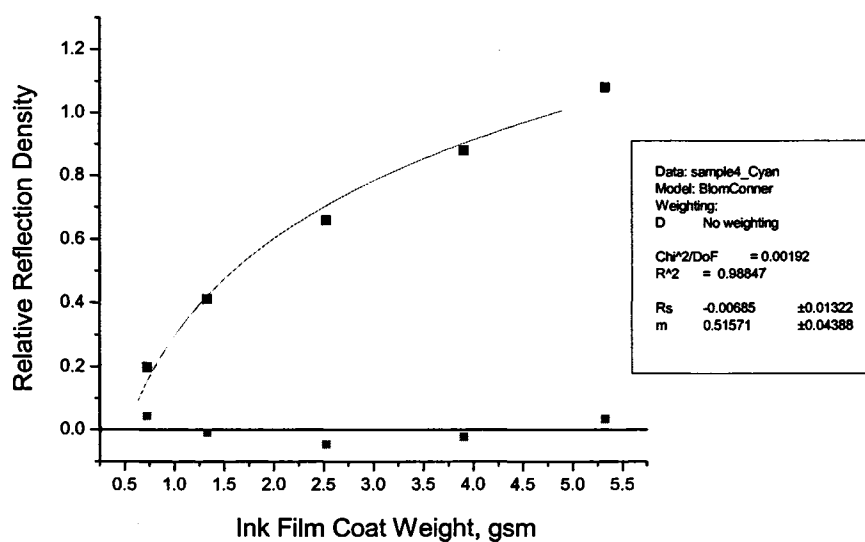


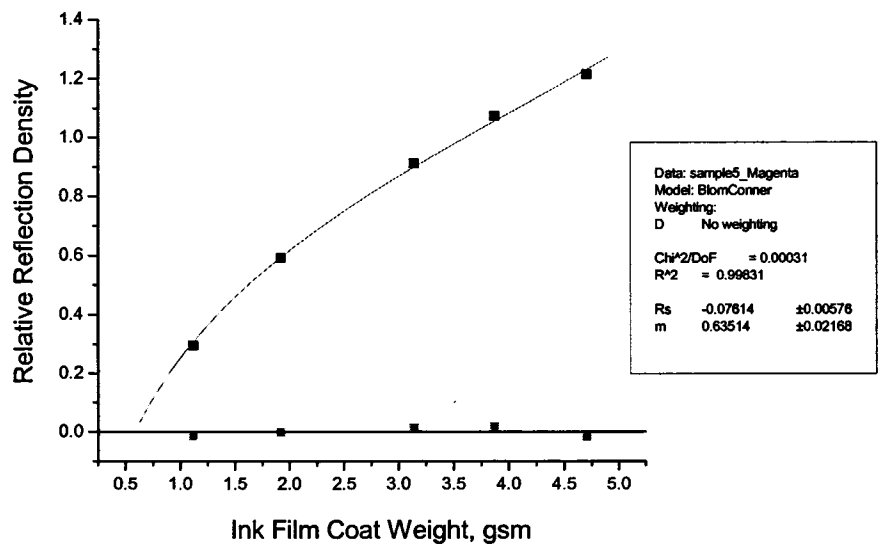
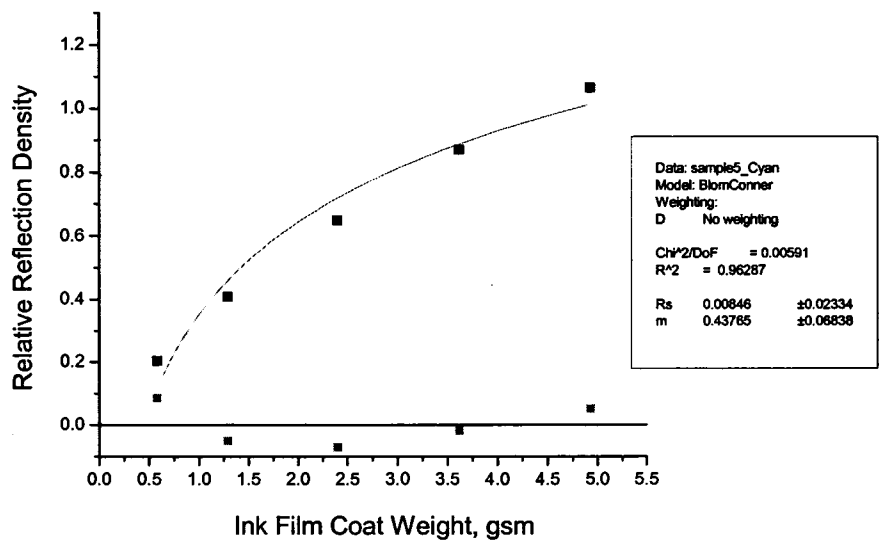


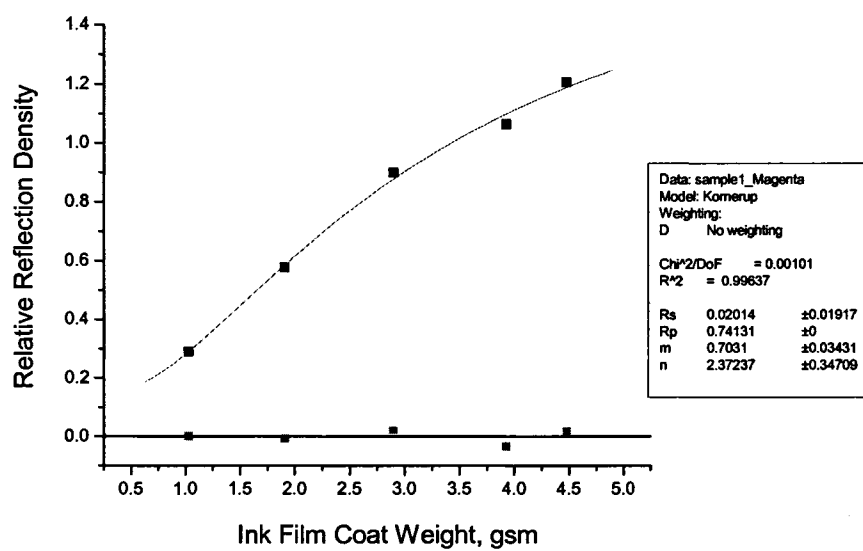
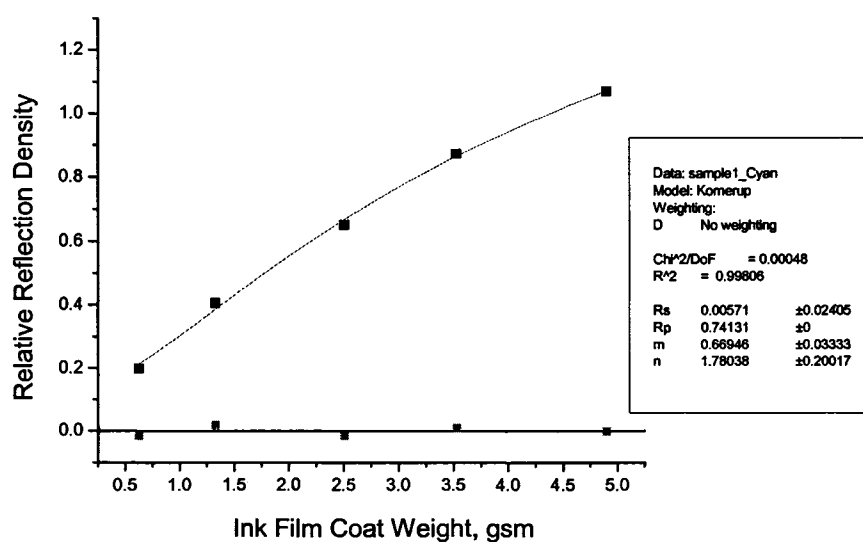


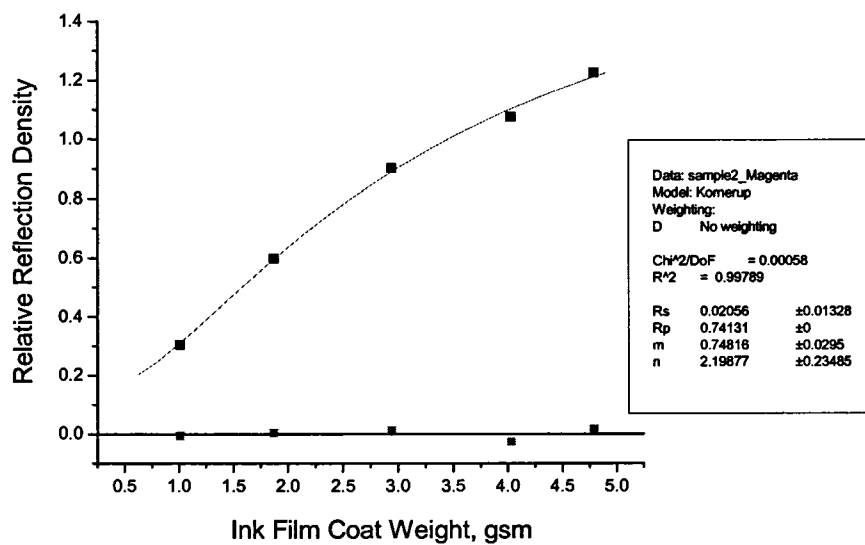
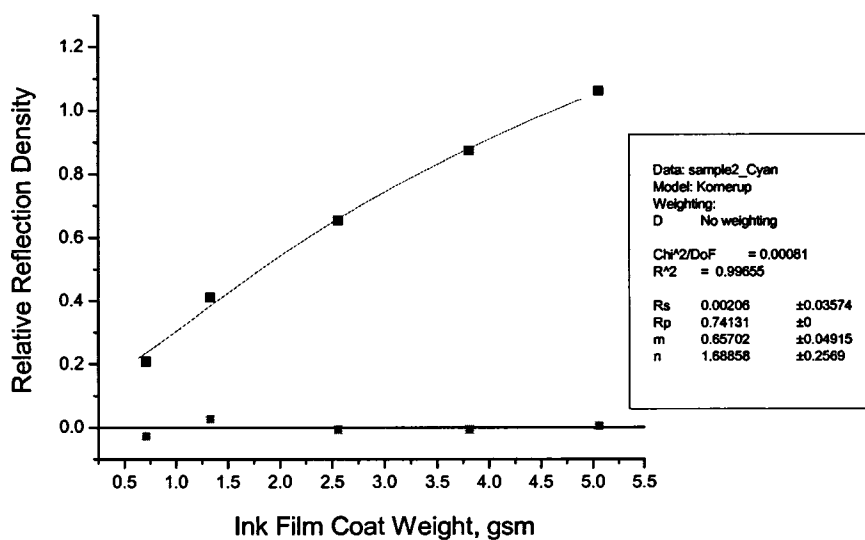


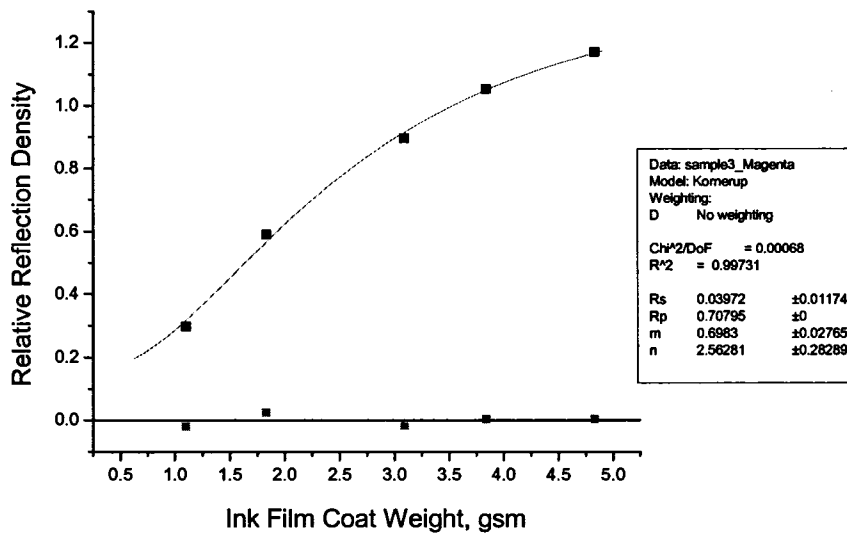
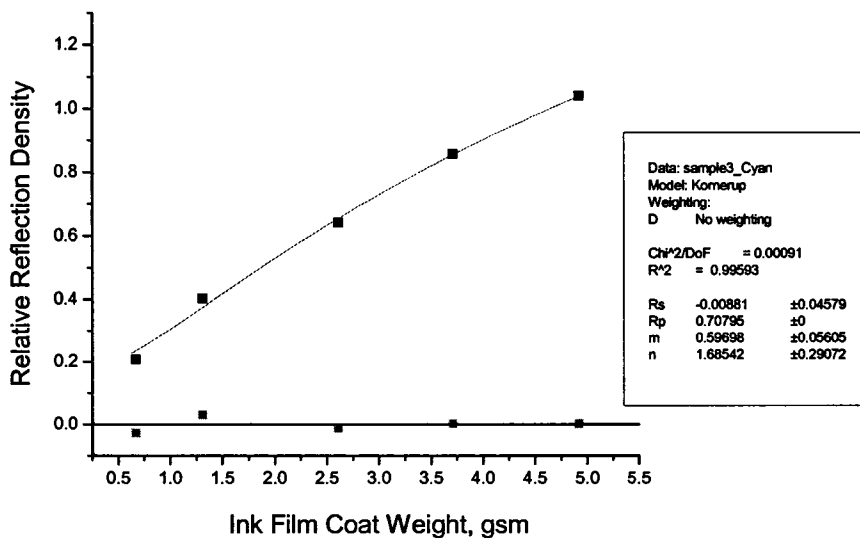


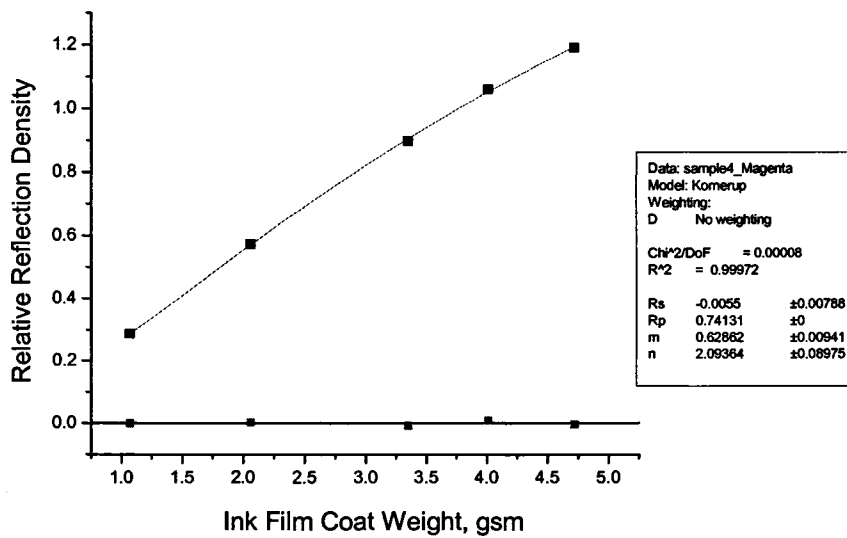
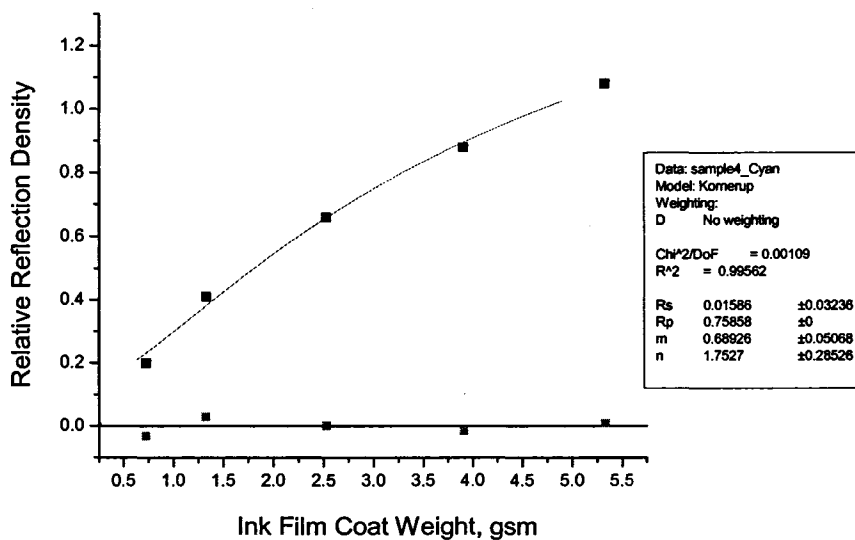


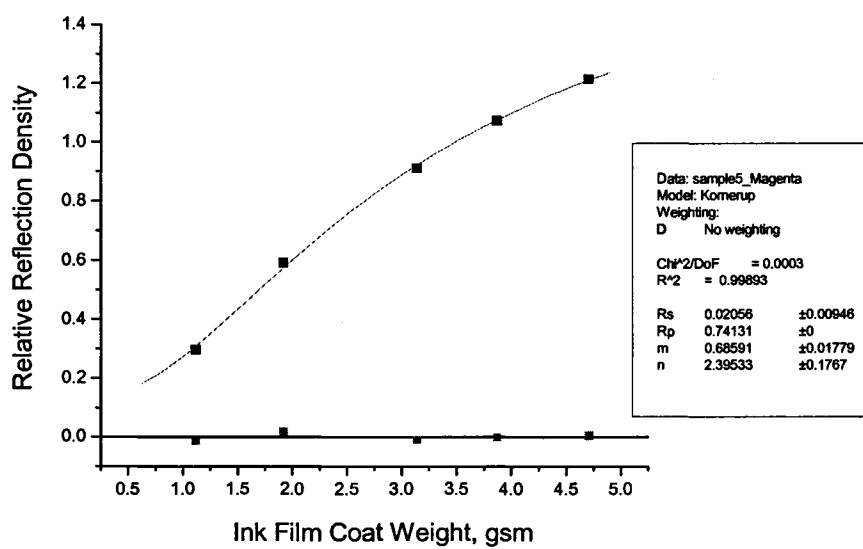
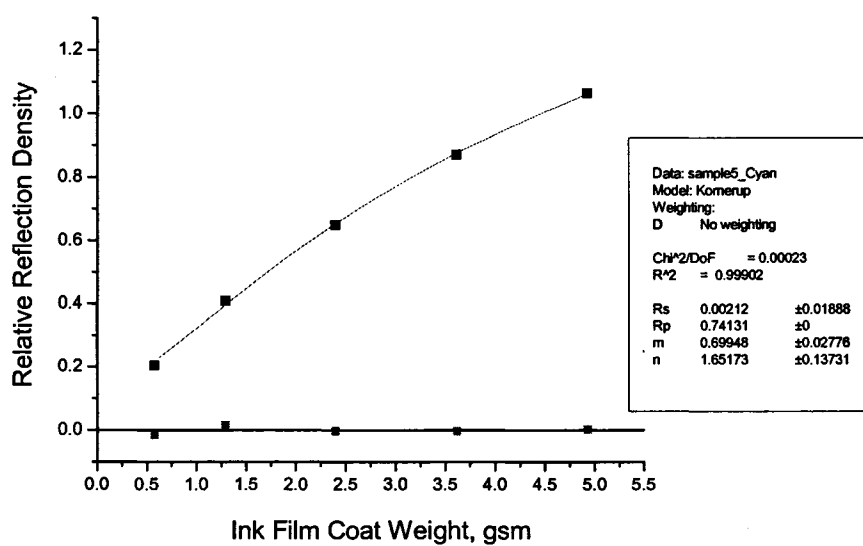












BIBLIOGRAPHY

- Adams, J. M., Faux, D. D., and Rieber, L. J. (1996), *Printing Technology*, 4th Edition, Delmar Publishers, Albany, pp. 465-469.
- Aspler, J. S. and Lepoutre, P. (1991), "Transfer and Setting of Ink on Coated Paper", *Progress in Organic Coating*, 19(4):333.
- ASTM (1998), American Society for Testing and Materials Standard E 284-98a "Standard Terminology of Appearance", Philadelphia.
- Béland, M.-C. and Bennett, J. M. (2000), "Effect of Local Microroughness on the Gloss Uniformity of Printed Paper Surfaces", *Applied Optics*, 39(16):2719-2726.
- Béland, M.-C., Lindberg, S., and Johansson, P.-Å. (2000), "Optical Measurement and Perception of Gloss Quality of Printed Matte-Coated Paper", *Journal of Pulp and Paper Science*, 26(3):120-123.
- Bernard, G., Farnood R., and Yan, N. (2004), "Relationship Between Microgloss Variation and Surface Texture of Paper", *Proceedings of the 2004 International Printing and Graphic Arts Conference*, TAPPI Press, Atlanta, pp. 217-222.
- Binnig, G., Quate, C. F., and Gerber, C. (1986), "Atomic Force Microscope", *Physical Review Letter*, 56(9):930-933.
- Blom, B. E. and Conner, T. J. (1990), "Optical Density and Ink Film Thickness; A Comparison of Models", *TAGA Proceedings*, TAGA Press, Rochester, pp. 213-225.
- Borch, J. (2002), "Optical and Appearance Properties", *Handbook of Physical Testing of Paper*, Volume 2, 2nd ed. (J. Borch, M. B. Lyne, R. E. Mark, and C. C. Habeger, Jr., eds.), Marcel Dekker, New York, p. 112.
- Borchers, C. H. (1958), "The Gloss of Offset Ink and Its Relationship to the Gloss and Absorptivity of Paper", *TAGA Proceedings*, TAGA Press, Rochester, pp. 191-198.
- Boumans, P. W. J. M. (1987), *Inductively Coupled Plasma Emission Spectroscopy, Part 1, Methodology, Instrumentation and Performance*, John Wiley and Sons, New York, p. 100.

- Calabro, G. and Mercatucci, F. (1974), "Method for Evaluating Newsprint Printability", *Advances in Printing Science and Technology: Proceedings of the Twelfth International Conference of Printing Research Institute*, Pentech Press, London, pp. 155-159.
- Calabro, G. and Savagnone, F. (1983), "A Method for Evaluating Printability", *Advances in Printing Science and Technology: Proceedings of the Seventeenth International Conference of Printing Research Institute*, Pentech Press, London, pp. 358-380.
- Casey, J. P. (1981), *Pulp and Paper*, John Wiley and Sons, New York, p. 3.
- Chinga, G. and Helle, T. (2003), "Relationships between the Coating Surface Structural Variation and Print Quality", *Journal of Pulp and Paper Science*, 29(6):179-184.
- Chinmayanandam, T. K. (1919), "On the Specular Reflection from Rough Surface", *Physics Review*, 13(2):96-101.
- Chou, S. M., Fadner, T. A., and Bain, L. J. (1990), "Structural Recovery of Printing Inks Studied by Steady Shear Rheometry", *TAGA Proceedings*, TAGA Press, Rochester, pp. 280-312.
- Chou, S. M. and Harbin, N. (1991), "Relationship between Ink Mileage and Ink Transfer", *TAGA Proceedings*, TAGA Press, Rochester, pp. 405-432.
- Chovancova, V., Howell, P., Fleming, P. D., and Rasmusson, A. (2004), "Printability of Different Epson Ink Jet Ink Sets", *Proceedings of IS&T NIP20: International Conference on Digital Printing Technologies*, IS&T, Springfield, pp. 457-463.
- Chovancova, V., Howell, P., Fleming, P. D., and Rasmusson, A. (2005), "Color and Lightfastness of Different Epson Ink Jet Ink Sets", *Journal of Imaging Science and Technology*, 49(6):652-659.
- Dalton, J. S., Preston, J. S., Heard, P. J., Allen, G. C., Elton, N. J., and Husband, J. C. (2002), "Investigation into the Distribution of Ink Components Throughout Printed Coated Paper Part 2: Utilising XPS and SIMS", *Colloids and Surface A*, 205:199-213.
- Donigian, D. W. (2004), "A New Mechanism for Setting and Gloss Development of Offset Ink", *Proceedings of the 1994 International Printing and Graphic Arts Conference*, TAPPI Press, Atlanta, pp. 77-94.
- Donigian, D., Dimmick A., Kim B.-S., and Bousfield, D. W. (2004), "Deviations from the Gloss-Tack Relationship", *Proceedings of the 1994 International Printing and Graphic Arts Conference*, TAPPI Press, Atlanta, pp. 59-65.

- Donigian, D. W., Ishley, J. N., and Wise, K. J. (1997), "Coating Pore Structure and Offset Printed Gloss", *TAPPI Journal*, 80(5):163-172.
- Dullien, F. A. L. (1979), *Porous Media, Fluid Transport and Pore Structure*, Academic Press, New York.
- Eldred, N. R. (2001), *What the Printer Should Know about Ink*, 3rd ed., GATF Press, Pittsburgh, p. 337.
- Enomae, T. and Lepoutre, P. (1995), "Stylus Profilometry: Marking by the Stylus", *TAPPI Journal*, 78(10):173-176.
- Eastman Kodak (2004), private communication with P. D. Fleming.
- Fetsko, J. M. and Zettlemoyer, A. C. (1962), *TAPPI Journal*, 45(8):667.
- Fu, Z. and Brown, J. T. (2003), "A Novel, Non-Mechanical Method for Producing Matte and Dull Papers with Exceptional Print Gloss", *TAPPI Journal*, 2(5):25-31.
- Gate, L. F., Windle, W., and Hine, H. (1973), "The Relationship between Gloss and Surface Microtexture of Coatings", *TAPPI Journal*, 56(3):61-65.
- Glatter, T. and Bousfield, D. W. (1997), "Print Gloss Development on a Model Substrate", *TAPPI Journal*, 80(7):125-132.
- Harrison, V. G. W. (1945), *Definition and Measurement of Gloss: a Survey of Published Literature*, Heffer and Sons Ltd., Cambridge.
- Hunter, R. S. (1952), "Gloss Evaluation of Materials", *ASTM Bulletin*, 186:48-55.
- ISO (1990), ISO Standard 8791-2 "Paper and Board – Determination of Roughness/smoothness (Air Leak Methods) – Part 2: Bendtsen Method", Geneva, Switzerland.
- ISO (1992), ISO Standard 8791-4 "Paper and Board – Determination of Roughness/smoothness (Air Leak Methods) – Part 4: Print-surf Method", Geneva, Switzerland.
- ISO (1994), ISO Standard 2813 "Paint and Varnishes – Determination of Specular Gloss of Non-Metallic Paint Films at 20 Degrees, 60 Degrees and 85 Degrees", Geneva, Switzerland.
- ISO (2005), ISO Standard 8791-2 "Paper and Board – Determination of Roughness/smoothness (Air Leak Methods) – Part 3: Sheffield Method", Geneva, Switzerland.

- Jeon, S. J., and Bousfield, D. W. (2004), "Print Gloss Development with Controlled Coating Structures", *Journal of Pulp and Paper Science*, 30(4):99-104.
- Johansson, P.-Å. (1983), "Evaluation of Grey Tone Evenness Using Band Pass Filtering", *Proceedings of the Third Scandinavian Conference on Image Analysis*, Lund, Sweden.
- Johnson, H. (2005), *Digital Printing Start-up Guide* [electronic resource] (C. D. Tobie, ed.), Thomson/Course Technology, Boston.
- Judd, D. B. and Wyszecki, G. (1975), *Color in Business, Science, and Industry*, 3rd ed., Wiley, New York.
- Khandekar A. (2000), "Ink Transfer in Rotogravure", *Gravure Magazine*, July/August, pp. 26-33.
- Kipphan, H., ed. (2001), *Handbook of Print Media: Technologies and Production Methods*, Springer, Berlin, p. 979.
- Kornerup, A., Fink-Jensen, P., and Rosted, C. O. (1969), "Tristimulus Values of Prints and Mileage of Printing Inks", *Die Farbe*, 18:29-64.
- Kubelka, P. and Monk, F. (1931), *Zeit. Fur Techn. Physik*, 12:593.
- Lee, H.-K., Joyce, M. K., and Fleming, P. D. (2004), "Interpretation of Paper Gloss and Associated Printability in Terms of Pigment Particle Size and Composition for Glossy Ink Jet Papers", *Proceedings of IS&T NIP20: International Conference on Digital Printing Technologies*, IS&T, Springfield, pp. 934-939.
- Lee, H.-K., Joyce, M. K., and Fleming, P. D. (2005a), "Influence of Pigment Particle Size and Pigment Ratio on Printability of Glossy Inkjet Paper Coatings", *Journal of Imaging Science and Technology*, 49(1):54-61.
- Lee, H.-K., Joyce, M. K., Fleming, P. D., and Cawthorne, J. E. (2005b), "Influence of Silica and Alumina Oxide on Coating Structure and Print Quality of Ink Jet Papers", *TAPPI Journal*, 4(2):11-16.
- Lipshitz, H., Bridger, M., and Derman, G. (1990), "On the Relationships between Topography and Gloss", *TAPPI Journal*, 73(10):237-245.
- MacGregor, M. A. (2001), "A Review of the Topographical Causes of Gloss Variation and the Effect on Perceived Print Quality", *Paper Technology*, 42(10):23-34.

- MacGregor, M. A. and Johansson, P.-Å. (1990), "Submillimeter Gloss Variations in Coated Paper Part 1: the Gloss Imaging Equipment and Analytical Techniques", *TAPPI Journal*, 73(12):161-168.
- MacGregor, M. A., Johansson, P.-Å., and Béland, M.-C. (1994), "Measurement of Small-Scale Gloss Variation in Printed Paper: Topography Explains Much of the Variation for one Paper", *Proceedings of the 1994 International Printing and Graphic Arts Conference*, TAPPI Press, Atlanta, pp. 33-43.
- MacPhee, J. and Lind J. T. (1991), "Measurements of Ink Film Thickness Printed by the Litho Process", *TAGA Proceedings*, TAGA Press, Rochester, pp. 550-573.
- MacPhee, J. and Lind J. T. (2002), "Insight into the Relationship between Print Density and Ink Film Thickness", *TAGA Proceedings*, TAGA Press, Rochester, pp. 479-496.
- Matsuda, N., Ichibashi, T., and Zama, Y. (2000), "Influence of Ultra Fine Surface Profile to Sheet and Print Gloss of Coated Paper", *Proceedings of the TAPPI Coating Conference and Trade Fair*, TAPPI Press, Atlanta, pp. 285-308.
- Myshkin N. K., Grigoriev A. Ya., Chizhik S. A., Choi K. Y., Petrokovets M. I. (2003), "Surface Roughness and Texture Analysis in Microscale", *Wear*, 254:1001-1009.
- Moreau-Tabiche, S. (2004), "Comparison of Different Developed Methods for Surface Characterisation", http://www.ind.tno.nl/en/cost_action_e11/Coating.
- Morita, S., Wiesendanger, R., and Meyer, E., eds. (2002), *Noncontact Atomic Force Microscopy*, Springer-Verlag Berlin, Heidelberg, Germany.
- Niskanen, K., ed. (1998), *Paper Physics*, Fapet Oy, Helsinki, Finland.
- Novak, G. and Muck, T. (2004), "Smoothness/Roughness Characterisation for Non-Impact Printing Papers", http://www.ind.tno.nl/en/cost_action_e11/calendering.
- Oittinen, P. (1972), "A Tentative Study of Back Transfer in Two-Colour Printing", *Graphic Arts in Finland*, 1(2):11-22.
- Oittinen, P. (1980), "Surface Reflection of Coated Papers and Prints", *Advances in Printing Science and Technology: Proceedings of the Fifteenth Advances in Printing Science and Technology Conference*, Pentech Press, London, pp. 344-372.
- Oittinen, P. and Saarelma, H. (1998), *Printing*, Fapet Oy, Helsinki, Finland.

- Pal, L., Joyce, M. K., and Fleming, P. D. (2005), "Pore Structure Parameters Properties - Effect on Barrier and Printing properties of Paper and Paperboard", Poster presented at the 2005 Coating & Graphic Arts Conference & Exhibit, Toronto, April 17-20.
- Pal, L., Joyce, M. K., and Fleming, P. D. (2006), "A Simple Method for Calculation of Permeability Coefficient of Porous Media", *TAPPI Journal*, accepted.
- Pauler, N. (1988), "A Model for the Interaction between Ink and Paper", *Advances in Printing Science and Technology: Proceedings of the International Conference of Printing Research Institute*, Pentech Press, London, pp. 116-136.
- Picollet, M., Morin, V., Piette, P., and Le Nest, J. F. (1998), "Competition Between Gravure Ink Penetration and Spreading on LWC Coated Papers", *Proceedings of the 1998 Coating/Papermakers Conference*, TAPPI Press, Atlanta, pp. 383-392.
- Preston, J. S., Elton, N. J., Husband, J. C., Dalton, J. S., Heard, P. J., and Allen, G. C. (2002), "Investigation into the Distribution of Ink Components on Printed Coated Paper Part 1: Optical and Roughness Considerations", *Colloids and Surface A*, 205:183-198.
- Preston, J., Nutbeem, C. Parsons, J., and Jones A. (2001), "The Printability of Coated Papers with Controlled Microstructure", *Paper Technology*, 42(2):33-41.
- Rutherford, B., ed. (1991), *Gravure: Process and Technology*, Gravure Education Foundation and Gravure Association of America, Rochester, pp. 346-350.
- Sandrueter, N. P. (1994), *TAPPI Journal*, 77(7):173.
- Serafano, J. and Pekarovicova, A. (1997), "Ink Consumption in Rotogravure – Determining Ink Mileage on Gravure Publication Papers", *TAGA proceedings*, TAGA Press, Rochester, pp. 511-523.
- Silver, G. A. (1984), *Professional Printing Estimating*, 2nd ed., Van Nostrand Reinhold Company, New York, p. 123.
- Steele, F. A. (1935), "The Optical Characteristics of Paper I. The Mathematical Relationships between Basis Weight, Reflectance, Contrast Ratio, and Other Optical Properties", *Paper Trade Journal*, 100(12):37-42.
- Ström, G., Englund, A., and Karathanasis, M. (2003), "Effect of Coating Structure on Print Gloss after Sheet-Fed Offset Printing", *Nordic Pulp and Paper Research Journal*, 18(1):108-115.

- Ström, G., Gustafsson, J., and Sjölin, K. (2000), "Separation of Ink Constituents During Ink Setting on Coated Substrates", *Proceedings of the 2000 International Printing and Graphic Arts Conference*, TAPPI Press, Atlanta, pp. 89.
- TAPPI (1992), TAPPI Test Method T 480 om-92 "Specular Gloss of Paper and Paperboard at 75 degree", TAPPI Press, Atlanta.
- TAPPI (1999), TAPPI Test Method T 555 om-99 "Roughness of Paper and Paperboard (Print-Surf Method)", TAPPI Press, Atlanta.
- TAPPI (2002), TAPPI Test Method T 410 om-02 "Grammage of Paper and Paperboard (Weight per Unit Area)", TAPPI Press, Atlanta.
- Tollenaar, D. and Ernst, P. A. H. (1962), "Optical Density and Ink Layer Thickness", *Advances in Printing Science and Technology: Proceedings of the International Conference of Printing Research Institute*, Pentech Press, London, pp. 214-234.
- Veenstra, P. (2004), "The Need to Develop Surface-Measuring Equipment", http://www.ind.tno.nl/en/cost_action_e11/calendering.
- Williams, C. (2001), *Printing Ink Technology*, Pira International, Leatherhead, p. 94.
- Xu, R., Fleming, P. D., Pekarovicova, A., and Bliznyuk, V. (2005), "The Effect of Ink Jet Paper Roughness on Print Gloss", *Journal of Imaging Science and Technology*, 49(6):660-666.
- Xu, R., Pekarovicova, A., Fleming, P. D., and Bliznyuk, V. (2005), "Physical Properties of LWC Papers and Gravure Ink Mileage", *Proceedings of 2005 TAPPI Coating Conference and Exhibit*, TAPPI Press, Atlanta, pp. 365-373.
- Yamauchi, T. and Murakami, K (2002), "Porosity and Gas Permeability", *Handbook of Physical Testing of Paper*, Volume 2, 2nd ed. (J. Borch, M. B. Lyne, R. E. Mark, and C. C. Habeger, Jr., Eds.), Marcel Dekker, New York, pp. 274-276.
- Yule, J. A. C. (1967), *Principles of Color Production*, John Wiley & Sons, New York, pp. 151-158.
- Zang, Y. H. and Aspler, J. S. (1994), "The Influence of Coating Structure on the Ink Receptivity and Print Gloss Development of Model Clay Coating", *Proceedings of the 1994 International Printing and Graphic Arts Conference*, TAPPI Press, Atlanta, pp. 193-199.
- Zhou, H. W. and Xie, H. (2003), "Direct Estimation of the Fractal Dimensions of a Fracture Surface of Rock", *Surface Review and Letters*, 10(5):751.